THE INTERACTIONS BETWEEN K^+ AND Tl^+ IN *C. RIPARIUS* LARVAE

INVESTIGATIONS OF THE INTERACTIONS BETWEEN K^+ AND Tl^+ IN *CHIRONOMUS RIPARIUS* LARVAE

By

RYAN F. BELOWITZ, B.Sc (Hons)

A thesis

Submitted to the School of Graduate Studies

in Partial Fulfillment of the Requirements

For the Degree

Master of Science

McMaster University

MASTER OF SCIENCE (2011) McMaster University
(Biology) Hamilton, Ontario

TITLE: Investigations of the interaction between K^+ and Tl^+ in *Chironomus riparius* larvae

AUTHOR: Ryan F. Belowitz, B.Sc. (Hons)

SUPERVISOR: Dr. Michael J. O'Donnell

NUMBER OF PAGES: xv, 185

ABSTRACT

Tl^+ is thought to be toxic to cells due to ionic mimicry of K^+. The aims of this study were two-fold. First, to identify whether K^+ and Tl^+ were interacting in isolated guts, whole animals and tissues in *Chironomus riparius,* and second, to determine the strategies of Tl^+ tolerance. *C. riparius.* were very tolerant towards Tl^+ with a 48-hr LC_{50} of 723 μmol l^{-1}. The Scanning Ion-selective Technique (SIET) allowed us to identify the caecae, AMG and PMG as the major K^+-transporting regions of isolated guts. Evidence for an interaction was based on the finding that Tl^+ was transported in the same directions at these segments (and others), and that 50 μmol l^{-1} Tl^+ decreased K^+ flux at the AMG and PMG. In addition, exposure to Tl^+ prior to flux measurements had significant effects on net K^+ transport by the gut. Measurements of Tl^+ and K^+ concentrations in the whole animal, gut and hemolymph by Atomic Absorption Spectroscopy (AAS) indicated that Tl^+ uptake was saturable in the whole animal and gut, and non-saturable in the hemolymph. Together with the SIET measurements, the AAS data suggests that high levels of Tl^+ can perturb K^+ transport and homeostasis. The absorption of Tl^+ from the gut to hemolymph, measured by SIET, was confirmed by hemolymph measurements of Tl^+ using AAS. This indicated that Tl^+ gains access to the hemolymph and that sensitive tissues (such as the nervous system) are thus exposed. However, survival of *C. riparius* at these concentrations implies efficient mechanisms for detoxification of Tl^+. This tolerance may involve sequestration in the gut, metal-binding proteins and increased secretion by the anal papillae and MTs. In addition, loss of K^+ from the muscle may prevent hypokalemia in the hemolymph and gut.

ACKNOWLEDGMENTS

Thank-you to my supervisor Dr. Michael O'Donnell, who initially took me on as a summer student in my third year. I had no training or experience (and probably no business!) being in the lab that summer. However, your patience was much appreciated. The excitement you show whenever someone has a new, interesting result is contagious within the lab, and made working on my Masters thesis a great experience.

Thank-you to my committee member Dr. Chris Wood. It was extremely helpful to hear your advice and comments on my project, whether it was at my committee meeting or over a beer (or six) at the Phoenix.

A huge thank-you to my science mentor Erin Leonard. You are a great teacher, and amazing friend. Thank you for all your help over the last three years, and for being so patient while teaching me the intricacies of SIET and Flame- and Graphite Furnace-Atomic Absorption Spectroscopy.

Thank-you to my family for their patience, especially my mom who provided me coffee just about every morning and ignored my outbursts at my computer. Thanks also to my brother for continuously distracting me with Halo.

To the O'Donnell and Wood Lab members – past and present. I have enjoyed every moment of my thesis, but mostly our times at the Phoneix, random bar Thursdays and soccer games. Good luck in the rest of your graduate careers.

Thank-you to my girlfriend Emma for encouragement and keeping me calm during my writing. And especially for checking over all 131 references.

THESIS ORGANIZATION AND FORMAT

This thesis is presented as a "sandwich thesis" with a general introduction and objectives of the research in chapter 1, followed by two research papers which are in the format of manuscripts to be presented for publication in peer-reviewed journals, followed by a general discussion.

Chapter 1: Introduction and project objectives

Chapter 2: Spatial and temporal transport patterns of K^+ and Tl^+ along the abdominal cuticle, anal papillae, gut and Malpighian tubules of *C. riparius* larvae: Investigations of the interaction between K^+ and Tl^+

Chapter 3: The effect of exposure to high concentrations of waterborne Tl^+ on K^+ and Tl^+ ion concentrations in *C. riparius* larvae.

Chapter 4: General discussion

TABLE OF CONTENTS

LIST OF FIGURES AND TABLES

CHAPTER 1

CHAPTER 2

CHAPTER 3

APPENDIX

CHAPTER 1:

General Introduction

1.1. Ion Transport

The regulated movement of substances into and out of cells is necessary for the normal functioning of any cell. Any abnormalities in this regulation can be detrimental to the organism, both at the micro- and macroscopic level. For example, cystic fibrosis is caused by the impaired conductance of chloride across the apical epithelia, causing the accumulation of mucus and resulting in numerous physiological problems (Widdicombe et al., 1985).

The cell is surrounded by a membrane composed of a lipid bilayer, which acts as a barrier to the movement of certain substances (both essential and non-essential) into or out of the cell. The lipid bilayer acts as a barrier by being an energetically unfavourable environment for hydrophilic substances (e.g. water and hydrated ions). However, the cell must overcome this barrier to allow the movement and regulation of essential substances, including physiological ions. To overcome the barrier, the cell contains many types of transporter proteins that span the lipid bilayer and allow movement of substances into or out of the cell. These transporters' can be highly specific to only one substance (e.g. K^+, glucose), and can be opened or closed by numerous mechanisms (e.g. voltage- or ligand-dependent), allowing the movement of specific substances to be precisely regulated.

The movement of ions across the membrane of a cell can occur by passive or active transport, the former requiring no energy and occurring due to electrochemical gradients, and the latter requiring energy. Primary active transport often involves

hydrolysis of adenosine triphosphate (ATP), which is produced by the cell, whereas secondary active transport uses potential energy caused by the movement of an ion down its electrochemical gradient to move another ion against its electrochemical gradient.

Passive transport of ions can occur by passive diffusion across the membrane due to electrochemical gradients, although this is quite slow for substances that are hydrophilic, such as hydrated ions. Facilitated diffusion is a type of passive transport that uses proteins embedded in the cell membrane to provide a channel for ions to move along their electrochemical gradient. These ion channels can be unregulated (i.e. always open) or regulated by voltage changes (voltage-dependent) or ligand-binding (ligand-dependent).

Active transport of ions requires a source of energy to move an ion against its concentration gradient. This energy can come from a chemical source, such as ATP, and be used to power ion pumps. A well known example is the Na^+-K^+ pump, which uses ATP to move three Na^+ out of the cell and two K^+ into the cell. The energy can also come from the movement of an ion down its electrochemical gradient to provide energy to move another ion against its gradient. For example, the ubiquitous sodium: proton exchanger (Na^+-H^+ exchanger) uses the favourable movement of Na^+ ions down their electrochemical gradient to move H^+ out of the cell against its gradient. The movement of both ions in the same direction is referred to as symport, whereas the movement of ions in the opposite direction it is referred to as antiport.

1.2. Potassium

The regulation of inter and extra- cellular potassium (K^+) is an essential process for the normal functioning of both the cell and the organism as a whole. At the cellular level, the resting membrane potential (E_M) is set by the potassium equilibrium potential (E_K) due to the high permeability of the membrane for potassium ions relative to other ions. This results in a high concentration of potassium within the cell (~ 150 mM) and a low concentration of potassium outside the cell (~ 4.5 mM) (Sperelakis, 1998). This unequal distribution occurs mainly from the action of the Na^+-K^+ pump. This pump relies on the energy from ATP and is essential for maintaining the sodium and potassium gradients. These gradients can then be utilized for indirect active transport of other ions into or out of the cell, a necessity for the daily processes which occur in the cell. Such processes relying on these gradients include the propagation of action potentials in excitable cells, such as neurons or muscle fibers. The propagation of these action potentials relies on the precise movement of both sodium and potassium ions due to changes in the membrane potential by the opening/closing of voltage gated Na^+ and K^+ channels. This was first demonstrated in giant axon of the squid *Loligo* by Hodgkin (1951). Potassium gradients are also essential for the proper functioning of Malpighian tubules, which compose the renal system of many invertebrates. In the mealworm, *Tenebrio molitor*, basolateral fluid secretion relies on the transport of potassium by K^+ channels, a Na^+:K^+:2Cl^- cotransporter and the Na^+-K^+ pump (Wiehart et.al, 2003). Thus, the ability of the cell to regulate their intercellular potassium concentration is extraordinarily important, and conditions which interfere with these regulatory processes

can lead to devastating effects on the organism. Such interferences can result from depletion of energy supplies (e.g. ATP) due to the application of certain drugs, such as cyanide, which interferes with the electron transport chain and can greatly hinder active transport (e.g. by the Na^+-K^+ pump). Another source of interference with the potassium gradient and transport results from blocking potassium channels by pharmacological agents, such as the scorpion toxin charybdotoxin (MacKinnon and Miller, 1988). Finally, competition for potassium transporters can occur from non-essential metals. Thallium (Tl^+) is one such toxic metal, and due to its similar ionic radius and holding the same charge as potassium, the displacement of potassium ions by thallium ions can greatly interfere with established potassium gradients and transport (Siegel and Siegel, 1976).

1.3. Thallium: Chemistry and Uses

Thallium was discovered in 1861 by W. Crookes, and metallic thallium was prepared by C. Lamy in 1862. It is classified as a group IIIA element in the periodic table, and exists in its inorganic forms as either monovalent (Tl^+) or trivalent (Tl^{3+}) thallium. Table I shows the physical and chemical properties of thallium (modified from Peter and Viraraghavan, 2005). Monovalent thallium is the more stable form in solution at neutral pH, making monovalent Tl-organocompounds (e.g. $TlNO_3$) more toxic (Galván-Arzate and Santamaria, 1998). However, there is evidence that the dominant form of thallium found in the Great Lakes is oxidized Tl^{3+}, which makes up 68% of total dissolved thallium (Lin and Nriagu, 1999). Furthermore, Tl^{3+} was shown to be more toxic

than Tl^+ to *Daphnia magna* with 48 hour LC_{50s} of 0.12 - 0.99 for Tl^{3+} (Lan and Lin, 2005) and 10.76 for Tl^+ (LeBlanc, 1980).

The hard soft acid and base [HSAB] principle helps predict metal-ligand binding characteristics, and as a general rule it states that soft acids/bases form more stable bonds with soft ligand donors, and vice versa for hard acids/bases (House, 2008). All compounds can be grouped as either a) *hard* Lewis acids/bases or b) *soft* Lewis acids/bases. Soft Lewis acids/bases have large atomic radii, low effective nuclear charge and high polarizability (Dong et al., 2006). Based on these criteria, Tl^+ is a soft Lewis acid and will form more stable complexes with soft ligand donors, such as sulfur or phosphorous containing compounds (House, 2008). When comparing the toxicity of organic thallium compounds (e.g. $TlNO_3$) and inorganic thallium (Tl^+), both share similar toxicity and distribution patterns, but Tl^+ shows a lower elimination rate constant (Aoyama, 1989).

Tl^+ has been used as a depilator for the treatment of ring worm, and is still used by poorer nations as a rodenticide and insectidicide (Galván-Arzate and Santamaria, 1998). Tl^+ can be employed as a catalyst in certain alloys, and in the production of imitation jewelry, low-temperature thermometers, fireworks, pigments and dyes. Expanding industries that require thallium include the production of fiber (optical) glass, semiconductors, lasers and specialized electronic research equipment. Thallium ions also demonstrate good nuclear magnetic resonance properties, making them useful markers for examining the biological function of K^+ and Na^+ ions (Peter and Viraraghavan, 2005). Thallous chloride 201 (Tl^{201}) also serves a clinical use for cardiac stress testing. This

alternative form of a cardiac stress test is particularly useful for patients who cannot perform the stressful and physical exercises required in regular cardiac stress testing. This includes elderly patients, or those who have just suffered myocardial infarction (Howard, 1991).

1.4. Thallium in the Environment: Natural and Anthropogenic Sources

Thallium is found within virtually all media on Earth. In the Earth's crust, thallium concentrations range from 0.45 – 8.32 μmol kg^{-1}, mainly complexed with sulfide ores of zinc, copper, lead and coal. However, Jurassic era coal contains much higher thallium concentrations, upwards of 4892 μmol kg^{-1} (Kazantzis, 2000). Within water, thallium concentrations range from 4.9 x 10^{-5} to 7.3 x 10^{-5} μmol l^{-1} in sea water (Flegal and Patterson, 1985); 2.5 x 10^{-5} to 4.9 x 10^{-5} μmol l^{-1} in unpolluted freshwater; and 9.9 x 10^{-5} to 25 x 10^{-5} μmol l^{-1} in polluted fresh water (Cheam et al., 1995). Overall, thallium concentrations in sea waters around the world are relatively constant, and their distribution is similar to other alkali metals (Peter and Viraraghavan, 2005).

Although only 15 tonnes of thallium is produced worldwide annually, it is estimated that between 2000-5000 tonnes is mobilized from industrial processes (Kazantzis, 2000). The major contributors are fossil fuel burning (especially Jurassic-era coal) and smelting and refining of ores. Other smaller contributors include oil refinement, cement production, brickworks and potash-derived fertilizers (Cheam, 2001).

The majority of mobilized thallium comes from coal-fired power plants. Due to the volatile properties of thallium at high temperatures, the electrostatic precipitators

which are used for emission control do not capture thallium as efficiently as other pollutants. The volatile nature of thallium at high temperatures also causes it to re-condense on ash particles from the coal. This precipitation occurs preferentially on smaller particles, resulting in higher thallium concentrations on ash particles than what is found in the coal itself (up to 10 times higher). These characteristics of thallium have further implications for emission control devices, as the smaller ash particles containing the highest concentrations of thallium pass through the filters the easiest. This allows thallium to enter aquatic and terrestrial environments, as well as be breathed in or consumed by humans, animals and plants (Cheam, 2001).

Metal ore refinement also mobilizes thallium into the atmosphere and aquatic environment. Streams and rivers which received industrial waste water and runoff from coal mines and power plants contained higher downstream concentrations of thallium (and other toxic metals) compared to upstream concentrations, 95% of the time (Cheam, 2001).

A well-known case of thallium poisoning occurred from cement production in Lengerich, Germany up until 1979. A factory produced a special type of cement which involved a pyrite roasting step, and this required an additive containing ferric oxide. This additive contained a very large amount of thallium which led to thallium accumulation in the local vegetation and atmosphere, leading to widespread thallium poisoning in the population. By simply switching the additive to one which contained less thallium, there was a huge improvement in air quality (Cheam, 2001).

Concentrations of thallium found in Canada (Table II) and from around the world (Table III) are shown below. In Table II it can be seen that the most Tl^+-contaminated aquatic sites in Canada are near east coast power plants and mines, which have Tl^+ concentrations ~28-fold higher than the Canadian Council of Ministers of the Environment (CCME) water quality guidelines for the protection of aquatic life. Of particular interest for this thesis are the data from the pore water samples. Figure 1, taken from Cheam (2001) shows a Tl^+ concentration profile curve from a 'peeper' which recorded Tl^+ concentrations in surface water and proceeded deeper into the sediment. A spike in thallium concentration (~3x the water concentration) occurs just below the sediment-water interface, which is the habitat of *C. riparius* being used in this study.

1.5. *Cellular Mechanisms of Thallium Toxicity*

Thallium can enter the body by inhalation, ingestion or by absorption through the skin (Galván-Arzate and Santamaria, 1998). However, the exact mechanism of Tl^+ toxicity is not known. Mulkey and Oehme (1993) have reported a number of possible mechanisms of Tl^+ toxicity. These include interference with potassium-dependent processes, such as substitution of Tl^+ for K^+ by the Na^+-K^+ pump. This is thought to occur because K^+ and Tl^+ have similar ionic radii (1.33 and 1.4 Å, respectively) and the same charge (Zhou and MacKinnon, 2003). Other mechanisms of Tl^+ toxicity suggested by Mulkey and Oehme (1993) include inhibition of cellular respiration, interferences with riboflavin and riboflavin based cofactors, and disruption of Ca^{2+} homeostasis. Tl^+ can also bind with a high affinity to sulfhydryl groups of proteins and enzymes and can lead

to inhibition of a wide range of cellular reactions and potential cell death. A study by Aoyama et al., (1988) looked a one such cellular reaction that may be affected by this unspecific binding. They have suggested that acute Tl^+ toxicity may result from the induction of lipid peroxidation, which has been shown to occur *in vivo* and *in vitro*. Gultathione and gultathione-peroxidase are two proteins involved in the protection of lipids from peroxidation. Increased Tl^+ concentrations were shown to decrease non-protein sulfhydryl levels (an indicator of glutathione levels) and the activity of glutathione-peroxidase. This resulted in widespread cellular damage in the liver and renal systems of mice due to lipid peroxidation (Aoyama et al., 1988).

1.6. Previous Studies of Tl^+ Toxicity in Aquatic Species

Less information is available on Tl^+ toxicity in aquatic species, compared to other toxic metals. In a study on juvenile Atlantic salmon (Zitko et al., 1975), it was found that acute toxicity to thallium (~0.147 μmol l^{-1}) was approximately 3- to 4-fold more toxic than copper. It was also found that neither humic acid (which reduces the toxicity of copper to juvenile Atlantic salmon) nor water hardness had an effect of thallium toxicity. Borgmann et al. (1998) performed chronic toxicity studies on the invertebrate *Hyalella azteca*. It was found Tl was more toxic than Ni, Cu and Zn, less toxic than Cd, and of similar toxicity as Pb. It was also found that K^+ was the only major ion that affected the uptake and toxicity of Tl^+. Table IV shows a summary of Tl^+ toxicity data for *Hyalella azteca,* and Table V provides a summary of Tl^+ toxicity values and endpoints from various studies.

The transfer of Tl^+ along food chains was studied by Dumas and Hare (2008). After exposing *Chironomus riparius* and *Tubifex tubifex* to sediment spiked Tl^+ (total concentration ~ 5 nmol g^{-1} dry weight), the sub-cellular distribution was determined for the cellular debris, granules, heat-denatured proteins (HDP), heat stable proteins (HSP) and organelles. Theoretically, Trophically Available Metal (TAM) is equal to the sum of the metal in the organelles, HDP and HSP. TAM was 74% and 49% of the total body concentration in *Chironomus riparius* and *Tubifex tubifex*, respectively. When these invertebrates were fed to *Sialis velata*, the assimilation efficiency was approximately 70% for both organisms, indicating both these organisms could be a source of Tl^+ poisoning in species at higher trophic levels.

1.7. Chironomus riparius *and the anatomy of the gut*

Chironomus riparius are members of the family Chironomidae. They are dipterans found in ecologically diverse habitats, and spend the majority of their life cycle as benthic larvae (Pinder, 1995). They are a source of food for many fishes, and are important bioindicators for water quality due to their abundance and widespread distribution in aquatic systems (Pinder, 1986). They are commonly found in extremely polluted aquatic environments, indicating that they are extremely tolerant towards a wide range of harmful xenobiotics (Pinder, 1995).

Ultrastructural studies of gut of *Chironomus thummi* have been performed by Seidman et al. (1986), and the gut anatomy of *C. riparius* has been previously described by Leonard et al (2009). Figure 2 shows a schematic diagram of the gut.

The gut of *C. riparius* is approximately 5 mm long and begins with the esophagus (ESO) at the most anterior side. The esophagus connects to the caecae, which are small projections which extend from the esophagus-caecae junction. The caecae connects to the anterior midgut (AMG), which has a characteristic basal surface on the anterior half, consisting of rows of projections in the shape of half-spheres. The measurement of K^+ and Tl^+ fluxes at the AMG in this study were performed within 500 μm of the esophagus-AMG junction, as this provided a distinct morphological feature from which AMG scans could be based on. The AMG connects to the posterior midgut (PMG), and the PMG connects to the ileum. The end of AMG and the beginning of the PMG does not show a distinct morphological change under the light microscope, so to decrease the likelihood of misidentifying the area scanned, the PMG scans were all performed within 500 μm of the PMG-ileum junction. The ileum-PMG junction is quite distinct, as this junction contains four Malpighian tubules (MTs) that join independently of each other (i.e. have no common ureter, as in *Drosophila*). The MTs are blind-ended tubes and together with the hindgut comprise the renal system of many insects. The MTs were arbitrarily divided into three segments for studies of K^+ and Tl^+ fluxes. The distal segment is furthest away from the PMG-ileum junction, the middle segment is approximately 750 μm from the PMG-ileum junction, and the proximal segment is within 250 μm of the PMG-ileum junction. The ileum connects to the rectum, which is divided into anterior and posterior segments.

1.8. Methods for measuring ion transport and concentrations

This study made use of the Scanning Ion-selective Electrode Technique (SIET) to measure ion fluxes. SIET is explained in detail in the methods of chapter II and is described only briefly here.

SIET exploits the ion gradients that are created in the unstirred boundary layer by transporting epithelia (figure 3). In epithelia that are transporting an ion from the bathing medium into the tissue, there will be a lower concentration of the ion closer to the tissue relative to the concentration a small distance (e.g. 50 µm) farther away. In epithelia that are transporting the ion in the opposite direction (tissue to bathing medium), the concentration of the ion within the unstirred boundary layer increases closer to the tissue. In either case, the concentration of the ion will eventually be equal to the background concentration of that ion in the bathing medium at a sufficient distance away from the tissue (~700-1000 µm). However, by measuring the voltage gradients created by ions between two points within the unstirred boundary layer (through the use of ion-selective microelectrodes), and by converting this voltage gradient to a concentration gradient (figure 3, equation 1), one can determine the ion flux using Fick's law (figure 3, equation 2). A schematic diagram showing the entire SIET setup is presented in figure 4.

K^+ concentrations in tissues and water samples were measured using flame atomic absorption spectroscopy (FAAS) and Tl^+ concentrations were measured using graphite furnace atomic absorption spectroscopy (GFAAS). These commonly used techniques are described in detail in the methods section of chapter III.

1.9. A Hypothesis for Toxic Metal Tolerance in Chironomus riparius

Chironomids have been shown to be highly tolerant towards a wide range of toxic metals, including Cd, Cu, Pb, Zn and Ni. The acute waterborne Cd LC_{50} (24 hour exposure) values for 1st instar chironomids, the most sensitive life stage, is 84 µmol l^{-1} (Bechard et al., 2008). This is thousands of times higher than the maximal allowable limit under Canadian Council of Ministers of the Environment (CCME) water quality guidelines for the protection of aquatic life.

Chronic toxicity tests are important for identifying sensitive endpoints for many aquatic species, however it is still important to perform acute toxicity tests in conjunction with chronic toxicity tests to help explain toxic effects (Watts and Pascoe, 2000). Gillis and Wood (2008) have proposed a potential mechanism for Cd tolerance using kinetic analysis of Ca and Cd uptake. Cd and Ca are of similar ionic radius and both hold a charge of 2+, and thus are thought to interact during Ca^{2+} transport. Gillis and Wood (2008) found chironomids have similar Ca^{2+} transport kinetics (i.e. maximum transport capacity (J_{max}) and affinity ($1/K_m$)) compared to other aquatic organisms. However, when looking at the transport kinetics of Ca transporters for Cd in chironomids, it was found that 1) the J_{max} is much higher, and 2) the affinity of the Ca transporters for Cd is quite low (large K_m) compared to other aquatic organisms. These findings suggest that the low affinity of Ca transporters for Cd prevents hypocalcaemia from occurring in chironomids, which is typically the cause of death by Cd poisoning in other aquatic organisms. However, chironomids still accumulate large amounts of Cd in their tissues due to the large J_{max}, and must find a way to detoxify this metal. One strategy employed is binding Cd^{2+} to metallothioneins, which renders Cd inert. Another strategy involves sequestering

and secreting the non-essential metal. A role of the gut and Malpighian tubules (MTs) in secretion and sequestration of Cd was investigated by Leonard et al., (2009). They found secretion of Cd^{2+} by the MTs to be the dominant form of tolerance at lower exposures (<100 μmol l^{-1}) whereas sequestration of Cd^{2+} by the posterior midgut (PMG) and MTs was more important at concentrations above 100 μmol l^{-1}. In addition, Leonard et al., found that the PMG was the primary site of sequestration, whereas the Malpighian tubules could both sequester and secrete Cd. A role for the anal papillae in Cd tolerance has also been explored (Appendix).

2.0. Thesis Objectives

This MSc has investigated the toxicity of a monovalent toxic metal, Tl^+, towards *C. riparius* and its effects on K^+ homeostasis. The experiments performed can be roughly divided into two types: those performed at the cellular level using electrophysiological techniques (chapter II), and those performed on the whole animal and/or entire tissue using toxicological approaches (chapter III).

In chapter II, K^+ and Tl^+ entry across the tissues exposed to the external environment (i.e. the abdominal cuticle and the anal papillae) were examined. Next, the spatial and temporal transport patterns of K^+ and Tl^+ along the basolateral (hemolymph-facing) surface of the gut and Malpighian tubules were characterized. This allowed me to identify the major K^+-transporting regions of the gut, and I was further able to examine the interaction of K^+ and Tl^+ at these sites through the use of competition studies and pharmacological blockers of K^+-transporters. Finally, I looked at the role of the gut as a

barrier to Tl^+ entry into the hemolymph by exposing the chironomid larvae to waterborne Tl^+ prior to dissection and conducting ion flux measurements along the gut. Exposing the larvae to Tl^+ prior to ion flux measurements also provided another means of identifying whether K^+ and Tl^+ were interacting by comparing K^+ fluxes in Tl^+-exposed and Tl^+-naïve larvae.

In chapter III, I examined the effect of waterborne Tl^+ exposure (48-hours) on Tl^+ uptake by the whole animal, gut and hemolymph. I was able to characterize which tissues showed saturable uptake, and which tissues did not. In addition I determined the relative roles for the gut, hemolymph and carcass in Tl^+ accumulation, taken as a percent of total Tl^+ present in the whole animal. Next, I compared the K^+ concentrations in unexposed larvae with larvae which were exposed to a range of Tl^+ concentrations. This allowed me to examine the interaction between K^+ and Tl^+ for the entire organism, as well as in the gut and hemolymph.

The transport of other ions (Ca^{2+}, Cd^{2+} and H^+) at the anal papillae has also been explored, and is presented in appendix.

References

Aoyama, H., Yoshida, M., Yamamura, Y. Induction of lipid peroxidation in tissues of thallous malonate treated hamster. *Toxicology*. **53** (1988), pp. 11-1

Aoyama, H. Distribution and excretion of thallium after oral and intraperitoneal administration of thallous malonate and thallous sulfate in hamsters. *Bull. Environ. Contam. Toxicol.* **42** (1989), pp. 456–463.

Bechard, K.M., Gillis, P.L., Wood, C.M. Acute toxicity of waterborne Cd, Cu, Pb, Ni and Zn to first-instar *Chironomus riparius* larvae. *Arch. Environ. Contam. Toxicol.* **54** (2008), pp. 454-459.

Borgmann, U., Norwood, W.P., Babirad, I.M. Relationship between chronic toxicity and bioaccumulation of cadmium in *Hyalella azteca. Canadian Journal of Fisheries and Aquatic Sciences* **48** (1991), pp. 1055-1060.

Borgrnann, U., Norwood, W.P., Clarke, C. Accumulation, regulation and toxicity of copper, zinc, lead and mercury in *Hyalella azteca. Hydrobiologia* **259** (1993), pp. 79-89.

Borgmann, U., Norwood, W.P. Toxicity and accumulation of zinc and copper in *Hyalella azteca* exposed to metal-spiked sediments. *Canadian Journal of Fisheries and Aquatic Sciences* **54** (1997), pp. 1046-1054

Borgmann, U., Cheam, V., Norwood, W.P., and Lechner, J. Toxicity and bioaccumulation of thallium in *Hyallela azteca*, with comparison to other metals and prediction of environmental impact. *Environ. Poll.* **99** (1998), pp.105-114.

Brockhaus, A., Dolgner, R., Ewers, U., Krämer, U., Soddemann, H., and Wiegand, H. Intake and health effects of thallium among a population living in the vicinity of a cement plant emitting thallium containing dust. *Int Arch Occup Environ Health* **48** (1981), pp. 375-389.

Buccafusco, R.J., Ells, S.J. and G.A. LeBlanc. Acute toxicity of priority pollutants to bluegill (*Lepomis macrochirus). Bull. Of Environ. Contam. And Toxic.* **26** (1981), pp. 446-452

Calleja, M.C., Persoone, G., and P. Geladi. Comparative acute toxicity of the first 50 multicenter evaluation of *in vitro* cytotoxicity chemicals to aquatic non-invertebrates. *Arch. Of. Environ. Contam. And Toxic.* **26** (1994), pp. 69-78.

Cheam, V., Lechner, J., Desrosiers, R., Sekerka, I., Lawson, G., and A. Mudroch. Dissolved and total thallium in Great Lakes waters. *J. Great Lakes Res.* **21** (1995), pp. 384-394.

Cheam, V. Thallium contamination of water in Canada. *Water Qual. Res. J. Canada* **36** (2001), pp. 851-877.

Dawson, G.W., Jennings, A.L., Drozdowski, D., and E. Rider. The acute toxicity of 47 industrial chemicals to fresh and saltwater fishes. *J. of. Hazard. Mat.* **1** (1975/1977), pp. 303-318.

Dong, H., Zheng, H. and Ye, B. Determination of thallium and cadmium on a chemically modified electrode with Langmuir–Blodgett film of *p*-allylcalix[4]arene. *Sensors and Actuators B: Chemical* **115** (2006) pp. 303-308.

Dumas, J., and Hare, L. The internal distribution of nickel and thallium in two freshwater invertebrates and its relevance to trophic transfer. *Environ. Sci. Technol* **42** (2008), pp. 5144-5149.

Flegal, A.R. and Patterson, C.C. Thallium concentrations in sea water. *Mar. Chem.* **15** (1985) 327-331.

Galván-Arzate, S. and Santamaria, A. Thallium toxicity. *Toxi. Letters* **99** (1998), pp.1-13.

Gillis, P., and Wood, C. Investigating a potential mechanism of Cd resistance in *Chironomus riparius* larvae using kinetic analysis of calcium and cadmium uptake. *Aqua. Toxi.* **89** (2008), pp.180-187.

Heitmuller, P.T., Hollister, T.A., and P.R. Parrish. Acute toxicity of 54 industrial chemicals to sheepshead minnows (*Cyprinodon variegates)*. **27** (1981), pp. 595-604.

Hodgkin, A.L. The ionic basis of electrical activity in nerve and muscle. *Biol. Rev*. **26** (1951), pp.339-409.

House, James E. 2008. Chemistry of Coordination Compounds. p. 582-583. In J. House, Inorganic Chemistry, Academic Press, Burlington, MA.

Howard, P.A. Intravenous dipyridamole: use in thallous chloride TL 201 stress imaging. *The Annals of Pharm.* **25** (1991), pp. 1085-1081.

Kazantzis, G. Thallium in the environment and health effects. *Envir. Geochem. and Heal.* **22** (2000), pp. 275-280.

Lan, C.H. and Lin, T.S. Acute toxicity of trivalent thallium compounds to Daphnia magna. *Ecotoxicology and Environmental Safety,* **61** (2005), pp. *432–4*

LeBlanc, G.A. Acute toxicity of priority pollutants to water flea (*Daphnia magna). Bull. Of Environ. Contam. And Toxic.* **24** (1980), pp. 684-691.

LeBlanc, G.A. Interspecies relationships in acute toxicity of chemicals to aquatic organisms. *Environ. Toxic.* **3** (1984), pp. 47-60.

Leblanc, G.A. and J.W. Dean. Antimony and thallium toxicity to embryos and larvae of fathead minnows (*Primephales promelas). Bull. Of Environ. Contam. And Toxic.* **32** (1984), pp. 565-569.

Leonard, EM., Pierce, L.M., Gillis, P.M., Wood, C.M., O'Donnell, M.J. Cadmium transport by the gut and Malpighian tubules of *Chironomus riparius. Aquat. Toxic*. **92** (2009), pp.179-186.

Lilius, H., Isomaa, B., and T. Holmstrom. A comparison of the toxicity of 50 reference chemicals to freshly isolated rainbow trout hepatocytes and *Daphnia magna*. *Aqua. Toxic.* **30** (1994), pp. 47-60.

Lin, T.S. and Nriagu, J.O. Thallium speciation in the Great Lakes. *Environ. Sci. Technol.* **33**(1999), pp. *3394-3397*

Linton, S.M., and M.J. O'Donnell. Contribution of K^+:Cl^- cotransport and Na^+/K^+-ATPase to basolateral ion transport in Malpighina tubules of *Drosophila melanogaster.* **202** (1999), pp. 1561-1570.

MacKinnon, R. and Miller, C. Mechanism of charybdotoxin block of the high-conductance, Ca2+-activated K+ channel. J. Gen. Physiol. **91** (1988), pp. 335–349.

MacLean, R.S., Borgmann, U., and D.G. Dixon. Bioaccumulation kinetics and toxicity of lead in *Hyalella azteca* (Crustacea Amphipoda). *Canad. J. of Fish. And Aquat. Scien.* **53** (1996), pp. 2210-2220

Mulkey, J.P. and Oehme, F.W. A review of thallium toxicity. *Veterinary and Human Toxicology* **35** (1993), pp. 445-453.

Peter, J.A.L. and Viraraghavan, T. Thallium: a review of public health and environmental concerns. *Environ. Int.* **31** (2005), pp. 493-501.

Pickard, J., Yang, R., Duncan, C., McDevitt, A., and C. Eickhoff. Acute and sublethal toxicity of thallium to aquatic organisms. *Bull. Of. Environ. Contam. And Toxic.* **66** (2001), pp. 94-101.

Pinder, L.C.V. Biology of freshwater chironomidae. *Ann. Rev. Entomol.* **31** (1986), pp. 1-23.

Pinder, L.C.V. The habitats of chironomid larvae. In: *The Chironomidae Biology and Ecology of Non-biting Midges*, edited by Armitage P.D., Cranston P.S., and L.C.V. Pinder. London: Chapman and Hall, 1995. pp. 107-135.

Seidman, L.A., Bergtrom, G., and C.C. Remsen. Structure of the larval midgut of the fly *Chironomus thummi* and its relationship to sites of cadmium sequestration. *Tissue and Cell.* 18 (1986), pp. 407-418.

Siegel, B.Z. and Siegel, S.M. Effect of potassium on thallium toxicity in cucumber seedlings: further evidence for potassium-thallium ion antagonism. *Bioinorganic Chem*. **6** (1976), pp. 341-345.

Sperelakis, Nicholas. 1998. Origin of Resting Membrane Potentials p. 178-201. In N. Sperelakis, Cell Physiology Source Book, Academic Press, San Diego.

Watts, M.M., and Pascoe, D. A comparative study of *Chironomus riparius* Meigen and *Chironomus tetnans* fabricius (Diptera: Chironomidae) in aquatic toxicity tests. *Arch Environ. Contam. Toxicol*. **39** (2000), pp. 299-306.

Wiehart, U. I. M., Nicolson, S. W. and Van Kerkhove, E. K+ transport in Malpighian tubules of *Tenebrio molitor* L.: a study of electrochemical gradients and basal K+ uptake mechanisms. *J. Exp. Biol.* **206** (2003), pp. 949-957.

Widdicombe, J.H., Welsh, M.J., and W.E. Finkbeiner. Cystic fibrosis decreases the apical membrane chloride permeability of monolayers cultured from cells of tracheal epithelium. *Proc. Natl. Acad. Sci. USA.* **82** (1985), pp. 6167-6171.

Xiao, T., Guha, J., Boyle, D., Liu, C., Chen, J. Environmental concerns related to high thallium levels in soils and thallium uptake by plants in southwest Guizhou, China. *The Science of The Total Environment* **318** (2004), pp. 223-244.

Zitko, V., Carson, W.V., Carson, W.G. Thallium: Occurrence in the environment and Toxicity to Fish. *Bull. Of Envir. Contam. and Tox.* **13** (1975), pp. 23-30.

Zhong, Z., Baogui, Z., Jiangping, L., Xingmao, Z., Guoli, C. Thallium pollution associated with mining and thallium deposits. *Science in China (Series D).* **41** (1998), pp 75-81.

Zhou, Y. and R. MacKinnon. The occupancy of ions in the K^+ selectivity filter: charge balance and coupling of ion binding to a protein conformational change underlie high conductance rates. *J. Mol. Biol.* **333** (2003), pp. 965-975.

Figure 1. Tl^{+} concentration profile of a peeper inserted into lake sediment from Lake Erie (taken from Cheam, 2001).

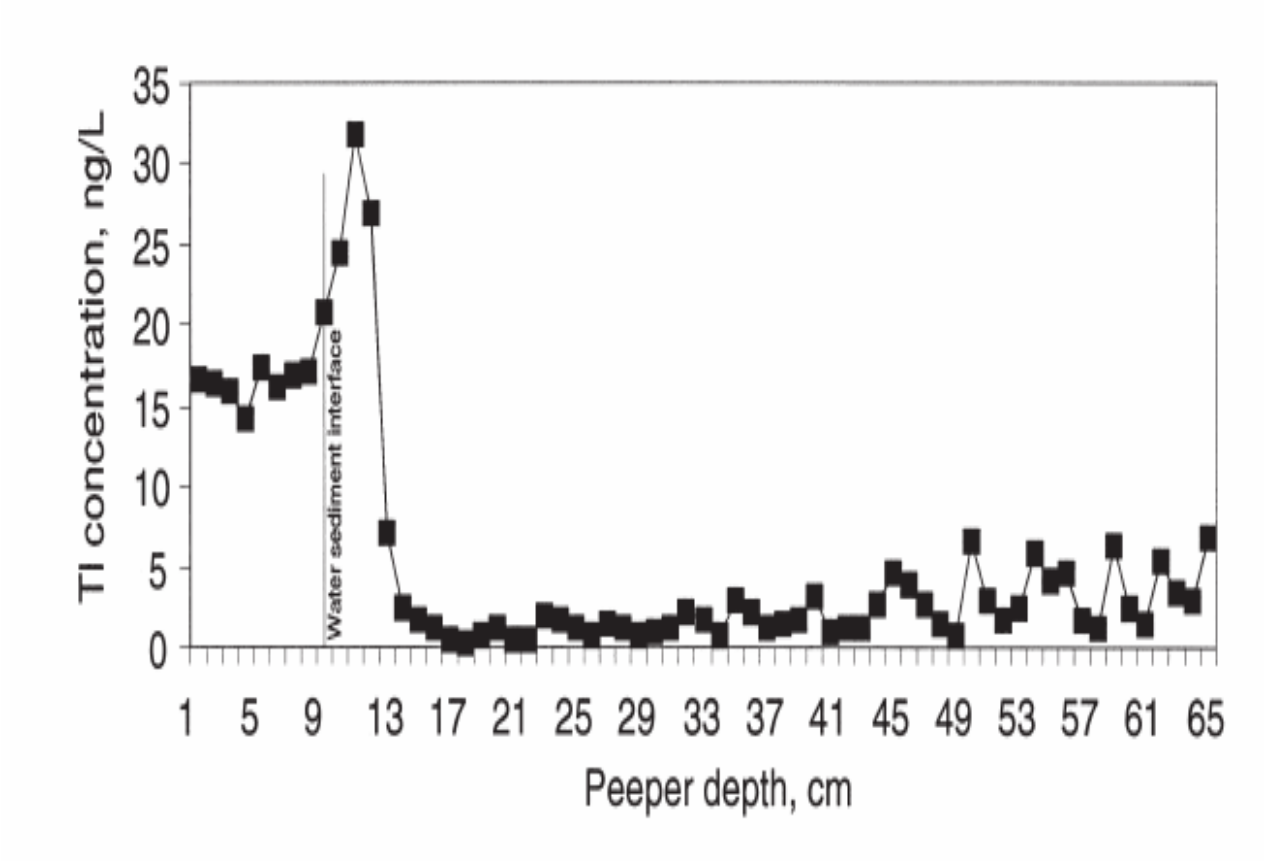
Tl concentration, ng/L
35
30
25
20
15
10
5
0
Water sediment interface
1
5
9
13
17
21
25
29
33
37
41
45
49
53
57
61
65
Peeper depth, cm

Figure 2. Schematic diagram of the *C. riparius* gut and Malpighian tubules. ESO = esophagus, CAE = caecae, AMG = anterior midgut, PMG = posterior midgut, LMT = lower Malpighian tubule, MMT = middle Malpighian tubule, DMT = distal Malpighian tubule, ILE = ileum, AR = anterior rectum, PR = posterior rectum.

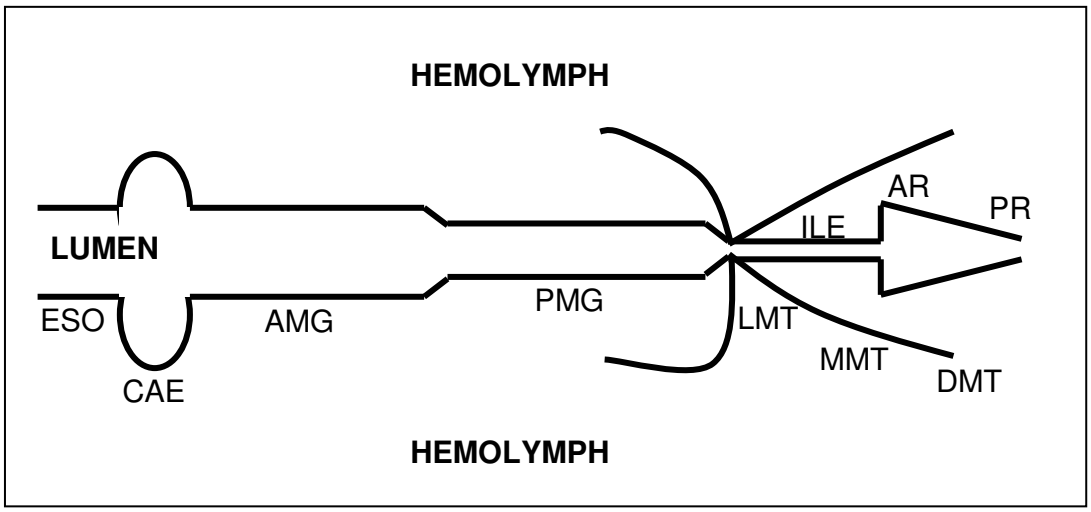
HEMOLYMPH
LUMEN
ESO
CAE
AMG
PMG
ILE
AR
PR
LMT
MMT
DMT
HEMOLYMPH

Figure 3. SIET technique for measurement of ion fluxes (K^+ used as an example). In this figure, K^+ is being transported out of the tissue (tissue to bathing medium) as indicated by the larger voltage at point A (V_A) relative to point B (V_B). In equation 1, C_B = background concentration of the ion (mmol l^{-1}), and S = the slope of the microelectrode (~58 mV for a 10-fold change in concentration of a monovalent ion). In equation 2, D = diffusion coefficient for the ion ($cm^2\ s^{-1}$), and ΔX = distance between V_A and V_B (cm). The units of ΔC are $\mu mol\ cm^{-3}$.

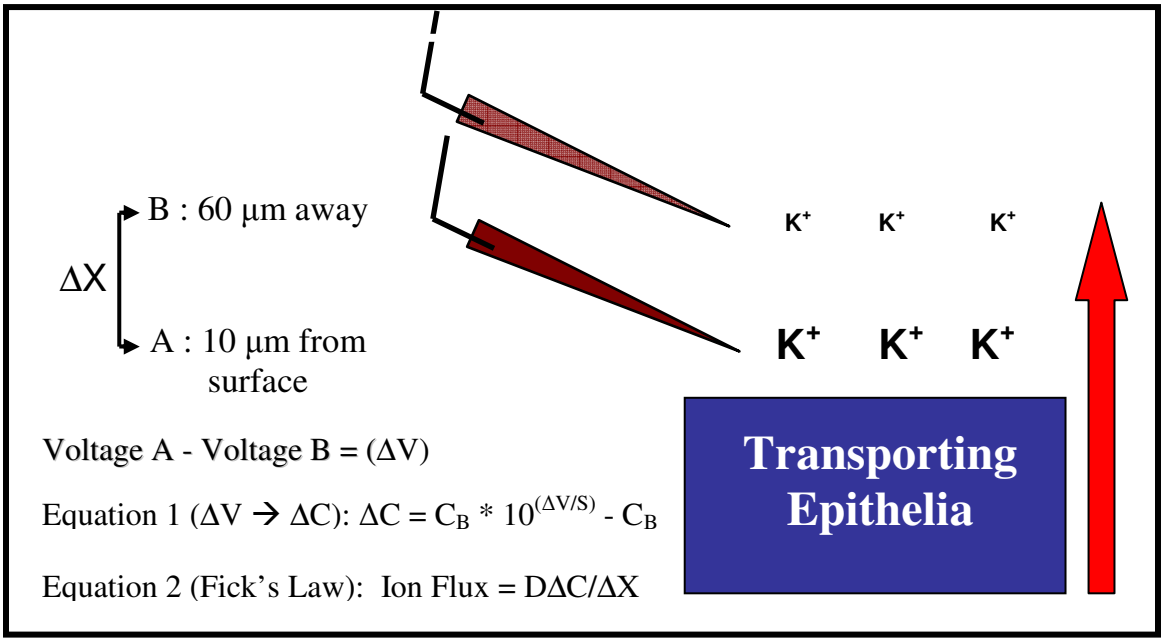
B : 60 µm away
ΔX
A : 10 µm from surface
K+ K+ K+
K+ K+ K+
Transporting Epithelia
Voltage A - Voltage B = (ΔV)
Equation 1 (ΔV → ΔC): ΔC = C_B * 10^(ΔV/S) - C_B
Equation 2 (Fick's Law): Ion Flux = DΔC/ΔX

Figure 4. Schematic representation of the SIET set up.

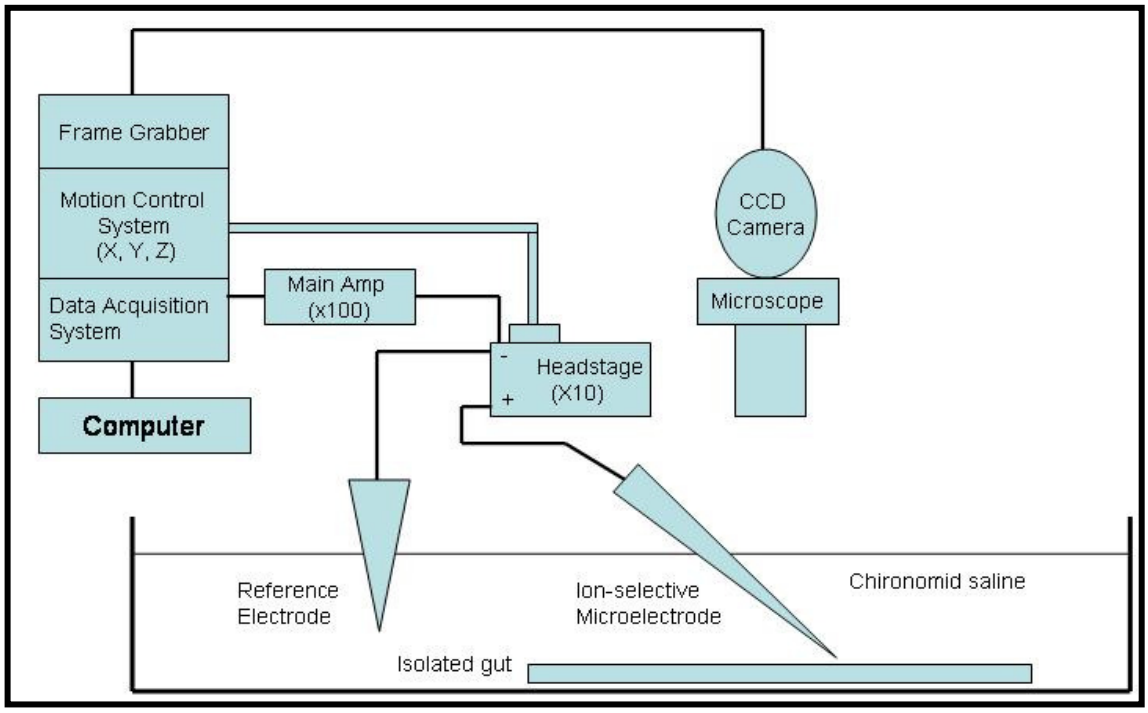
Frame Grabber
Motion Control System (X, Y, Z)
Data Acquisition System
Computer
Main Amp (x100)
Headstage (X10)
-
+
CCD Camera
Microscope
Reference Electrode
Ion-selective Microelectrode
Chironomid saline
Isolated gut

Table I. Physical and chemical properties of Thallium (modified from Peter and Viraraghavan, 2005)

Property	**Value**
Atomic Number	81
Molecular Weight (g/mol)	204.38
Ground state electronic configuration	[Xe] $4f^{14}5d^{10}6s^{2}6p^{1}$
Melting point (K)	577
Boiling point (K)	1746
Density (g/cc)	11.85
Atomic radius	1.704 (α-form)
Single-bond covalent radius	1.55
Van der Waals radius (2)	2.0

Table II: Thallium concentrations in aquatic environments collected from sites across Canada (data summarized from Cheam, 2001). The maxim allowable Tl^+ concentration according to the Canadian Council of Ministers of the Environment (CCME) water quality guidelines for the protection of aquatic life is provided for comparison.

Location	**Thallium (µmol l^{-1})**
Arctic Snow (i.e. 'natural' levels)	4.11×10^{-5}
Great Lakes	0.0002
Pore Waters	0.001
Western Power Plants and Mines (aquatic discharge sites)	0.0065
Central Power Plants (aquatic discharge sites)	0.0004
Eastern Power Plants (aquatic discharge sites)	0.1155
Miscellaneous Sites	0.0215
CCME Water Quality Guidelines (maximum allowed concentration)	0.004

Table III: Thallium concentrations in aquatic environments and soil samples taken from across the world.

Location	Thallium (µmol l^{-1} or µmol kg^{-1})
Sea water (low)[a]	$5.87x10^{-5}$
Sea water (high)[a]	$7.83x10^{-5}$
Cement additive (Germany)[b]	1957.1
Soil from mining area (China, low)[c]	195.7
Soil from mining area (China, high)[c]	606.7
Slope wash materials (China, low)[c]	97.8
Slope wash materials (China, high)[c]	136.9
Alluvial deposits downstream (China, low)c	68.4
Alluvial deposits downstream (China, high)[c]	303.3
Undisturbed natural soils (China, low)[c]	7.3
Undisturbed natural soils (China, high)[c]	33.7
Soil background area (China, low)[c]	0.97
Soil background area (China, high)[c]	2.4
Plants (Nanhua, low)[d]	1.02
Plants (Nanhua, high)[d]	69.8
Plants (Lanmuchang, low)[d]	0.04
Plants (Lanmuchang, high)[d]	171.2

a: Flegal and Patterson, 1985
b: Brockhaus et al., 1981
c: Xiao, T et al., 2004.
d: Zhong et al., 1998.

Table IV: Comparison of Tl toxicity to other toxic metals in *Hyallela azteca* in Lake Ontario water. (modified from Borgmann et al., 1998).

Metal	1-week LC_{50} (range) ($\mu mol\ l^{-1}$)	N	4-Week LC_{25} ($\mu mol\ l^{-1}$)	Source
Tl	**0.25 (0.19-0.31)**	**5**	**0.048**	**Borgmann et al., 1998**
Cd	0.068 (0.04-0.084)	8	0.0035	Borgmann et al., 1991
Hg	0.05	1	0.0084	Borgmann et al., 1993
Pb	0.560 (0.5-0.64)	3	0.042	Borgmann et al., 1993
Ni	1.350 (1.16-1.72)	3	-	unpublished
Cu	2.190 (1.78-2.73)	9	0.33	Borgmann and Norwood, 1997
Zn	6.220 (5.68-6.82)	2	1.7	Borgmann and Norwood, 1997

Table V: A summary of Tl toxicity values and endpoints in aquatic organisms

Species	**Effective [Tl] (umol l^{-1})**	**End Point**	**Reference**
C. riparius	**726**	**48 hr LC_{50}**	**This study**
D. magna	17.61	LC50 (24 Hr)	LeBlanc, 1980
D. magna	10.76	LC50 (48 Hr)	LeBlanc, 1980
D. magna	8.32	NOEC (48 Hr)	LeBlanc, 1980
D. magna	39.51	EC50 (immobility, 24 Hr)	Lilius et al., 1994
D. magna	9.83	LC50 (48 hr)	Pickard et al., 2001
C. dubia	1.81	LC50 (7 days)	Pickard et al., 2001
C. dubia	0.49	IC50 (reproduction)	Pickard et al., 2001
Daphnia	10.76	LC50 (48 hr)	LeBlanc, 1984
D. magna	8.3	EC50 (immobility, 24 Hr)	Calleja et al., 1993
Brine Shrimp	79	LC50 (24 Hr)	Calleja et al., 1993
Fairy Shrimp	0.8	LC50 (24 Hr)	Calleja et al., 1993
Rotifer	18.8	LC50 (24 Hr)	Calleja et al., 1993
Tadpoles	1.96	Lethality	Zitko, 1975
Atlantic salmon	0.147	LD50	Zitko et al., 1975
Rainbow trout	48.9-73.4	Lethality	Zitko, 1975
Rainbow trout	20.89	LC50 (96 Hr)	Pickard et al., 2001
Fathead Minnows	4.21	LC50 (96 Hr)	LeBlanc and Dean, 1984
Bluegill Sunfish	> 2900	LC50 (24 hr)	Buccafucso et al., 1981
Bluegill Sunfish	645.86	LC50 (96 hr)	Dawson, 1975/1977
Tidewater silversides	117.43	LC50 (96 hr)	Dawson, 1975/1977
Sheepshead minnows	102.75	LC50 (96 hr)	Heitmuller et al., 1981
Fathead minnow	4.21	LC50 (96 hr)	LeBlanc, 1984
Bluegill Sunfish	587.14	LC50 (96 hr)	LeBlanc, 1984

CHAPTER 2:

Abstract

Tl^+ is mobilized through industrial processes and can enter aquatic environments where it acts as a toxic metal at low concentrations. However, the aquatic larvae of the midge, *Chironomus riparius,* are exceptionally tolerant towards many waterborne toxic metals, with LC50s several orders of magnitude above CCME and USEPA guidelines. Few studies have looked at the cellular mechanism of this tolerance. Tl^+ and K^+ ions share the same charge and have similar ionic radii, resulting in competition between these ions for K^+ transporters. Using a recently developed Tl^+-selective microelectrode in conjunction with the Scanning Ion Selective Electrode Technique (SIET) and a two-microelectrode holder, precise measurements of K^+ and Tl^+ fluxes were made along the abdominal cuticle, anal papillae, gut tract and Malpighian tubules of *C. riparius* larvae. We determined that the major K^+ transporting regions of the gut and MTs were the caecae, anterior midgut (AMG) and posterior midgut (PMG) in Tl^+-naïve larvae, and that Tl^+ was also transported in the same direction at these locations. When the concentration of Tl^+ was increased to 50 μmol l^{-1}, K^+ transport was inhibited at the AMG and PMG. Larvae exposed to 300 μmol l^{-1} waterborne Tl^+ for 48 hours prior to ion flux measurements showed impaired K^+ flux at the AMG and PMG, but not the caecae, and Tl^+ was absorbed into the hemolymph across all three gut regions. In Tl^+-naïve larvae, net K^+ transport by the whole gut and MTs was absorption (4200 fmol s^{-1}) and net Tl^+ transport was secretion (-3.5 fmol s^{-1}). In contrast, Tl^+ exposed larvae had a net K^+ secretion (-2400 fmol s^{-1}) and net Tl^+ absorption (60 fmol s^{-1}). The absorption of Tl^+

would cause hemolymph levels to reach the concentration of the exposure medium (300 μmol l^{-1}) within ~2 hours, and the secretion of K^+ would cause whole body K^+ to be lost after ~12 hours. However, the survival of *C. riparius* larvae at the Tl^+ concentrations studied indicates that this does not occur, indicating efficient mechanisms of detoxification are present, possibly involving excretion of Tl^+ by the anal papillae or by binding it to proteins such as metallothionein that render Tl^+ inert. This study adds to the growing body of research looking at mechanisms of tolerance displayed by *C. riparius* towards non-essential metals.

Introduction

Chironomus riparius are dipterans found in ecologically diverse habitats, and spend the majority of their life cycle as benthic larvae (Pinder, 1995). They are a source of food for many fishes, and are important bioindicators for water quality due to their abundance and widespread distribution in aquatic systems (Pinder, 1986). They are commonly found in extremely polluted aquatic environments, indicating that they are extremely tolerant towards a wide range of harmful xenobiotics (Pinder, 1995). *C. riparius* have acute (24 hour) LC_{50} values for the waterborne toxic metals Cd, Cu, Pb, Ni and Zn that are significantly higher than CCME and USEPA guidelines (Béchard et al., 2008), indicating *C. riparius* are both well protected and extremely tolerant to non-essential metals.

There are three main strategies that can be employed, either separately or in conjunction, to increase tolerance towards toxicants. An increase in tolerance can be achieved by decreasing the uptake of the toxicant. This can involve avoidance through behavioural changes (Olla et al., 1980; Mohlenberg and Kiorboe, 1983) or the presence of a physical barrier to uptake (e.g. presence of an exoskeleton or limiting uptake across the gut). However, if the toxicant enters the species, particularly the blood or hemolymph, sensitive tissues (such as the nervous system) are exposed, and thus the toxicant must be detoxified. Detoxification may involve elimination (i.e. secretion) by transporting epithelia (O'Donnell, 2008), sequestration in the gut (Krantzberg and Stokes, 1990), or binding it to special proteins, such as metallothionein, rendering the toxicant inert (Hamilton and Mehrle, 1986).

Tolerance towards Cd^{2+}, a divalent toxic metal, has been previously studied in *C. riparius* (Gillis and Wood, 2008a; 2008b). Cd^{2+} can use Ca^{2+} transporters to enter aquatic organisms due to the similar size and ionic radii of the two ions, as has been observed in *C. staegeri* (Craig et al., 1999). Gillis and Wood (2008a) examined the kinetics of Cd^{2+} and Ca^{2+} uptake by 3rd and 4th instar larvae. They found *C. riparius* are able to tolerate high exposures to Cd^{2+} due to the uniquely low affinity (compared to other aquatic organisms) of Ca^{2+}-transporters for Cd^{2+}, thus preventing hypocalcaemia. However, Gillis and Wood (2008a) also showed that the transport capacity for Cd^{2+} is quite high, causing Cd^{2+} to accumulate in the tissues of *C. riparius*.

The role of the gut and Malpighian tubules (MTs) in detoxification of Cd^{2+} by secretion and sequestration was studied by Leonard et al., (2009). They found that the PMG is a site of sequestration of Cd^{2+}, and that the MTs can secrete Cd^{2+} at rates that would eliminate 10 μmol l^{-1} Cd^{2+} from the hemolymph within ~15 hours. The relative roles of secretion and sequestration were found to be dependent on the concentration of Cd^{2+}, with secretion predominant at low concentrations (<100 μmol l^{-1} $Cd^{2+)}$ and sequestration more important at higher concentrations. Detoxification of Cd^{2+} in *C. riparius* can also involve rendering Cd^{2+} inert by binding the toxic metal to metallothionein, a sulfur-rich protein. Metallothionein levels increase with exposure to higher concentrations of Cd^{2+} in *C. riparius* (Gillis et al., 2002; Fabrik et al., 2008).

By contrast to the Cd^{2+}:Ca^{2+} interaction in *C. riparius* described above, no studies have looked at the interaction of a monovalent toxic metal, such as Tl^{+}, with a physiological ion, such as K^{+}. K^{+} is a physiologically relevant ion that is found in high

concentrations in plant material. The large amount of K^+ obtained from the diet can subsequently be used to drive nutrient absorption in insects (Harvey, 2009). The diet of *C. riparius* relies heavily upon detritus, which contains a mixture of decaying plant and animal material, and thus is K^+-rich (Pinder, 1986).

The majority of Tl^+ enters the aquatic environment due to anthropogenic activities such as mining and the burning of fossil fuels (Kazantzis, 2000; Cheam, 2001). K^+ and Tl^+ share the same charge and have similar ionic radii (Peter and Viraraghavan, 2005). Due to the similar chemical properties, Tl^+ can act as an ionoregulatory toxicant and interfere with K^+ homeostasis in plants (Siegel and Siegel, 1976) and aquatic organisms (Pickard et al., 2001; LeBlanc, 1980; Zitko, et al., 1975). Tl^+ can also act as a toxicant by binding to sulfur-rich proteins and interfering with their function (Peter and Viraraghavan, 2005).

The aims of the study were five-fold. First, we wanted to identify the major K^+ transporting regions of the gut and MTs in *C. riparius*. Second, we wanted to identify the spatial transport patterns of Tl^+ along the gut and MTs and compare this to K^+ transport patterns. Similar directions and magnitudes of fluxes would be consistent with a shared transport mechanism. Third, we performed competition studies to identify whether K^+ and Tl^+ were competing for K^+-transporters at the three major K^+-transporting regions of the gut. In addition, we used pharmacological blockers to elucidate which K^+-transporters were involved. Fourth, we examined whether the gut would act as a barrier to Tl^+ entry into the hemolymph by exposing *C. riparius* larvae to Tl^+ prior to ion flux measurements. We also looked at the role of the anal papillae and abdominal cuticle in

acting as a barrier to Tl^+ entry in Tl^+-naïve larvae. Our fifth aim was to identify net K^+ and Tl^+ flux by the whole gut and MTs in Tl^+-naïve larvae, and to determine if net transport of the two ions was perturbed by Tl^+-exposure. We have considered the mechanism(s) of Tl^+ tolerance displayed by *C. riparius* in the discussion.

Methods

1.1. Chironomid larvae

C. riparius larvae were cultured at McMaster University, initiated from egg ropes obtained from Environment Canada. *C. riparius* egg ropes were hatched in Petri dishes, and first instar larvae were transported to 10 L aquaria containing fine-grained silica sand and aerated dechlorinated Hamilton tap water ('culture water'). The ionic composition of the culture water (in mmol l^{-1}) was Na^+ (0.6), Cl^- (0.8), Ca^{2+} (1.8), K^+ (0.4), Mg^{2+} (0.5) and Tl^+ (<1.25 x 10^{-5}). The water was moderately hard (140 mg l^{-1} $CaCO_3$) and pH was 7.8-8.2. The water was replaced once every ~10 days. The larvae were fed *ad labitum* on ground Nutrafin™ fish flakes (45% protein, 5% crude fat, 2% crude fibre, 8% moisture) and maintained at 21 ± 2 ºC under a 16:8 h light:dark photoperiod. Dissolved organic content (DOC) has been reported as 3.0 mg l^{-1} for our culture water (Gillis and Wood, 2008b). Once the larvae pupated and emerged as adults, the tanks were fitted with an equal sized lid. The lid contained an opening that could be covered with a removable mesh net, allowing egg ropes to be removed and hatched so that the colony was continuously replenishing itself.

1.2. Preparation and isolation of gut, anal papillae (AP) and abdominal cuticle

Ion flux measurements by the **S**canning **I**on-selective **E**lectrode **T**echnique (SIET) were all performed on 3^{rd}-4^{th} instar chironomid larvae. Ion flux measurements along the isolated gut were performed *in vitro*. The isolation of the gut for ion flux measurements using SIET has been described previously (Leonard et al., 2009). Figure 1

shows an image of the whole gut, and figures 2A-F shows images of the individual gut segments and the anal papillae which were scanned. For ion flux measurements in Tl^+-naïve larvae, the chironomids were transferred from the holding tank into a beaker containing 200 mL of dechlorinated Hamilton tapwater the day of the scan. The beaker was kept in the lab where dissections and scans were performed, and unused chironomids were returned to the holding tank at the end of the day. For ion flux measurements in Tl^+-exposed larvae, chironomids were transferred from the holding tank into a beaker containing 200 mL of dechlorinated Hamilton tapwater with 300 μmol l^{-1} Tl^+. They were exposed to Tl^+ for 48 hours prior to gut dissection and subsequent measurement of ion fluxes by SIET.

For the gut dissection, the chironomid was transferred from the beaker to a 5 mL Petri dish containing chironomid saline. The composition of chironomid saline is based on measurements of chironomid hemolymph, performed by Leonard et al., (2009). The ionic composition (in mmol l^{-1}) was K^+ (5), Na^+ (74), Ca^{2+} (1), Mg^{2+} (8.5), HCO_3^- (10.2), HEPES (10), glucose (20), and pH was titrated to 7 before use.

Using a pair of fine tipped forceps, the chironomid was pinched on the anterior and posterior ends, and holding one end firmly in place, the other end was tugged slightly which caused the gut to slide out from the exoskeleton. After the gut was removed, it was placed in a poly-L-lysine coated Petri dish, which adhered the gut to the bottom of the dish. The dish was filled with physiological saline and transferred to a Faraday cage for SIET measurements. The solutions used for ion flux measurements along the whole gut are listed in Table I.

Ion flux measurements at the anal papillae were performed *in vitro.* The isolation of the anal papillae for ion flux measurements has been described previously (Donini and O'Donnell, 2005; Nguyen and Donini, 2010). Briefly, the chironomids were removed from the beaker and placed in a Petri dish with 5 mL of chironomid saline. A pair of fine tipped forceps was used to pinch the posterior end of the abdomen containing the anal papillae. The posterior segment with the attached papillae was excised from the larva, and a clamp was placed on the forceps to ensure it remained closed to prevent hemolymph from leaking out. A small amount of petroleum jelly was also placed on the forceps opposite the side holding the papillae to seal the opening and ensure that the hemolymph did not leak out. The forceps holding the papillae were attached to a micromanipulator which allowed them to be moved in the X, Y and Z axes, thus facilitating their positioning in the Petri dish for ion flux measurements.

Ion flux measurements at the cuticle were performed *in vivo*. The chironomid was removed from the beaker and carefully dried using a Kimwipe™. It was placed in an empty Petri dish, and petroleum jelly was applied to cover the posterior end and the anterior head region. Once both ends of the chironomid were completely covered and isolated by the petroleum jelly, the appropriate solution was added to the dish and ion fluxes were measured at segments along the length of the abdomen.

1.3. Construction of reference electrodes and ion-selective microelectrodes (ISMEs)

Reference electrodes were made from 10 cm borosilicate glass capillaries (TW150-4; WPI, Sarasota, FL, USA) that were bent at a 45º angle, 1-2 cm from the end,

to facilitate placement in the sample dish. Capillaries were filled with boiling 500 mmol l^{-1} KCl saline solution containing 3% - 5 % agar and were stored at 4 ºC in 500 mmol l^{-1} KCl.

Tl^+ and K^+ ion concentrations were determined using ion-selective microelectrodes which were calibrated in the solutions listed in table I. This method has been previously described in detail (Rheault and O'Donnell, 2001; Donini and O'Donnell, 2005; Leonard et al., 2009). Borosilicate glass capillaries were pulled to a tip diameter of approximately 5-8 µm on a P-97 Flaming-Brown pipette puller (Sutter Instruments Co., Novato, CA, USA). The micropipettes were silanized with ~200 µl of N,N-dimethyltrimethylsilylamine (Sigma-Aldrich) or dichlorodimethylsilane (Sigma-Aldrich) at 200 ºC for 60 min and kept in a desiccator until needed. Salinization made the interior of the micropipette hydrophobic which allowed the ionophore cocktail to be frontloaded into the micropipette tip via capillary action.

Tl^+ micropipettes were backfilled with a solution of 1 mmol l^{-1} $TlNO_3$ (Sigma-Aldrich) and 150 mmol l^{-1} NaCl. Tl ionophore cocktail containing 5% w/w calyx[4]arene tetra-n-propyl-ether, 0.5% w/w potassium tetrakis (3,5 bis-[trifluromethyl]phenyl)borate, and 94.5% w/w o-NPOE (Harskamp et al., 2010). The Tl^+ cocktail was frontloaded into the electrode until it reached a column length of approximately 100-125 µm.

K^+ micropipettes were backfilled with 100 mmol l^{-1} KCl and used K^+ Ionophore I Cocktail B, which was frontloaded into the tip of the micropipette via capillary action until it reached a column length of approximately 100-150 µm.

1.4. *Scanning ion-selective electrode technique (SIET) measurements of ion (Tl^+ and K^+) gradients adjacent to the gut, anal papillae (AP) and abdominal cuticle*

Tl^+ and K^+ fluxes were determined using SIET for measurements of the ion gradients created by the transporting epithelial tissue of the gut. SIET measurements were made using hardware from Applicable Electronics (Forestdale, MA, USA) and automated scanning electrode technique (ASET) software (version 2.0, Science Wares Inc., East Falmouth, MA, USA).

The microelectrode was placed 5-10 μm from the tissue surface and voltage was recorded. The microelectrode was then moved a further 50 μm away and voltage was recorded again. The "wait" and "sample" times at each limit of the microelectrode excursion were 5 and 0.5 seconds, respectively. The average of three consecutive measurements was taken at five individual points along the gut, and the mean of these five individual points was calculated. The process was repeated four times and generated a total of 60 measurements (1 scan = 3 replicates x 5 sites x 4 repetitions), and an average of 1 scan was taken as a single measurement for that region of the gut. In the figures, consecutive scans at the same tissue are denoted as scan 1, scan 2 and scan 3. The voltage differences (ΔV) were converted to the corresponding Tl^+ concentration difference by the following equation (Donini and O'Donnell, 2005; Leonard et al., 2009):

$$\Delta C = C_B * 10^{(\Delta V/S)} - C_B \qquad \text{(Equation 1)}$$

where ΔC is the Tl^+ concentration difference between the two limits of the excursion distance (μmol cm^{-3}); C_B is the background Tl^+ concentration within the media (μmol cm^{-3}); ΔV is the voltage gradient (μV); and S is the slope of the electrode (μV $decade^{-1}$)

obtained from the calibration solutions. Tl^+ flux was calculated from the concentration difference and excursion distance using Fick's law of diffusion:

$$J_{Tl} = D_{Tl}(\Delta C)/\Delta X \qquad \text{(Equation 2)}$$

where J_{Tl} is the net flux in pmol cm^{-2} s^{-1}; D_{Tl} is the diffusion coefficient of Tl^+ (1.989 x 10^{-5} cm^2 s^{-1}); ΔC is the Tl^+ concentration gradient (µmol l^{-1} cm^{-3}) and ΔX is the excursion distance between the two points (cm).

K^+ flux was calculated using the equations listed above and the diffusion coefficient of K^+ (1.957 x 10^{-5} cm^2 s^{-1}). Diffusion coefficients for K^+ and Tl^+ were taken from the CRC handbook of chemistry and physics (Lide, 2002).

1.5. *Simultaneous measurement of K^+ and Tl^+ fluxes*

The previously mentioned scans used a set-up in which only one microelectrode (K^+ or Tl^+) was used. We also made use of a specialized microelectrode holder which allowed two ion-selective microelectrodes to be positioned so that measurements of both K^+ and Tl^+ flux could be made at the same location for studying K^+-Tl^+ competition and the effects of blockers (Ba^{2+} and ouabain). This relatively new technique has been described by Nguyen and Donini (2010). Figure 3 shows a comparison of the single microelectrode holder and double microelectrode holder. Using this set-up, guts were dissected and isolated as described above. The experimental studies were performed as paired measurements (i.e. each tissue preparation acted as its own control) due to the variability between tissues.

1.6 *Statistical analysis*

Comparisons between three treatment groups studied using the double electrode holder used repeated-measures analysis of variance (ANOVA) followed by Tukey's post-hoc test and Bonferoni post-hoc test. Comparisons between two treatment groups of experimental studies used the Students two-tailed paired t-test. For ion fluxes measured using the single microelectrode holder at the anal papillae and cuticle, one-way analysis of variance (ANOVA) followed by Tukey's post-hoc test and Bonferoni post-hoc test was used. All statistical analyses was performed using GraphPad Instat software (GraphPad InStat, GraphPad software, Inc San Diego, CA, USA). Statistical significance was designated if $p<0.05$. Data are reported as mean ± SEM.

Results

2. K^+ and Tl^+ flux measurements using a single-microelectrode holder

2.1. K^+ transporting regions of the gut in Tl^+-naïve C. riparius *larvae*

K^+ fluxes were measured along the entire gut tract and Malpighian tubules (MTs) of Tl^+-naïve *C. riparius* larvae to determine the major K^+ transporting regions. In all figures, negative fluxes denote movement of the ion from the bathing saline (i.e. hemolymph) towards the lumen (secretion), whereas positive fluxes denote absorption. The K^+ fluxes were compared to the corresponding Tl^+ fluxes measured at the same regions of the gut and MTs to determine if the direction of transport was the same (i.e. secretion or absorption). Transport of K^+ and Tl^+ in the same direction is consistent with a shared transport mechanism. In the figures below, K^+ fluxes for each tissue and condition are presented first, followed by Tl^+.

Figure 4A shows the rate at which the different gut segments and MTs transport K^+ per unit surface area (pmol $cm^{-2}s^{-1}$). For the esophagus (ESO), lower Malpighian tubule (LMT), middle Malpighian tubule (MMT) and distal Malpighian tubule (DMT), standard errors about the mean fluxes overlapped with zero, implying that these tissues were not physiologically important in transporting K^+. The highest rates of K^+ transport were seen at the caecae, anterior midgut (AMG) and posterior midgut (PMG), respectively.

Total K^+ transport by each gut region was calculated by multiplying the flux per unit area (pmol $cm^{-2}s^{-1}$) by the surface area (cm^2) of the corresponding tissue. Surface area measurements (taken from Leonard et al., 2009) were calculated from micrographs

by assuming a cylindrical shape of the gut. Figure 4B shows that the major K^+ transporting regions are the caecae, AMG and PMG. The values in figure 4B are expressed as fmol s^{-1} for easier comparison to Tl^+ transport below. Absorption of K^+ by the AMG is in excess of the sum of K^+ secretion by the caecae and PMG by ~2.5 fold. The other gut segments transport K^+ at rates which are negligible compared to the caecae, AMG and PMG.

Net K^+ transport by the entire gut and MTs can be determined by taking the sum of the fluxes for each segment in figure 4B. Calculations of net K^+ transport indicate whether the net movement of the ion by the whole gut and MTs is absorption or secretion. The positive sum (grey bar in figure 4B) indicates that the net transport of K^+ is absorption into the hemolymph at a rate equaling 4200 fmol s^{-1}, which is the equivalent of a daily uptake of 0.36 μmoles of K^+. The significance of this is addressed in the discussion. Net K^+ absorption in Tl^+-naïve larvae is compared to net K^+ transport in Tl^+-exposed larvae in section 2.3a, below.

2.2. Tl^+ transporting regions of the gut in Tl^+-naïve C. riparius *larvae*

Tl^+ fluxes were measured along the entire gut tract and MTs of Tl^+-naïve (i.e. no *prior* Tl^+ exposure) *C. riparius* larvae in order to compare the direction and magnitude of fluxes with the corresponding K^+ fluxes at each gut and MT segment (figure 4C). As seen for K^+ fluxes at the ESO and ILE, Tl^+ fluxes at these segments had standard errors about the mean that were close to overlapping with zero. Unlike K^+ flux at the AMG, Tl^+ flux at the AMG was quite variable and its standard errors about the mean also overlapped with

zero. The results indicated the ESO, ILE and AMG do not play a major role in transporting Tl^+. The apparent disagreement in K^+ and Tl^+ fluxes at the AMG was explored further (section 3.2b, below) and reasons for the difference are considered in the discussion (4.5b)

The direction of K^+ and Tl^+ fluxes were the same at the caecae, PMG, anterior rectum (AR) and posterior rectum (PR). All three segments of the MTs transported Tl^+, even though K^+ was not transported at measurable rates at these locations. Tl^+ was secreted by the middle and distal segments, and reabsorbed by the lower segment.

Total Tl^+ transport by each gut segment or tubule, calculated as the product of the Tl^+ flux in figure 4C (pmol $cm^{-2}s^{-1}$) and the surface area of the corresponding segment (cm^{-2}) is shown in figure 4D. The figure shows clearly that the major Tl^+ transporting region was the PMG.

Net Tl^+ flux is the sum of transport across all gut and tubule segments from figure 4D. The net Tl^+ flux was -3.44 fmol s^{-1} (grey bar in figure 4D), indicating that the gut and tubules together were moving more Tl^+ into the gut (and towards the lumen) than into the hemolymph. The PMG accounted for ~85% of this secretion. A very different picture emerged from studies of Tl^+-exposed larvae, described in section 2.3a below.

2.3. K^+ and Tl^+ transport at the anal papillae (AP) and abdominal cuticle of Tl^+-naïve C. riparius *larvae*

K^+ and Tl^+ transport (pmol $cm^{-2}s^{-1}$) were measured independently at the distal and proximal anal papillae (AP), as well as the cuticle of the abdominal wall of Tl^+-naïve *C.*

riparius larvae. The cuticle and AP are bathed in the external medium, so measurements were performed in dechlorinated Hamilton tap water to which a buffer had been added. K^+ was found to be absorbed (bath to AP) at the distal segment and secreted (AP to bath) at the proximal segment (Figure 5A). As a result, net transport of K^+ across the whole AP was negligible. By contrast, Tl^+ was absorbed at both the distal and proximal segments (Figure 5B), perhaps indicating the AP are a route of entry for Tl^+ into the hemolymph. There was no significant K^+ or Tl^+ flux at the abdominal cuticle.

3. Simultaneous K^+ and Tl^+ flux measurements using a two-microelectrode holder

3.1a K^+ and Tl^+ transport at the caecae of Tl^+-exposed C. riparius *larvae*

C. riparius larvae were exposed to 300 μmol l^{-1} Tl^+ for 48 hours prior to dissection of the gut and subsequent measurement of K^+ and Tl^+ fluxes. This concentration was chosen as it was close to the 48 hour LC_{50} for Tl^+ (723 μmol l^{-1} Tl^+, chapter 3). This allowed for investigations into whether the gut could act as a barrier to Tl^+ entry into the hemolymph.

Figure 6A shows that K^+ secretion was maintained during scans 1-3 (~60 minutes) at the caecae of Tl^+-exposed larvae.

Tl^+ was absorbed across the caecae and into the hemolymph in Tl^+-exposed larvae (figure 6B), but the rate of absorption declined 47% below the value in scan 1 by scan 3. In the descriptions below, percent changes in scan 2 or 3 are relative to the value in scan 1. The significance of this Tl^+ absorption is two-fold; it indicated that the caecae were not

acting as a barrier to Tl^+ entry into the hemolymph, and it also showed that Tl^+ was transported in the opposite direction from K^+.

3.1b K^+ and Tl^+ transport at the caecae of Tl^+-naive C. riparius *larvae*

K^+ and Tl^+ fluxes (pmol $cm^{-2}s^{-1}$) were measured at the caecae over a period of ~60 minutes to ensure that fluxes remained stable over time. Scans 1-3 took approximately 15 minutes each to complete, with an additional ~5 minutes between scans for solution changes. Figures 7A and 7B show that both K^+ and Tl^+ fluxes remained stable for scans 1-3 in Tl^+-naïve larvae. Changes in K^+ or Tl^+ flux would thus be attributed to the experimental treatment. There was no significant difference between K^+ gradients in Tl^+-naïve and Tl^+-exposed *C. riparius* larvae (figures 7A and 6A, respectively).

However, Tl^+ fluxes at the caecae were very different in Tl^+-naïve and Tl^+-exposed larvae. Tl^+ was secreted towards the lumen at the caecae of Tl^+-naïve organisms (figure 7B), whereas it was absorbed into the hemolymph in Tl^+-exposed larvae (figure 6A).

A decrease in K^+ flux in response to an increase in the concentration of Tl^+ in the bathing saline could result if the two ions competed for a shared transport mechanism. Figure 8 shows there was no significant effect of 5 or 50 μmol l^{-1} Tl^+ on K^+ flux at the caecae in Tl^+-naïve larvae.

Effect of Ba^{2+} and ouabain on K^+ and Tl^+ fluxes at the caecae

Ba^{2+} is a well known K^+-channel blocker (e.g. Alagem et al., 2001; Armstrong and Taylor, 1980; Hibino et al., 2010). The sensitivity of the transport of K^+ and Tl^+ to Ba^{2+} was therefore examined. Figure 9A shows that there was no significant effect of 2

mmol l^{-1} Ba^{2+} on K^+ flux in Tl^+-naïve larvae. However, a complete inhibition of Tl^+ flux occurred after Ba^{2+} was applied (figure 9B).

To determine if K^+ and/or Tl^+ transport into the caecae (in Tl^+-naïve larvae) involved the Na^+ pump, the Na-K ATPase inhibitor ouabain was applied. Ouabain exerts its blocking effect on the K^+-transporting (i.e. basolateral) side of the tissue (Harvey, et al., 1983). Controls showed that 0.2% DMSO (the vehicle for ouabain) had no significant effect on either K^+ or Tl^+ transport (figures 10A and 10B, respectively). K^+ flux decreased slightly by 15% during scan 3 in response to 100 µmol l^{-1} ouabain (figure 11A). Tl^+ flux was more strongly affected, and there was a clear reversal from secretion to absorption during both scans 2 and 3 (figure 11B).

3.2a K^+ and Tl^+ transport at the AMG of Tl^+-exposed C. riparius *larvae*

In Tl^+-exposed larvae, K^+ was secreted into the AMG (figure 12A). The K^+ secretion decreased to ~0 by scan 2.

Figure 12B shows that Tl^+-exposed larvae absorbed Tl^+ across the AMG and into the hemolymph. However, Tl^+ absorption decreased 47% by scan 2. These fluxes are compared to K^+ and Tl^+ fluxes in Tl^+-naïve larvae, below. The findings show that the AMG was not acting as a barrier to Tl^+ entry into the hemolymph.

3.2b K^+ and Tl^+ transport at the AMG of Tl^+-naive C. riparius *larvae*

Figure 13A shows that in Tl^+-naïve larvae, K^+ absorption by the AMG remained stable for ~60 minutes during scans 1-3. This was in marked contrast to the secretion of K^+ in Tl^+-exposed larvae (figure 12A).

In Tl^+-naïve larvae, Tl^+ fluxes increased over the duration of the scan (figure 13B). It was thought that this increase over time was due either to Tl^+ entering the gut lumen by transport across the caecae or bulk flow through the open end of the esophagus. To test this, the caecae and esophagus were removed at the caecae-AMG junction so that the gut was open and the bathing solution had access to the lumen. This resulted in a dramatic increase in Tl^+ flux (absorption) during scan 1 (figure 13C) in the caecae-removed gut compared to the same time point in the intact gut (figure 13B, scan 1). It is worth noting that Tl^+ fluxes at the AMG of Tl^+-naïve larvae whose guts were open (figure 13C) were similar to Tl^+ fluxes in Tl^+-exposed larvae (figure 12B), as both these gut preparations were provided with a Tl^+-source in the lumen.

The effect of an increase in Tl^+ concentration in the bathing saline on K^+ flux was tested to determine if Tl^+ affected K^+ transport at the AMG. Figure 14A shows that K^+ flux decreased 56% in the presence of 50 μmol l^{-1} Tl^+. To ensure that the observed effect was due to the increase in Tl^+ concentration, and not due to increased duration of exposure to 5 μmol l^{-1} Tl^+, the effect of 5 μmol l^{-1} Tl^+ over a longer time (i.e. during scan 2 and 3) was tested. Figure 14B shows no significant difference in K^+ flux when 5 μmol l^{-1} Tl^+ was applied for an increased duration, indicating the effect observed in figure 13A was in fact caused by an increase in the concentration of Tl^+ to 50 μmol l^{-1}.

3.3a K^+ and Tl^+ transport at the PMG of Tl^+-exposed C. riparius *larvae*

Figure 15A shows K^+ secretion at the PMG of Tl^+-exposed larvae. However, the rate of secretion decreased 76% by scan 3.

Tl^+ was absorbed into the hemolymph across the PMG of Tl^+-exposed larvae, and the flux remained stable during scans 1-3 (Figure 15B). K^+ and Tl^+ fluxes in Tl^+-exposed larvae were quite different than what was observed at the PMG in Tl^+-naïve *C. riparius*, described in section 2.3b, below.

Net K^+ transport by the caecae, AMG and PMG in Tl^+-exposed larvae

Total K^+ transport by the caecae, AMG and PMG in Tl^+-exposed larvae was calculated by multiplying the K^+ fluxes (scan 1) in figures 6A, 12A and 15A (pmol cm^{-2} s^{-1}) by the corresponding gut surface area (cm^{-2}). In figure 16A, the net K^+ transport (grey bar) was determined by taking the sum of the transport at the caecae, AMG and PMG. Given that these three gut regions account for ~77% of the surface area of the entire gut and were the major K^+ transporting regions, they provide a good estimate of net K^+ transport by the whole gut. Net K^+ transport in Tl^+-exposed larvae was -2443 fmol s^{-1}, indicating gut secretion of K^+. This secretion was equivalent to -0.21 μmol K^+/day. This was opposite to the K^+ absorption by the entire gut in Tl^+-naïve *C. riparius* (figure 4B). The effect of the net K^+ loss in Tl^+-exposed larvae is considered in the discussion (section 4.6c).

Net Tl^+ Transport by the caecae, AMG and PMG in Tl^+-exposed larvae

Total Tl^+ transport in Tl^+-exposed larvae was calculated for the caecae, AMG and PMG in the same manner as total K^+ transport above, using the scan 1 Tl^+ fluxes from

figures 6B, 12B and 15B. In figure 16B, net Tl^+ transport (grey bar) by these three gut regions was 50 fmol s^{-1}, indicating that Tl^+-exposed *C. riparius* were absorbing Tl^+. This indicated the gut was not acting as a barrier to Tl^+ entry into the hemolymph. The net absorption of Tl^+ was opposite to the net secretion of Tl^+ observed in Tl^+-naïve larvae (figure 4D). The significance of this is addressed in the discussion (sections 4.6b and 4.6c).

3.3b K^+ and Tl^+ transport at the PMG of Tl^+-naive C. riparius *larvae*

Figure 17A shows that K^+ flux at the PMG of Tl^+-naïve larvae remained stable for ~60 minutes during scans 1-3. The stable K^+ flux at the PMG indicated that any changes in flux could be attributed to the experimental treatment. As mentioned above, in Tl^+-exposed larvae K^+ secretion decreased during scans 2 and 3 (figure 12A), indicating that prior exposure of the larvae to Tl^+ affected the ability of the PMG to maintain stable K^+ fluxes.

In Tl^+-naïve larvae, Tl^+ was initially secreted at the PMG. However, it showed a significant and linear decrease with time (64% and 100% for scans 2 and 3, respectively. (figure 17B)). Due to this time dependant decrease in Tl^+ flux, it was not possible to make clear conclusions about the effects of Ba^{2+} on Tl^+ flux. The secretion of Tl^+ by Tl^+-naïve larvae is in stark contrast to the absorption of Tl^+ by the PMG of Tl^+-exposed larvae, described above. Explanations for the differences are considered in the discussion (section 4.5c).

The effect of 5 and 50 µmol l^{-1} Tl^{+} on K^{+} flux at the PMG was examined (Figure 18). K^{+} flux was completely inhibited by 50 µmol l^{-1} Tl.

Effect of Ba^{2+} on K^{+} flux at the PMG

The effect of Ba^{2+} at the PMG was investigated to determine if K^{+} transport was Ba^{2+} sensitive. Figure 19 shows K^{+} flux decreased significantly by 60% and 80 % for scans 2 and 3 in response to 2 mmol l^{-1} Ba^{2+}.

Discussion

This study examined transport of the physiological ion K^+ and the toxic metal Tl^+ by epithelial cells of *C. riparius*. We made use of a newly developed ion-selective microelectrode (ISME) for Tl^+ in conjunction with a specialized two-microelectrode holder. The Tl^+ ISME has been previously used only once in an analysis of Tl^+ fluxes along plant roots (Harskamp et al., 2010). Until now, no studies have been performed using an ISME to measure Tl^+ fluxes in isolated animal tissues in physiologically relevant conditions. The single-microelectrode holder allowed us to measure K^+ or Tl^+ fluxes along the entire gut and MTs to identify spatial transport patterns, whereas the two-microelectrode holder allowed us to study the fluxes of two ions (K^+ and Tl^+) simultaneously. The two microelectrode method provided us with a means to study mechanisms of ion transport and to examine competition between the two ions. In addition, this study has provided some insight into mechanisms of acute toxicity at the cellular level and adds to the growing body of research looking at how *C. riparius* larvae are able to tolerate extremely toxic conditions.

4.1. Comparison of K^+ and Tl^+ flux magnitudes

The relative rates of K^+ and Tl^+ transport can be compared if the Tl^+ flux is multiplied by 1000 to compensate for the 1000-fold lower concentration of Tl^+ relative to K^+ (5 µmol l^{-1} Tl^+ versus 5 mmol l^{-1} K^+). The adjusted Tl^+ fluxes are all within an order of magnitude of K^+ fluxes, suggesting that the two ions can be transported at comparable rates. At the caecae, K^+ flux is only 4-fold larger than the adjusted Tl^+ flux. The

differences in magnitudes are even less at the PMG, AR and PR; K^+ fluxes are all within 3-fold of the adjusted Tl^+ fluxes. The similarities between the directions and magnitudes of K^+ and Tl^+ fluxes suggests that Tl^+ may be substituting for K^+ at these tissues. Given that 5 mmol l^{-1} K^+ was present in the saline during all measurements, the detection of measurable Tl^+ fluxes suggests that the transporters involved have a high affinity for Tl^+ relative to K^+.

4.2. Malpighian tubules

An interesting finding was the lack of K^+ transport by any segment (distal, middle or proximal) of the MTs, even though Tl^+ fluxes were detected at all three segments (figures 4A and 4C). We suggest a two-part explanation. First, published and unpublished studies in our lab by Leonard et al., (2009) have used the Ramsay assay to measure fluid secretion and K^+ flux by *C. riparius* MTs. They found that K^+ flux is very low in the absence of cAMP, a 2^{nd} messenger implicated in stimulation of fluid and K^+ secretion. Our K^+ flux measurements at the tubule were done in the absence of cAMP, and as a result the tubules do not transport K^+. Secondly, it has also been shown in our lab that *C. riparius* tubules preferentially transport Na^+ in the absence of cAMP, and this is thought to drive the small amount of fluid secretion observed in unstimulated tubules. It has been shown by Boudker et al., (2007) that Tl^+ can bind to the Na^+ sites of a sodium-dependent aspartate transporter. Nriagu (1998) reports that Tl^+ ions have also been used as probes for determining biological functions of both K^+ and Na^+ ions. Taken together, we suggest that Tl^+ flux along the MTs may involve the contribution of Na^+ transporters.

4.3. Abdominal cuticle

The insect cuticle is composed of multiple layers; the outermost layer (epicuticle) contains lipoid materials and waxes, allowing it to act as an effective barrier to water loss (Wigglesworth, 1945). However, few studies have looked at ion transport at the insect cuticle. Credland (1978) found the cuticle of *C. riparius* is structurally similar to other insect cuticles in the post-cephalic region, and is between 3-4 μm, thus providing a barrier for water or ion transport. The lack of K^+ or Tl^+ transport at the abdominal cuticle is consistent with these findings (figures 5A and 5B).

4.4. Anal papillae

Ultrastructural studies have found that the cuticle surrounding the anal papillae is thin (1.6 μm) relative to the abdominal cuticle and that the hemolymph is continuous with the lumen of the AP (Credland, 1976). The structure of the epidermis surrounding the AP is characteristic of transporting epithelium, with a highly folded apical and basal membrane to increase surface area, and a high density of mitochondria (Credland, 1978). Ion flux measurements at the AP have been performed previously by Donini and O`Donnell (2005) in *Aedes aegypti* larvae. They found K^+ absorption (towards hemolymph) across the distal and proximal AP at rates approximately 10-fold higher than found in this study. However, the larger transport rates may be due to the approximately 10-fold higher concentration of K^+ in the bathing medium (5 mmol l^{-1} K^+ versus ~0.5 mmol l^{-1} K^+). K^+ fluxes have also been measured at the AP of *C. riparius* by Nguyen and Donini (2010). They measured K^+ fluxes along the entire AP (proximal and distal

segments) at rates averaging 6.4 ± 12.1 pmol cm^{-2} s^{-1}, while our measured K^+ flux along the entire anal papillae (the mean of the distal and proximal K^+ flux, figure 5A) was -2.0 ± 2.62 pmol cm^{-2} s^{-1}. However, both these rates had standard errors about the mean fluxes that overlapped with zero (i.e. no net transport). Nguyen and Donini also found that there was no significant difference between the proximal and distal AP. This discrepancy may be the result of differences in the ionic composition of the bathing medium in which K^+ fluxes were measured [dechlorinated Hamiltion tapwater (this study) vs. 1 mmol l^{-1} KCl in deionzed water (Nguyen and Donini)].

An interesting finding was Tl^+ absorption by the distal and proximal AP (figure 5B), indicating the AP as a potential source of Tl^+ entry into the hemolymph. The absorption of Tl^+ across the AP may be a reflection of the concentration gradient present, since these measurements were performed on Tl^+-naïve larvae. To elucidate whether Tl^+ is using K^+ transporters to cross the AP and access the hemolymph, future studies using K^+ transport blockers (e.g. Ba^{2+}) at the AP would be useful.

Although no measurements of Tl^+ flux were performed at the AP of Tl^+-exposed larvae, it would be of interest to do so. It may be that the AP can eventually act as a site of Tl^+ excretion. P-glycoproteins are ATP-dependant efflux pumps capable of transporting of wide range of xenobiotics, including the toxic metal Cd^{2+} (Callaghan and Denny, 2002) and have been detected in the AP of *C. riparius* (Podsiadlkowski, 1998). An increase in measured P-glycoproteins levels can be induced by exposure to inorganic arsenic in rat liver cell lines (Liu et al., 2001;), and an increase in multixenobiotic protein levels (related to mammalian P-glycoprotein) in the clam *Corbicula fluminea* was shown

to be induced by heavy metal exposure (Achard et al., 2004). This may implicate the AP as a site of excretion for toxic metals including Tl^+, although more studies would need to be completed.

4.5 Transport of K^+ and Tl^+ across the major K^+-transporting regions of the gut (caecae, AMG and PMG)

Figure 20 provides a summary of K^+ and Tl^+ fluxes along the entire gut and MTs in Tl^+-naïve larvae, and shows the effects of experimental treatments. Figures 21A and 21B show the fluxes of K^+ and Tl^+ during scans 1-3 for the Tl^+-naïve and Tl^+-exposed larvae, respectively. The information presented in figures 20 and 21 are discussed in detail in the following sections

4.5a Caecae

The caecae are involved in water absorption in the locust *Schisrocercn gregarra* (Dow, 1981), mosquito larvae *Aedes aegypti* (Jones and Zeve, 1968) and fly larvae *Rhynchosciara* (Ferreira et al., 1981). Osmotically obliged water absorption tends to follow the absorption of ions, such as K^+. The caecae of *C. thummi* (a close relative of *C. riparius*) are ultrastructurally similar to the salivary glands of *Calliphora erythrocephala* (Seidman et al., 1986b), which produce a K^+-rich primary saliva (Oschman and Berridge, 1970). Our study measured secretion of both K^+ and Tl^+ by the caecae (figure 20), consistent with the suggestion of Seidman et al., (1986b) of a role for the caecae in ion

secretion. The same direction of transport of K^+ and Tl^+ raises the possibility that they share a common transport pathway.

However, the caecae are unique compared to the AMG and PMG in that K^+ flux appears to be *unaffected* by any of the experimental treatments (figure 20) or by Tl^+-exposure (figure 21B). Increasing the concentration of Tl^+ in the bathing saline of Tl^+-naïve larvae had no effect on K^+ transport, an unexpected result if K^+ and Tl^+ are using a shared transport mechanism. The simplest explanation is that K^+ and Tl^+ are transported by separate pathways at the caecae. An alternative explanation for the findings is that Tl^+ is transported across the caecae via multiple types of K^+ transporters, some which are more selective for K^+. Surprisingly, neither of the pharmacological blockers (Ba^{2+} or ouabain) exerted an effect on K^+ flux, whereas they both inhibited Tl^+ flux (Figure 20). This unusual result may be explained by simple competition between the three substrates for a shared transporter, since the concentration of K^+ >> ouabain/Ba^{2+} > Tl^+. We suggest that most K^+ is transported at the caecae by Ba^{2+}- and ouabain-insensitive transporters that have a low affinity for Tl^+. In addition, a small proportion of K^+ and the majority of Tl^+ are transported by Ba^{2+}- and ouabain- sensitive pathways that have a relativity high affinity for Tl^+. As a result, Ba^{2+} and ouabain have a measurable effect on Tl^+ flux but not K^+ flux. It is not uncommon for physiologically relevant ion transporters to have a higher affinity for a non-essential metal. This has been demonstrated by Verbost et al., (1989) at the gills of freshwater trout, where a Ca^{2+}-ATPase has a 100-fold higher affinity for Cd^{2+} over Ca^{2+}.

The rundown of Tl^+ absorption (at the caecae) over the course of three scans in Tl^+-exposed larvae (figure 21B) may be caused by a decrease in the concentration gradient since there is very little Tl^+ in the bathing medium (5 µmol l^{-1}) compared to the amount that may be present in the caecae after a 48 hour exposure to 300 µmol l^{-1} Tl^+. Identifying whether the Tl^+ flux is passive (and due to a lumen to hemolymph concentration gradient) could be achieved by the administration of cyanide, an inhibitor of oxidative phosphorylation (Way (1984), and/or by iodoacetate, an inhibitor of glycoylsis (Pirolo and Allen (1986).

The absorption of Tl^+ across the caecae and into the hemolymph (figure 21B) indicates that the gut does not provide a barrier for Tl^+ entry into the hemolymph. Once Tl^+ gains access to the hemolymph, it can exert toxic effects on sensitive tissues, such as the nervous system. Survival of *C. riparius* in the presence of high concentrations of Tl^+ (chapter III) thus implies the presence of efficient mechanisms for detoxification. Possible mechanisms of detoxification are discussed in section 4.7 below.

4.5b Anterior midgut (AMG)

Structural studies by Seidman et al., (1986b) indicate the AMG of *C. thummi* is a mitochondrial rich region involved in active transport, and Cioffi and Harvey (1981) have demonstrated K^+ transport across the anterior midgut in *Manduca sexta*. We found the AMG absorbed K^+ into the hemolymph, however, there was no net transport of Tl^+ (figure 20). We propose that this was an artifact of the experimental set-up in Tl^+-naïve organisms. Since there is no Tl^+ present within the lumen or cells of the AMG in Tl^+-

naïve larvae, when the gut is placed within the bathing medium there is no initial Tl^+ source available to be absorbed. However, given enough time (~45 minutes) there is a small absorption of Tl^+ into the hemolymph (figure 13B, scan 3). The source of this Tl^+ appears to be secretion upstream at the caecae, and from a small amount of bathing saline (containing 5 μmol l^{-1} Tl^+) entering the gut lumen via the opening at the esophagus. This explanation is based on the finding that a large absorption of Tl^+ across the AMG occurs as soon as the gut is opened at the caecae-AMG junction (figure 13C), which allows the bathing medium to freely enter the gut lumen and act as a Tl^+ source. Similarly, when a Tl^+ source is provided in the lumen of the AMG by Tl^+-exposure of larvae prior to dissection (figure 21B), there is a large absorption of Tl^+ across the AMG *without* opening the gut (figure 13C). These findings suggest that the opposite direction of K^+ and Tl^+ flux in Tl^+-naïve larvae reflects the absence of a Tl^+ source in the gut lumen. The K^+ flux across the AMG matches the direction of Tl^+ flux as long as a luminal source of Tl^+ is available, either by opening the gut and allowing Tl^+-containing saline to enter, or by exposing the larvae to Tl^+ in the water prior to dissection. In addition, we found that increasing the concentration of Tl^+ in the bathing saline (to 50 μmol l^{-1}) causes K^+ flux to decline (figure 20). Taken together with the finding that the stable rate of K^+ absorption seen in Tl^+-naïve larvae (figure 21A) was inhibited by >95% in Tl^+-exposed larvae (figure 21B), these findings suggest competition between K^+ and Tl^+ across the AMG.

4.5c Posterior midgut (PMG)

Ba^{2+}-sensistive K^+ secretion (transport towards the lumen) has been observed at the PMG in *Manduca sexta* (Zeiske et al., 1986; Moffet and Koch, 1988), and is driven by H^+-VATPases on the luminal membrane (Harvey, 2009). Our findings of Ba^{2+}-sensitive K^+ secretion at the PMG in *C. riparius* (figure 20) are consistent with the latter studies. Tl^+ was also secreted at the PMG in Tl^+-naïve larvae, although this secretion declined to zero over ~60 minutes (figure 21A). The rundown of Tl^+ flux is thought to be caused by a decrease in the concentration gradient (from hemolymph to lumen) for Tl^+ as the cells and lumen of the PMG accumulate Tl^+. The use of cyanide and/or iodoacetate would help to confirm whether this is passive transport.

The PMG has been implicated in the sequestration of Cd^{2+} by Seidman et al., (1986a), who used radiolabeled Cd^{2+} to determine regions of Cd^{2+} accumulation in *C. thummi*. Leonard et al., (2009) also found that the PMG of *C. riparius* can sequester Cd^{2+}, as evidenced by the finding that Cd^{2+} is secreted into the cells across both the apical and basolateral membranes. However, we cannot make the same claim for Tl^+ due to the rundown of Tl^+ secretion at the basolateral surface, and the absence of flux measurements at the apical membrane. Due to the decrease in Tl^+ flux over time, it was not possible to identify what effect, if any, Ba^{2+} had on Tl^+ transport.

The same directions of transport of both K^+ and Tl^+ ions across the PMG, and the suppression of K^+ flux by increasing Tl^+ in the bathing saline (to 50 μmol l^{-1}) in Tl^+-naïve larvae (figure 20) suggests an interaction between K^+ and Tl^+ ions. The finding that K^+ secretion decreases with time in larvae exposed to waterborne Tl^+ (figure 21B), while the

secretion remains stable in unexposed larvae (figure 21A) further suggests an interaction between K^+ and Tl^+ at the PMG.

Our findings implicate the PMG as another gut region where K^+ and Tl^+ interaction occurs. We interpret the results as follows: the PMG is a site of continuous Tl^+ access into the hemolymph in Tl^+-exposed larvae (figure 21B). This continuous Tl^+ flux increases Tl^+ concentrations in the unstirred layer on the basolateral surface, where the Tl^+ inhibits K^+ secretion. It is possible that Tl^+ interferes with K^+ transport across the basolateral surface of the PMG directly, by using K^+ channels to exit the cell and enter the hemolymph, thus preventing K^+ transport from hemolymph into the cell. This is proposed based on two pieces of evidence. First, our finding that K^+ transport was Ba^{2+}-sensitive, indicating that K^+-channels play a role in K^+ secretion at the PMG, and second, that Tl^+ transport by the KcsA K^+ channel has been directly observed by x-ray crystallography (Zhou and MacKinnon, 2003).

4.6 Net K^+ and Tl^+ transport by guts of Tl^+-naïve and Tl^+-exposed C. riparius *larvae*

4.6a Net K^+ transport by Tl^+-naïve larvae

In Tl^+-naïve organisms, a net absorption of K^+ was observed (figure 20 and 21A). If this absorption remained stable over one day, it would equal ~80 times total hemolymph K^+ (Leonard et al., 2009), or ~3.5 times total body K^+ (Chapter III). Thus, uptake is sufficient to exchange total body K^+ in approximately 7 hours. One caveat is that transport was measured in isolated guts in saline and in the absence of hemolymph factors such as neuropeptides, which may alter the rate of K^+ transport *in vivo*

The net K^+ absorption may be important for *C. riparius* larvae which are continually growing until they moult into adults. A similar condition is seen for caterpillars, which grow rapidly. The diet of caterpillars is mainly leaves, and thus K^+ rich. The excess K^+ is coupled to nutrient absorption (Harvey, 2009). The diet of *C. riparius* is more variable and depends on the environment, but gut contents have been shown to most frequently contain detritus (Pinder, 1986), which contain moderate amounts of K^+ (Fahey, 1983). This excess K^+ may also be coupled to nutrient absorption in Tl^+-naïve *C. riparius* larvae.

4.6b Net Tl^+ transport by Tl^+-naïve larvae

The net Tl^+ secretion observed in Tl^+-naïve larvae (figure 20 and 21A) may demonstrate secretion as a method of detoxification at low exposure concentrations. Leonard et al., (2009) has reported that secretion is the dominant form of detoxification for Cd^{2+} at low exposure concentrations. However, it may also reflect an artifact of the experimental set-up. Net Tl^+ transport towards the lumen is likely to occur due to concentration gradients (zero Tl^+ in the gut lumen and 5 μmol l^{-1} in the bathing medium), and a lack of absorption due to the absence of a Tl^+ source within the gut. Exposing the larvae to low Tl^+ concentrations prior to flux measurements would provide a better estimate for the role of the gut in Tl^+ tolerance.

4.6c Net K^+ and Tl^+ transport by Tl^+-exposed larvae

A very different pattern of net K^+ and Tl^+ transport emerges in Tl^+-exposed larvae. Net K^+ transport is reversed in Tl^+-exposed larvae, and becomes a net K^+ loss (figure 21B), which would cause *C. riparius* to lose total hemolymph K^+ after ~40 minutes (Leonard et al., 2009), and total body K^+ after ~12 hours (chapter III). This is in conjunction with a net Tl^+ absorption, which would result in Tl^+ concentration in the hemolymph being equal to that of the exposure medium (300 μmol l^{-1}) after ~2 hours if net absorption was sustained. The reversal of K^+ transport in Tl^+-exposed larvae suggests an interaction of the two ions at the level of the gut. Our results suggest that interference with K^+ transport and subsequent effects on hemolymph ion homeostasis may contribute to Tl^+ toxicity. It should be noted that waterborne exposures to 300 μmol l^{-1} Tl^+ would not be encountered in even the mot Tl^+-contaminated sites in Canada.

4.7 Suggested mechanisms of Tl^+ detoxification in Tl^+-exposed C. riparius *larvae*

The net absorption of Tl^+ requires detoxification for survival. Mechanisms of detoxification of Tl^+ may include the formation of inert Tl^+-containing compounds. This may include the binding of Tl^+ to sulphur rich proteins, such as metallothionein. This is supported by research showing metallothionein can lessen the Tl^+-induced oxidative stress in rat livers (Kılıç and Kutlu, 2010), and that metallothionein is present within *C. riparius* larvae and increases in response to exposure to increased concentrations of toxic metals, such as Cd^{2+} (Gillis et al., 2002; Fabrik et al., 2008). It has also been shown that the hemoglobin present in the hemolymph can play a passive role in detoxification by

providing supplies of oxygen to accelerate metabolic secretion (Osmulski and Leyko, 1986).

C. riparius larvae are quite tolerant towards Tl^+ compared to other organisms (chapter I), although the mechanism of this tolerance is not well understood. Tolerance may be similar to detoxification strategies employed for divalent toxic metals like Cd^{2+}, which rely more heavily on sequestration at higher concentrations and secretion at lower concentrations. We have examined secretion of Tl^+, but not sequestration within tissues such as the gut. Future studies looking at the role of the gut in sequestration at various exposure concentrations would be helpful in identifying the detoxification strategy. A more careful examination of a role by the anal papillae in toxic metal secretion/sequestration would also help in understating how *C. riparius* larvae are able to tolerate high levels of Tl^+.

References

Achard, M., Baudrimont, M., Boudou, A., and J.P. Bourdineaud. Induction of multixenobiotic resistance protein (MXR) in the Asiatic clam *Corbicula fluminea* after heavy metal exposure. *Aquat. Toxic.* **67** (2004), pp. 347-357.

Alagem, N., Dvir, M., and E. Reuveny. Mechanism of Ba^{2+} block of a mouse inward rectifying K^+ channel: differential contribution by two discrete residues. *J. Physiol.* **534.2** (2001), pp. 381-393.

Armstrong, C.M. and S.R. Taylor. Interaction of Barium Ions With Potassium Channels in Squid Giant Axons. *Biophys. J.* **30** (1980), pp. 473-488.

Boudker, O., Ryan, R.M., Yernool, D., Shumamoto, K., and E. Gouaux. Coupling substrate and ion binding to extracellular gate of a sodium-dependant aspartate transporter. *Nature* **445** (2007), pp. 387-393.

Béchard, K.M., Gillis, P.L., and C.M. Wood. Acute toxicity of waterborne Cd, Cu, Pb, Ni, and Zn to first-instar *Chironomus riparius* larvae. *Arch. Environ. Contam. Toxicol.* **54** (2008), pp. 454-459.

Callaghan, L., and N. Denny. Evidence for an interaction between p-glycoprotein and cadmium toxicity in cadmium-resistant and –susceptible strains of Drosophila melanogaster. *Ecotoxicol. Environ Saf.* **52** (2002), pp. 211-213.

Cheam, V. Thallium contamination of water in Canada. *Water Qual. Res. J. Canada* **36** (2001), pp. 851-877.

Cioffi, M., and W.R. Harvey. Comparison of Potassium Transport in Three Structurally Distinct Regions of the Insect Midgut. *J. of Expt. Biol.* **91** (1981), pp. 103-116.

Craig, A., Hare, L., and A. Tessier. Experimental evidence for cadmium uptake via calcium channels in the aquatic insect *Chironomus staegeri*. *Aquat. Toxic.* **4** (1999), pp. 255-262.

Credland, P.F. An Ultrastructural study of the anal papillae of the midge, *Chironomus riparius* meigen (Diptera: Chironomidae). *Cell and Tiss. Resear.* **166** (1976), pp. 531-540.

Credland, P.F. An Ultrastructural study of the larval integuement of the midge, *Chironomus riparius* meigen (Diptera: Chironomidae). *Cell and Tiss. Resear.* **186** (1978), pp. 327-335.

Donini, A., O'Donnell, M.J.Analysis of Na^+, Cl^-, K^+, H^+ and NH_4^+ concentration gradients adjacent to the surface of the anal papillae of the mosquito *Aedes*

aegypti: application of self-referencing ion-selective microelectrodes. *J. Exp. Biol.* **208** (2005), pp. 603-610.

Dow, J.A.T. Counter current flows, water movements, and nutrient absorption in the locust midgut. *J. Insect Physio.* **27** (1981), pp. 579-585.

Fabrik, I., Ruferova, Z., Hilscherova, K., Adam, V., Trnkova, L and R. Kizek. A determination of metallothionein in larvae of freshwater midges (*Chironomus riparius)* using Brdicka reaction. *Sensors*. **8** (2008), pp. 4081-4094.

Fahey, T.J. Nutrient dynamics of above ground detritus in lodgepole pine (*Pinus contorta ssp. Latifolia*) ecosystems, southeastern Wyoming. *Ecological Monographs.* **53** (1983), pp. 51-72.

Ferreira, C., Ribeiro, A.F., and W.R. Terra. Fine structure of the larval midgut of the fly *Rhynchosciara* and its physiological implications. *J. Insect. Physio.* **27** (1981), pp. 559-570.

Gillis, P.L., Diener, L.C., Reynoldson, T.B., and D.G. Dixon. Cadmium induced production of a metallothionein-like protein in *Tubifex tubifex* (Oligochaeta) and *Chironomus riparius* (Diptera): correlation with whole body (reproduction and

growth) endpoints of toxicity. *Environ. Toxicol. Chem.*, **21** (2002), pp. 1836–1844.

Gillis, P., and C.Wood. Investigating a potential mechanism of Cd resistance in *Chironomus riparius* larvae using kinetic analysis of calcium and cadmium uptake. *Aqua. Toxicol.* **3** (2008a), pp.180-187.

Gillis, P., and C.Wood. The effect of extreme waterborne cadmium exposure on the internal concentrations of cadmium, calcium and sodium in *Chironomus riparius* larvae. *Aqua. Toxicol.* **1** (2008b), pp. 56-64.

Hamilton, S.J. and P.M. Mehrle. Metallothionein in Fish: Review of Its Importance in Assessing Stress from Metal Contaminants. *Transactions of the American Fisheries Society*. **115**, (1986), pp. 596-609

Harskamp, J.G., O'Donnell, M.J., and E.Berkelaar. Determining the fluxes of Tl^+ and K^+ at the root surface of wheat canola using Tl(I) and K ion-selective microelectrodes. *Plant and Soil*. **335** (2010), pp. 299-310.

Harvey, W.R. Voltage coupling of H^+ V-ATPases to secondary Na^+- or K^+ -dependant transporters. *J. of Exp. Biol.* **212** (2009), pp. 1620-1629.

Harvey, W.R., Cioffi, M., Dow, J.A. and M.G. Wolfersberger. Potassium Ion Transport in Insect Epithelia. *J. Exp. Biol.* **106** (1983), pp. 91-117.

Hibino, H., Inanobe, A., Furutani, K., Murakami, S., Findlay, I., and Y. Kurachi. Inwardly Rectifying Potassium Channels: Their Structure, Function, and Physiological Roles. *Physiol. Rev.* **90** (2010), pp. 291-366.

Jones, J.C., and V.H. Zeve. The fine structure of the gastric caecae of Aedes aegypti larvae. *J. Insect Physio.* **14** (1968), pp. 1567-1575.

Kazantzis, G. Thallium in the environment and health effects. *Envir. Geochem. and Heal.* **22** (2000) pp. 275-280.

Kılıç, G.A., and M. Kutlu. Effects of exogenous metallothionein against thallium-induced oxidative stress in rat liver. *Food and Chem. Toxic.* 48 (2010), pp. 980-987.

Krantzberg, G., and P.M. Stokes. Metal concentrations and tissue distributions in larvae of *Chironomus* with reference to X-ray microprobe analysis. *Arch. Environ. Contam. Toxicol.* **19** (1990), pp. 84-93.

LeBlanc, G.A. Acute toxicity of priority pollutants to water flea (*Daphnia magna*). *Bull. Environ. Contam. Toxicol.* **24** (1980), pp. 684-691.

Leonard, EM., Pierce, L.M., Gillis, P.M., Wood, C.M. and M.J. O'Donnell. Cadmium transport by the gut and Malpighian tubules of *Chironomus riparius. Aquat. Toxic*. **92** (2009), pp.179-186.

Lide, D.R. CRC handbook of chemistry and physics, 3rd edn. (2002) CRC, Boca Raton.

Liu, J., Chen, H., Miller, D., Saavedra, J.E., Keefer, L.K., Johnson , D.R., Klaassen, C.D., and M.P. Waalkes. Overexpression of glutathione S-trasnferease II and multidrug resistance transport proteins associated with acquired tolerance to inorganic arsenic. *Molec. Pharm.* **60** (2001), pp. 302-309.

Moffett, D.F., and A.R. Koch. Electrophysiology of K+ transport by midgut epithelium of Lepidopteran insect larvae: the transbasal electrochemical gradient. *J. Exp. Biol.* **135** (1988), pp. 25-38.

Mohlenberg, F., and T. Kiorboe. Burrowing and avoidance behaviour in marine organisms exposed to pesticide-contaminated sediment. *Mari. Pollu. Bulle.* **14** (1983), pp. 57-60.

Ngyuen, H. and Donini, A. Larvae of the midge *Chironomus riparius* possess to distinct mechanisms for ionoregulation in response to ion-poor conditions. *American Journal of Physiology.* **299** (2010), pp. 762-773.

Nriagu, J.O. Thallium in the environment. Wiley Series in Advances in Environment Sceience and Technology, 29 (1998) John Wiley and Sons.

O'Donnell, M.J. Insect excretory mechanisms. *Adv. In Insec. Physio.* **35** (2008), pp. 1-122.

Olla, B.L., Studholme, A.L., and W.H. Pearson. Applicability of behavioural measures in environmental stress assessment. *Rapp. P-v. Réun. Int. Explor. Mer.* **197** (1980), pp. 162-173.

Oschmann, J.L. and M.J. Berridge. Structural and functional aspects of salivary fluid secretion in *Calliphora*. *Tiss. And cell.* **2** (1970), pp. 281-310.

Osmulski, P.A., and W. Leyko. Structure, function and physiological role chironomus haemoglobin. *Comp. Biochem. Physiol.* **4** (1986), pp. 701-722.

Peter, J.A.L. and T. Viraraghavan. Thallium: a review of public health and environmental concerns. *Environ. Int.* **31** (2005), pp. 493-501

Pickard, J., Yang, R., Duncan, B., McDevitt, C.A., and C. Eickhoff. Acute and sublethal toxicity of thallium to aquatic organisms. *Bull. Environ. Contam. Toxicol.* **66** (2001), pp. 94-101.

Pinder, L.C.V. Biology of freshwater chironomidae. *Ann. Rev. Entomol.* **31** (1986), pp. 1-23.

Pinder, L.C.V. The habitats of chironomid larvae. In: *The Chironomidae Biology and Ecology of Non-biting Midges*, edited by Armitage P.D., Cranston P.S., and L.C.V. Pinder. London: Chapman and Hall, 1995. pp. 107-135.

Pirolom J.S. and D.G. Allen. Assesement of techniques for preventing glycolysis in cardiac muscle. *Cardiovasc. Res.* **20** (1986), pp. 837-844.

Podsiadlowski, L., Matha, V., and A. Vilcinskas. Detection of a p-glycoprotein related pump in *Chironomus* larvae and its inhibition by verapamil and cyclosporine A. *Comp. Biochem. And Physiol. Part B: Biochem. And Molec.Biol.* **121** (1998), pp. 443-450.

Rheault, M.R., O'Donnell, M.J. Analysis of epithelial K^+ transport in Malpighian tubules of *Drosophila melanogaster*: evidence for spatial and temporal heterogeneity. *J. Exp. Biol.* **204** (2001), pp. 2289-2299.

Rheault, M.R., O'Donnell, M.J., Organic cation transport by *Drosophila melanogaster*: application of two novel electrophysiological methods. *J. Exp. Biol*. **207** (2004), pp. 2173-2184.

Seidman, L.A., Bergtrom, G., Gingrich, D.J., and C.C. Ramsen. Accumulation of cadmium by the fourth instar larva of the fly *Chironomus thummi*. **18** (1986a), pp. 395-405.

Seidman, L.A., Bergtrom, G., and C.C. Remsen. Structure of the larval midgut of the fly *Chironomus thummi* and its relationship to sites of cadmium sequestration. *Tissue and Cell.* 18 (1986b), pp. 407-418.

Siegel, B.Z. and S.M. Siegel. Effect of potassium on thallium toxicity in cucumber seedlings: further evidence for potassium-thallium ion antagonism. *Bioinorganic Chem*. **6** (1976), 341-345.

Verbrost, P.M., Rooij, J.V., Flik, G., Lock, R.A.C., and S.E. Wendelaar Bonga. The movement of cadmium through freshwater trout brachial epithelium and its interference with calcium transport. *J. Exp. Biol.* **145** (1989), pp. 185-197

Way, J.L. Cynaide intoxication and its mechanism of antagonism. *Ann. Rev. Pharmacol. Toxicol.* **24** (1984), pp. 451-481.Wigglesworth, V.B. Transpiration through the cuticle of insects. *J. Exp. Biol.* **21** (1945), pp. 97-114.

Zeiske, W., Driessche, W., and R. Ziegler. Current-noise analysis of the basolateral route for K^+ ions across a K^+-secreting insect midgut epithelium. *Europ. J. Physiol.* **407** (1986), pp. 657-663.

Zhou, Y. and R. MacKinnon. The occupancy of ions in the K^+ selectivity filter: charge balance and coupling of ion binding to a protein conformational change underlie high conductance rates. *J. Mol. Biol.* **333** (2003), pp. 965-975.

Zitko, V., Carson, W.V., and W.G Carson. Thallium: Occurrence in the environment and Toxicity to Fish. *Bull. Of Envir. Contam. and Tox.* **13** (1975), pp. 23-30.

Figure 1: Light-microscope image (25x) of the gut tract and MTs of a 4th instar *C. riparius* larvae. The anterior is the leftmost side, beginning at the esophagus.

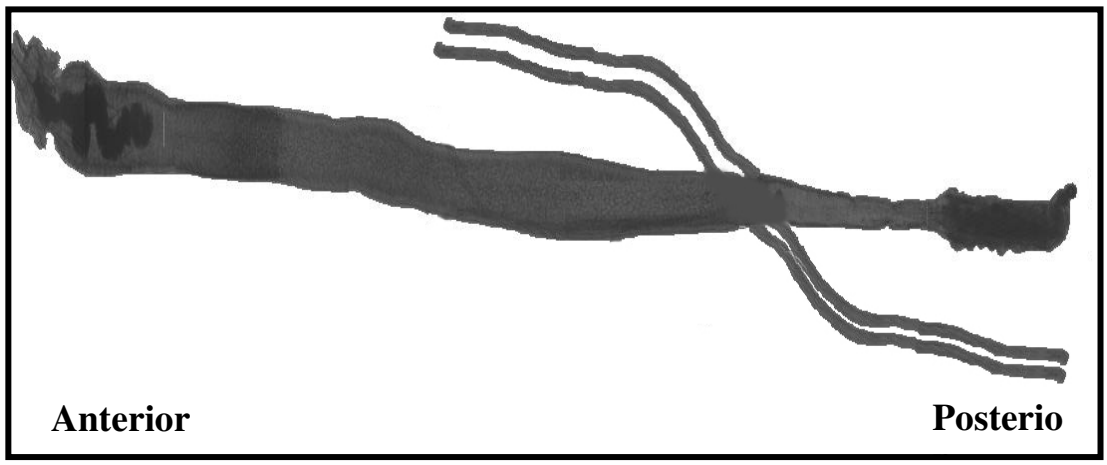
Anterior
Posterio

Figure 2. Light-microscope images (40X) of the gut segments and Malpighian tubules of a 4th instar *C. riparius* larvae. ESO = esophagus, CAE = caecae, AMG = anterior midgut, PMG = posterior midgut, ILE = ileum, LMT = lower Malpighian tubule, MMT = middle Malpighian tubule, DMT = distal Malpighian tubule, AR = anterior rectum, PR = posterior rectum.

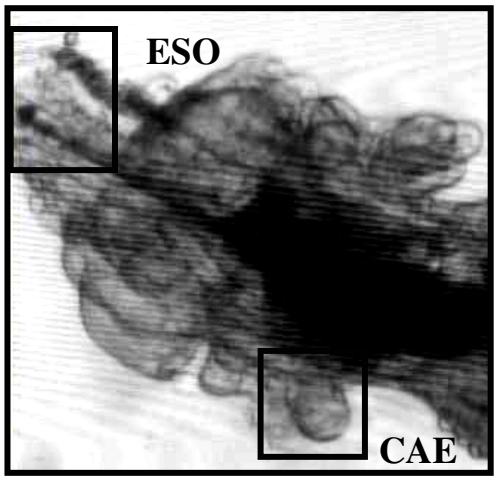

A

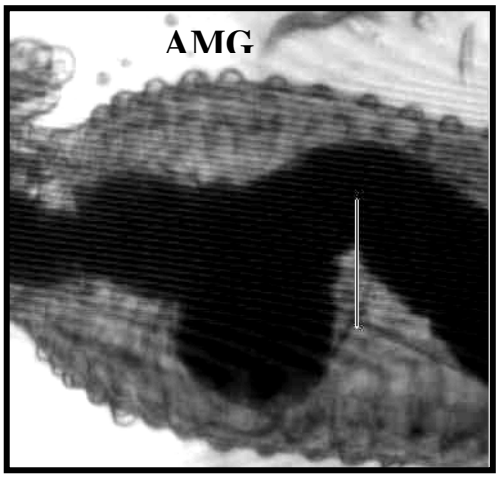

B

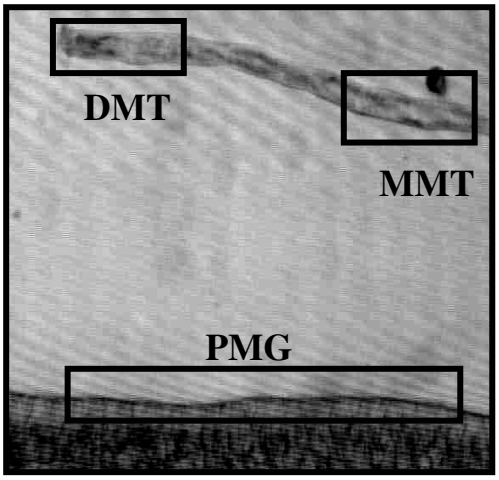

C

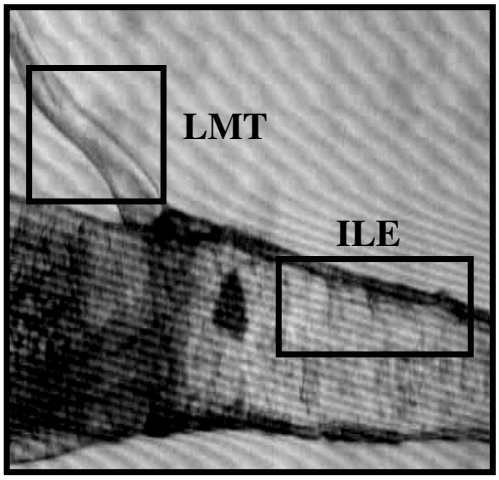

D

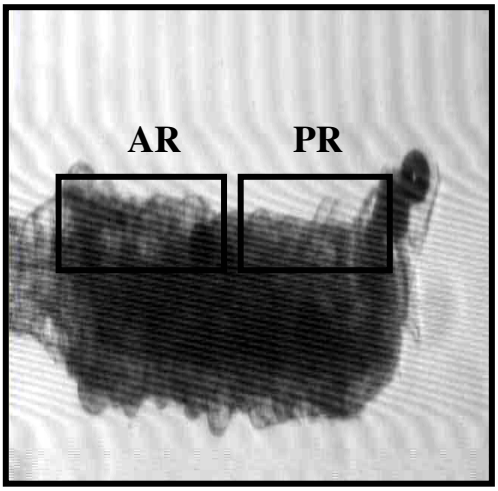

E

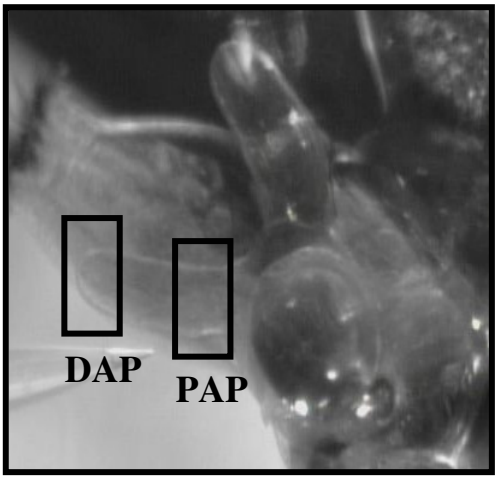

F

Figure 3. Light-microscope images (40x) of the (A) one-ISME holder and (B) two-ISME holder.

A

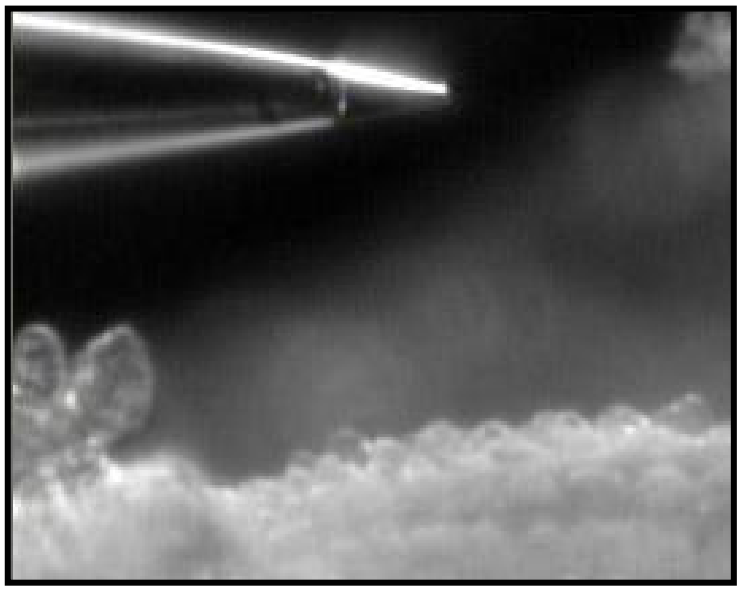

B

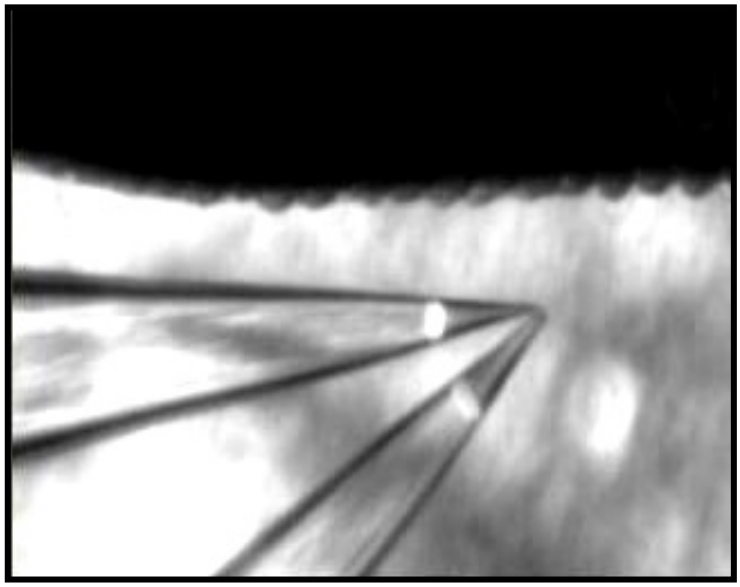

Figure 4. SIET measurements of ion (K^+ and Tl^+) fluxes along the gut and MTs of *C. riparius* larvae. Negative fluxes denote movement of the ion from bathing medium to gut lumen, whereas positive values denote movement from gut lumen to bathing medium. A flux of zero was interpreted when the SEM of the mean overlapped with zero. Bars are means ± SEM. (A) K^+ fluxes (pmol $cm^{-2}s^{-1}$) in Tl^+-naïve larvae. N = 5-24 per each tissue segment. (B) K^+ fluxes (fmol s^{-1}) in Tl^+-naïve larvae, corrected for surface area of the corresponding tissue segment. Net K^+ transport by the entire gut and MTs is the sum of the fluxes for each tissue segment, shown on the right as the gray bar. N = 5-24 per each tissue segment. (C) Tl^+ fluxes (pmol $cm^{-2}s^{-1}$) in Tl^+-naïve larvae. N = 5-24 per each tissue segment. (D) Tl^+ fluxes (fmol s^{-1}) in Tl^+-naïve larvae, corrected for surface area of the corresponding tissue segment. Net Tl^+ transport by the entire gut and MTs is the sum of the fluxes, shown on the right as the gray bar. N = 5-10 for ESO, LMT, MMT, DMT, AR and PR. N= 18-24 for CAE, AMG and PMG.

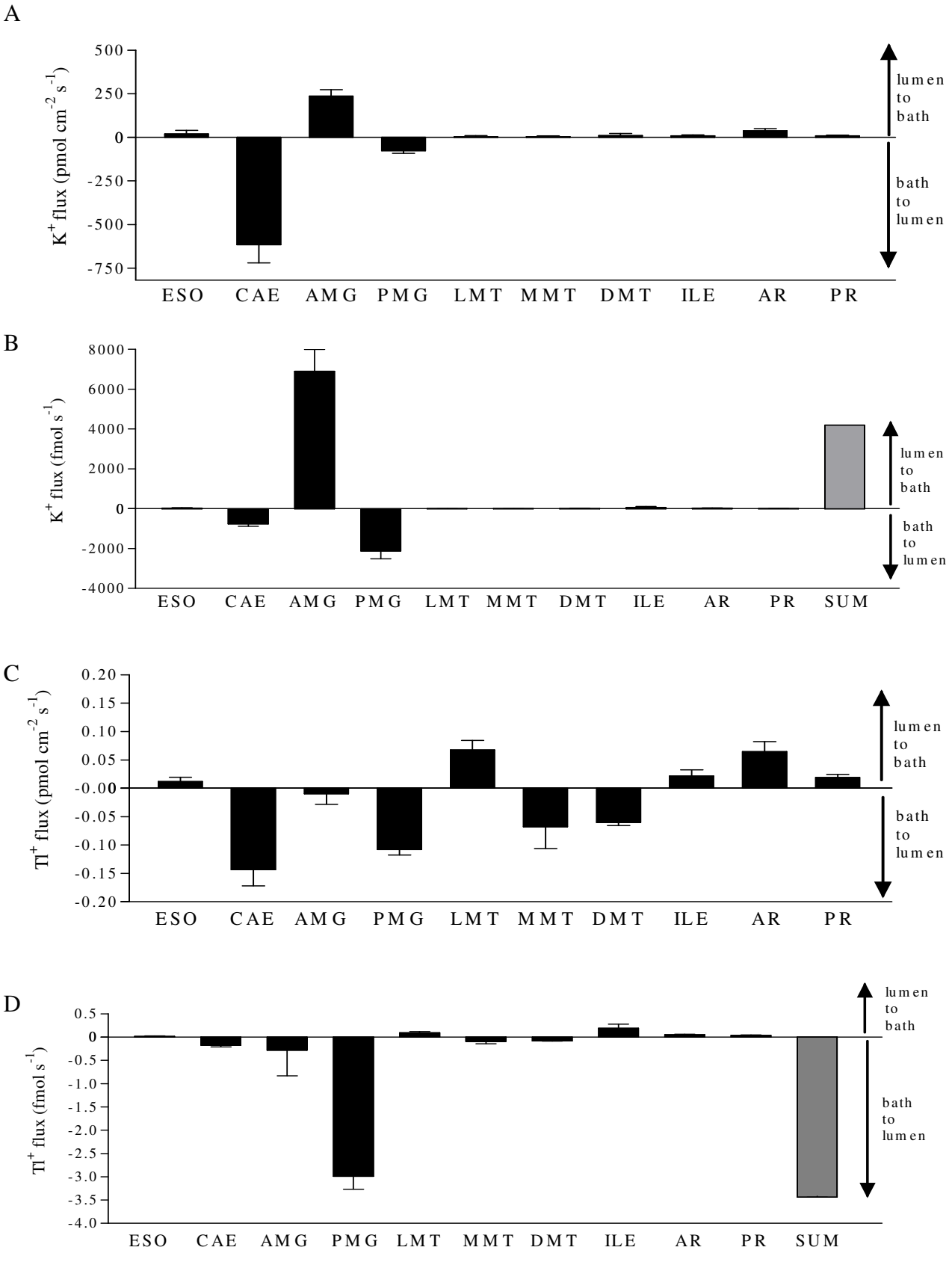
A
500
250
0
-250
-500
-750
K+ flux (pmol cm-2 s-1)
lumen to bath
bath to lumen
ESO CAE AMG PMG LMT MMT DMT ILE AR PR
B
8000
6000
4000
2000
0
-2000
-4000
K+ flux (fmol s-1)
lumen to bath
bath to lumen
ESO CAE AMG PMG LMT MMT DMT ILE AR PR SUM
C
0.20
0.15
0.10
0.05
0.00
-0.05
-0.10
-0.15
-0.20
Tl+ flux (pmol cm-2 s-1)
lumen to bath
bath to lumen
ESO CAE AMG PMG LMT MMT DMT ILE AR PR
D
0.5
0
-0.5
-1.0
-1.5
-2.0
-2.5
-3.0
-3.5
-4.0
Tl+ flux (fmol s-1)
lumen to bath
bath to lumen
ESO CAE AMG PMG LMT MMT DMT ILE AR PR SUM

Figure 5. SIET measurement of ion flux at the distal and proximal anal papillae (AP) and abdominal cuticle of Tl^+-naïve *C. riparius* larvae. Bars are means ± SEM. Statistical analysis was performed by one-way ANOVA with Tukey's and Bonferroni's post-hoc test if $p<0.05$. Bars sharing the same letter are not statistically different from each other. (A) K^+ flux. (B) Tl^+ flux

A

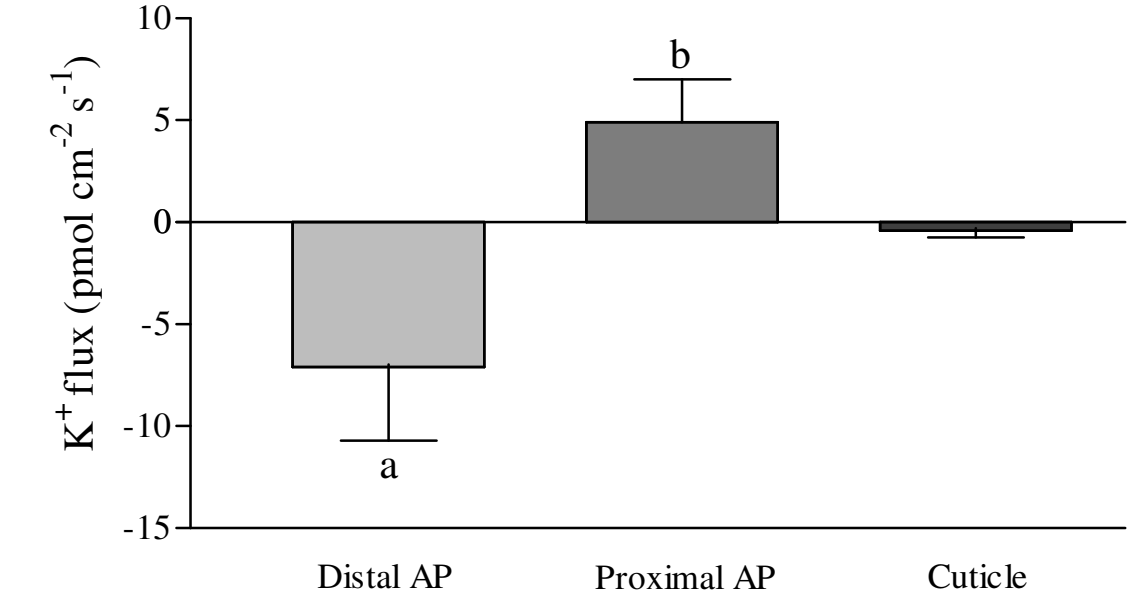
10
5
0
-5
-10
-15
K+ flux (pmol cm-2 s-1)
b
a
Distal AP
Proximal AP
Cuticle

B

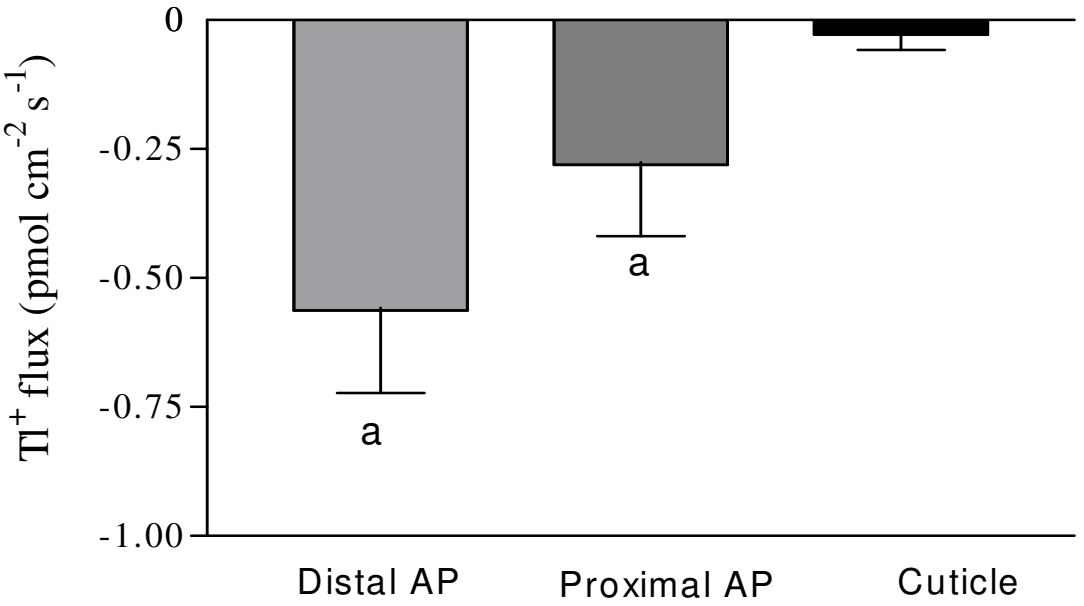
0
-0.25
-0.50
-0.75
-1.00
Tl+ flux (pmol cm-2 s-1)
a
a
Distal AP
Proximal AP
Cuticle

Figure 6. The effect of 48 hour exposure to 300 μM Tl^+ on ion flux at the caecae of *C. riparius*. Bars are means ± SEM. N = 5. Statistical analysis was performed by repeated measures ANOVA with Tukey's and Bonferroni's post-hoc test if $p<0.05$. Bars sharing the same letter are not statistically different from each other. (A) K^+ flux. (B) Tl^+ flux.

A

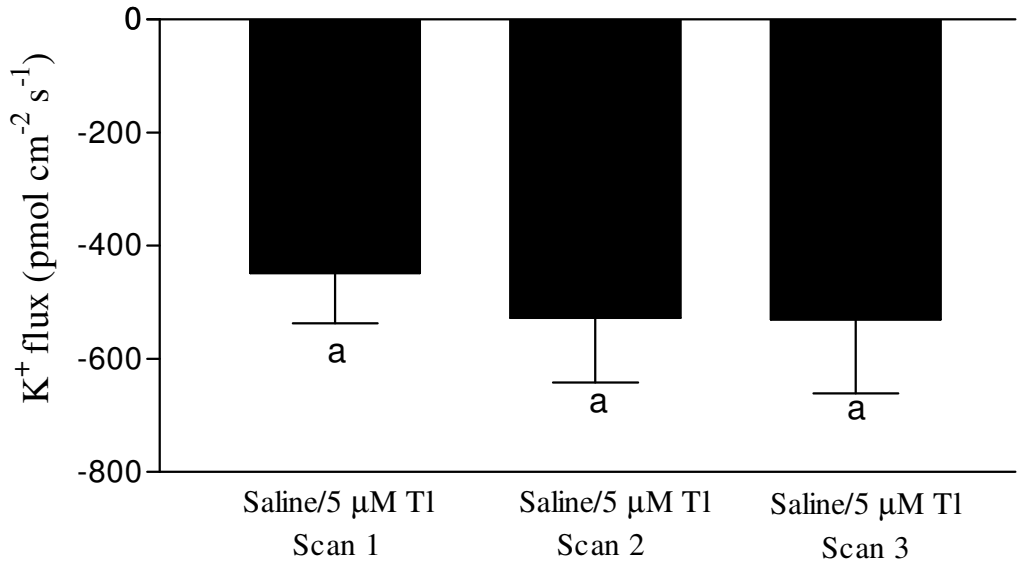
0
-200
-400
-600
-800
K+ flux (pmol cm-2 s-1)
a
a
a
Saline/5 µM Tl
Scan 1
Saline/5 µM Tl
Scan 2
Saline/5 µM Tl
Scan 3

B

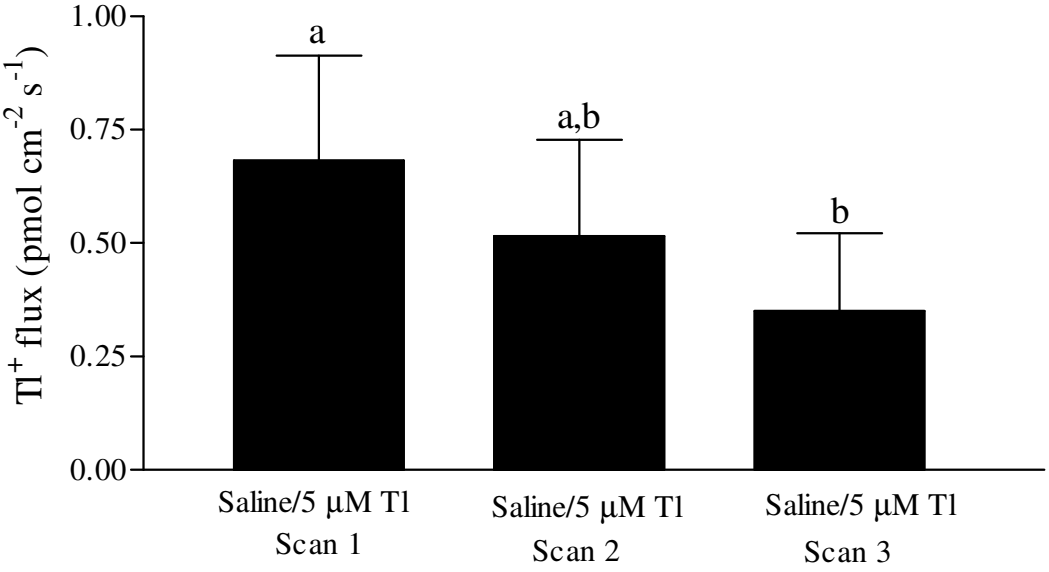
1.00
0.75
0.50
0.25
0.00
Tl+ flux (pmol cm-2 s-1)
a
a,b
b
Saline/5 µM Tl
Scan 1
Saline/5 µM Tl
Scan 2
Saline/5 µM Tl
Scan 3

Figure 7. SIET measurement of ion flux at the caecae of Tl^+-naïve *C. riparius* larvae over ~60 minutes; controls for the effects of time and changing solutions between scans. Bars are means ± SEM. Statistical analysis was performed by repeated measures ANOVA with Tukey's and Bonferroni's post-hoc test if $p<0.05$. (A) K^+ flux. N = 4. (B) Tl^+ flux. N = 6.

A

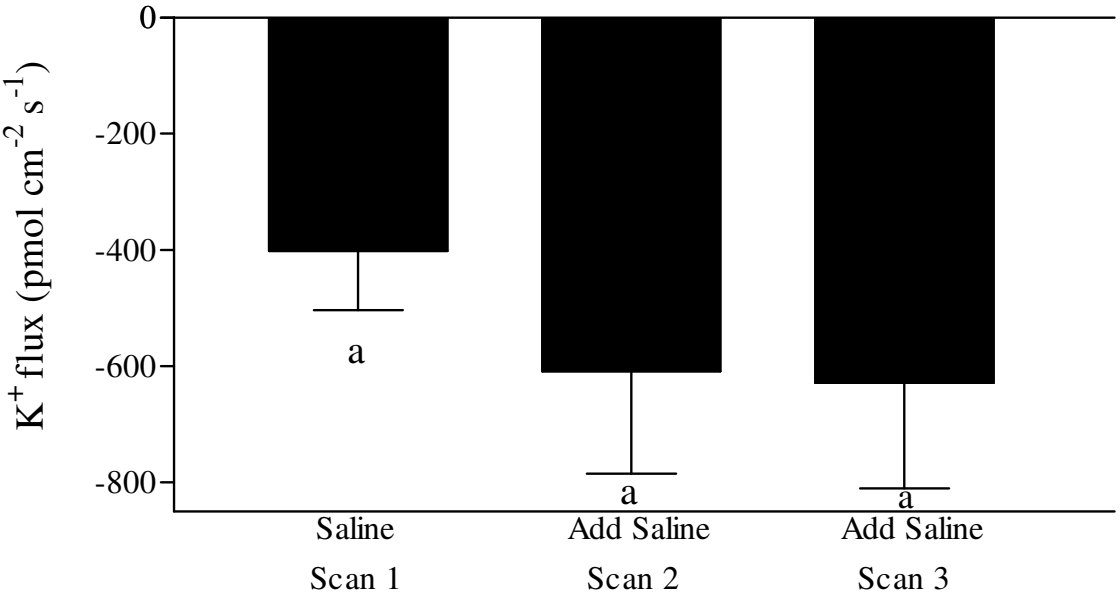
0
-200
-400
-600
-800
K+ flux (pmol cm-2 s-1)
a
a
a
Saline
Scan 1
Add Saline
Scan 2
Add Saline
Scan 3

B

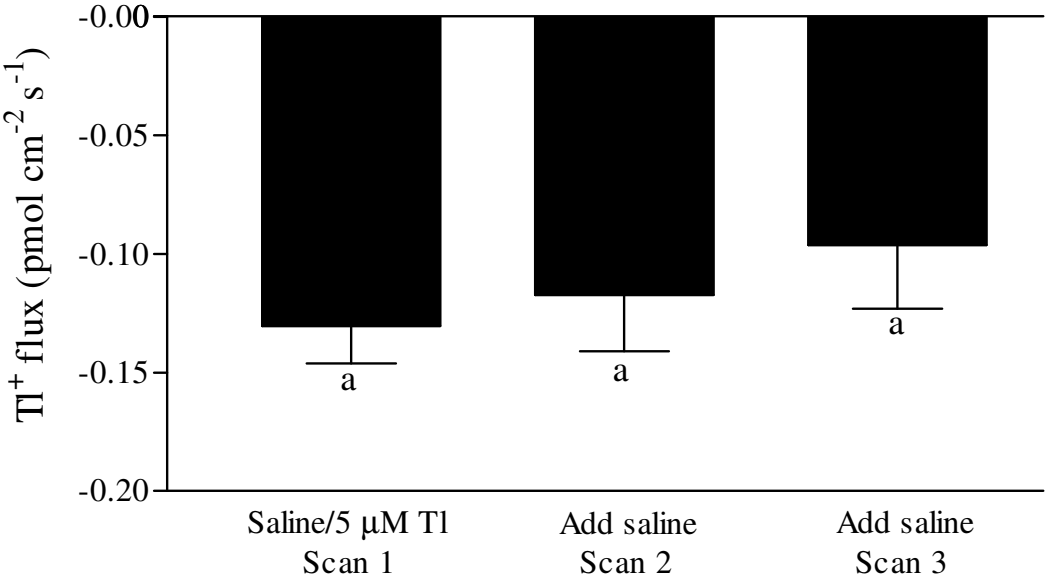
-0.00
-0.05
-0.10
-0.15
-0.20
Tl+ flux (pmol cm-2 s-1)
a
a
a
Saline/5 µM Tl
Scan 1
Add saline
Scan 2
Add saline
Scan 3

Figure 8. The effect of 5 and 50 μM Tl^+ on K^+ flux at the caecae of Tl^+-naïve *C. riparius* larvae. Bars are means ± SEM. N = 5. Statistical analysis was performed by repeated measures ANOVA with Tukey's and Bonferroni's post-hoc test if $p<0.05$.

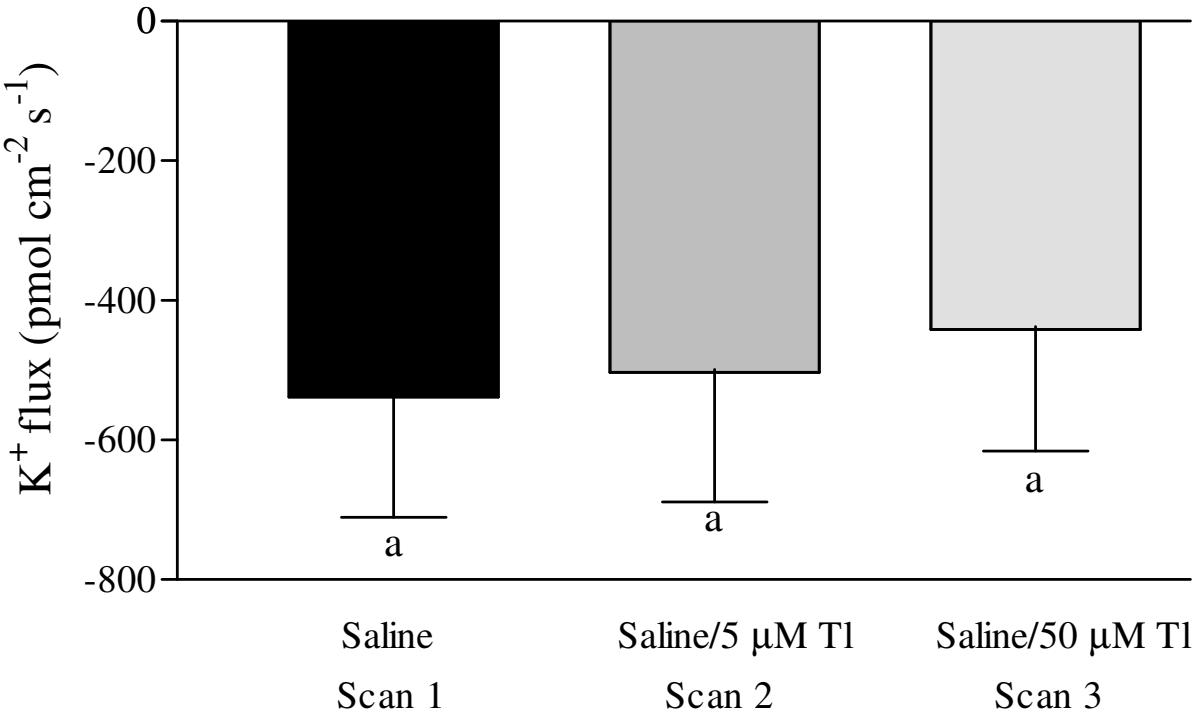
0
-200
-400
-600
-800
K+ flux (pmol cm-2 s-1)
a
a
a
Saline
Scan 1
Saline/5 µM Tl
Scan 2
Saline/50 µM Tl
Scan 3

Figure 9. The effect of 2 mmol l^{-1} Ba^{2+} on ion flux at the caecae of Tl^{+}-naïve *C. riparius* larvae. Bars are means ± SEM. N = 5. Statistical analysis was performed by repeated measures ANOVA with Tukey's and Bonferroni's post-hoc test if $p<0.05$. Bars sharing the same letter are not statistically different from each other. (A) Effect of Ba^{2+} on K^{+} flux. (B) Effect of Ba^{2+} on Tl^{+} flux

A

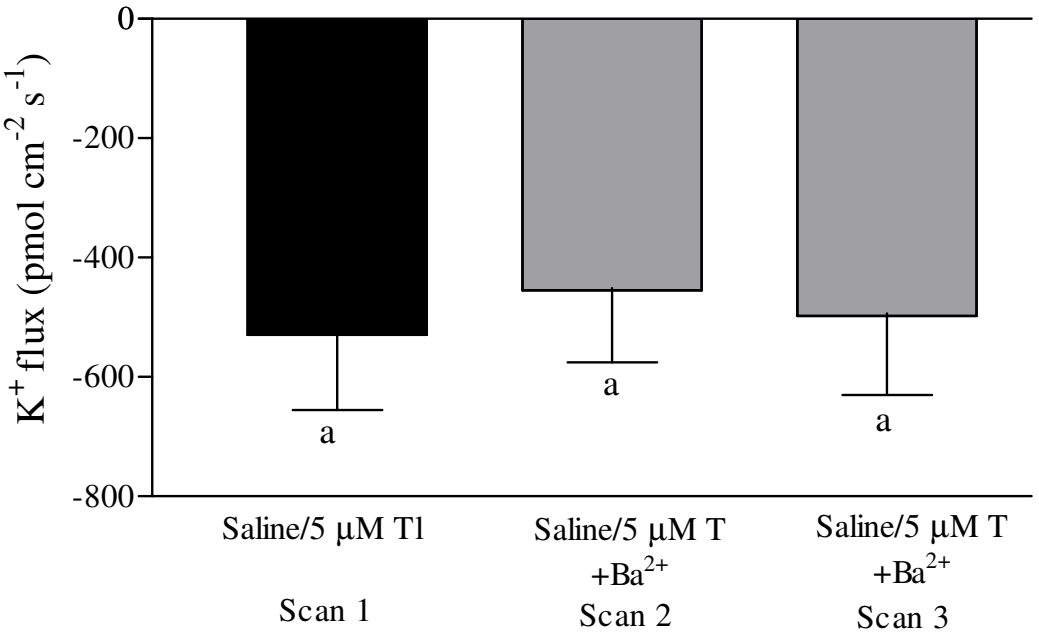
0
-200
-400
-600
-800
K+ flux (pmol cm-2 s-1)
a
a
a
Saline/5 µM Tl
Scan 1
Saline/5 µM T
+Ba2+
Scan 2
Saline/5 µM T
+Ba2+
Scan 3

B

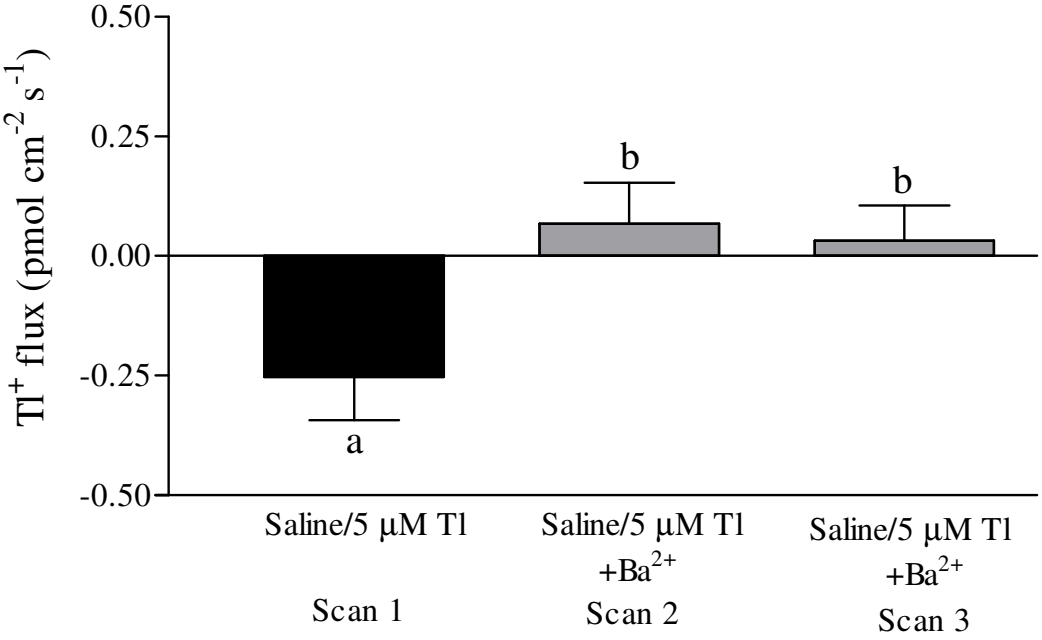
0.50
0.25
0.00
-0.25
-0.50
Tl+ flux (pmol cm-2 s-1)
a
b
b
Saline/5 µM Tl
Scan 1
Saline/5 µM Tl
+Ba2+
Scan 2
Saline/5 µM Tl
+Ba2+
Scan 3

Figure 10. The effect of 0.2% DMSO (the vehicle for ouabain) on ion flux at the caecae of Tl^+-naïve *C. riparius* larvae. Bars are means ± SEM. N = 5. Statistical analysis was performed by repeated measures ANOVA with Tukey's and Bonferroni's post-hoc test if $p<0.05$. (A) Effect of DMSO on K^+ flux. (B) Effect of DMSO on Tl^+ flux.

A

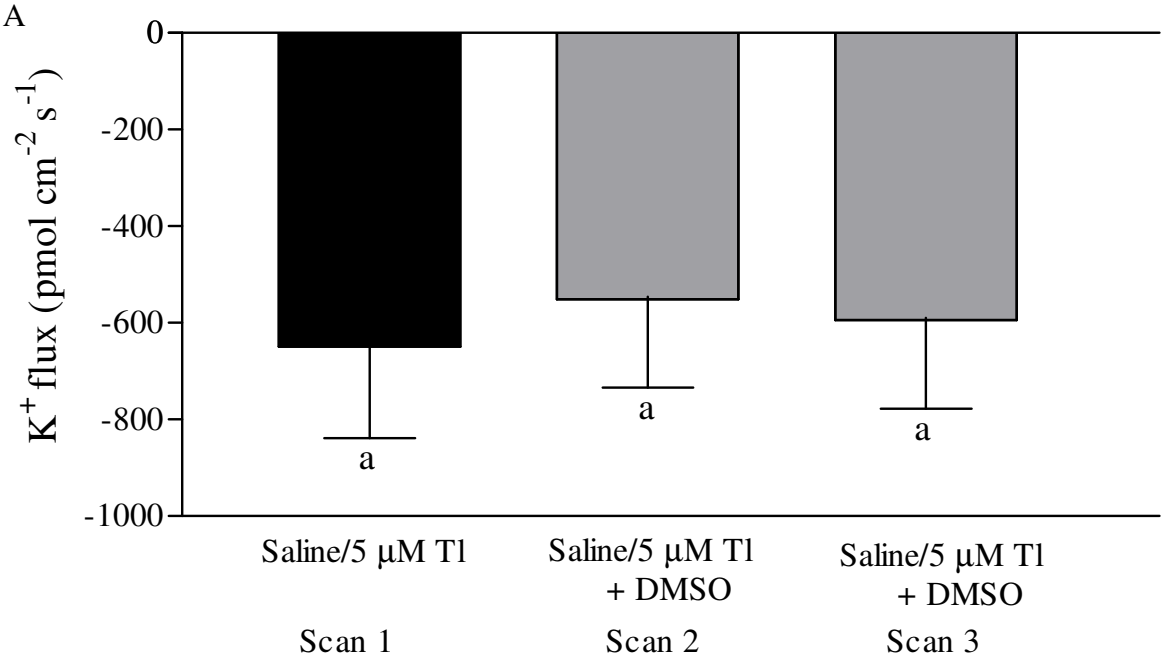
0
-200
-400
-600
-800
-1000
K+ flux (pmol cm-2 s-1)
a
a
a
Saline/5 µM Tl
Saline/5 µM Tl + DMSO
Saline/5 µM Tl + DMSO
Scan 1
Scan 2
Scan 3

B

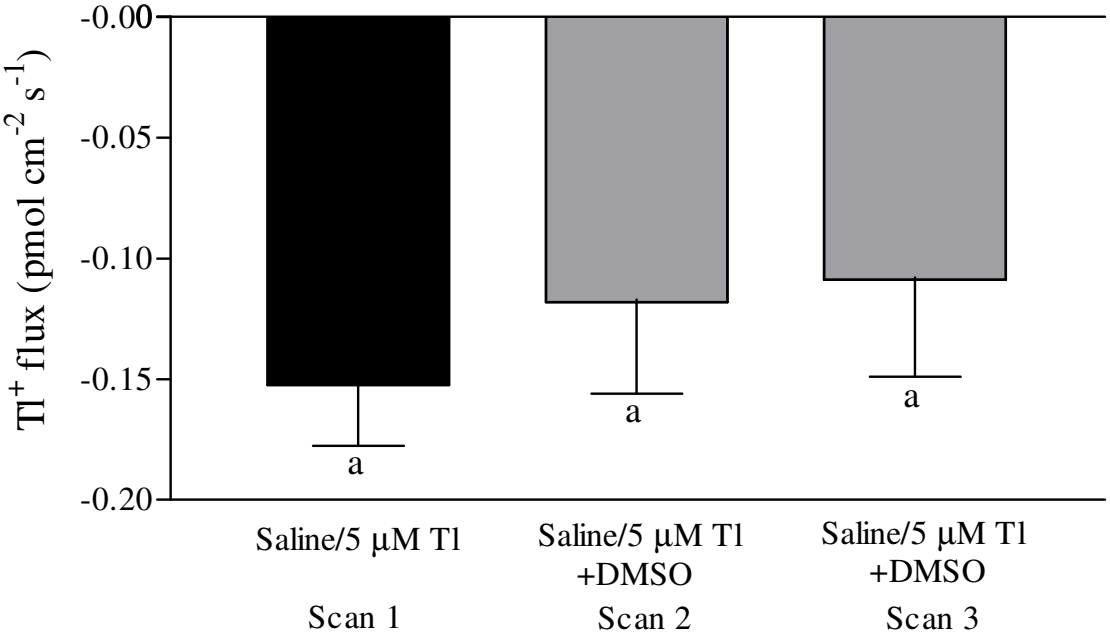
-0.00
-0.05
-0.10
-0.15
-0.20
Tl+ flux (pmol cm-2 s-1)
a
a
a
Saline/5 µM Tl
Saline/5 µM Tl +DMSO
Saline/5 µM Tl +DMSO
Scan 1
Scan 2
Scan 3

Figure 11. The effect of 100 μmol l^{-1} ouabain (in 0.2% DMSO) on ion flux at the caecae of Tl^+-naïve *C. riparius* larvae. Bars are means ± SEM. N = 5. Statistical analysis was performed by repeated measures ANOVA with Tukey's and Bonferroni's post-hoc test if $p<0.05$. Bars sharing the same letter are not statistically different from each other. (A) Effect of ouabain on K^+ flux. Significance was detected by Tukey's post-hoc test only. (B) Effect of ouabain on Tl^+ flux.

A

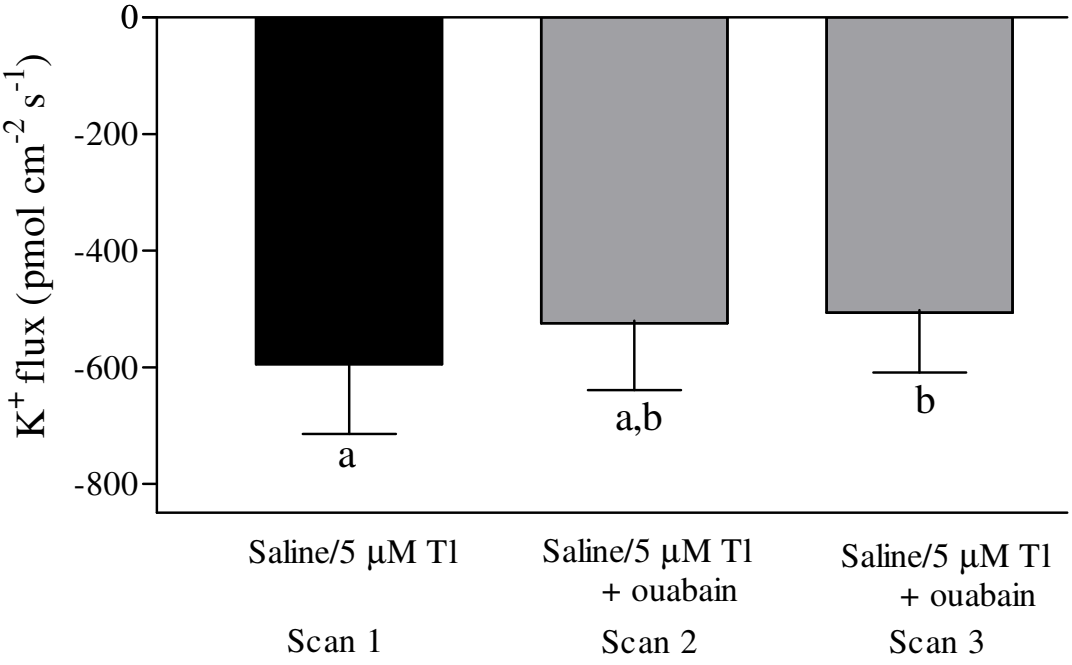
0
-200
-400
-600
-800
K+ flux (pmol cm-2 s-1)
a
a,b
b
Saline/5 µM Tl
Saline/5 µM Tl + ouabain
Saline/5 µM Tl + ouabain
Scan 1
Scan 2
Scan 3

B

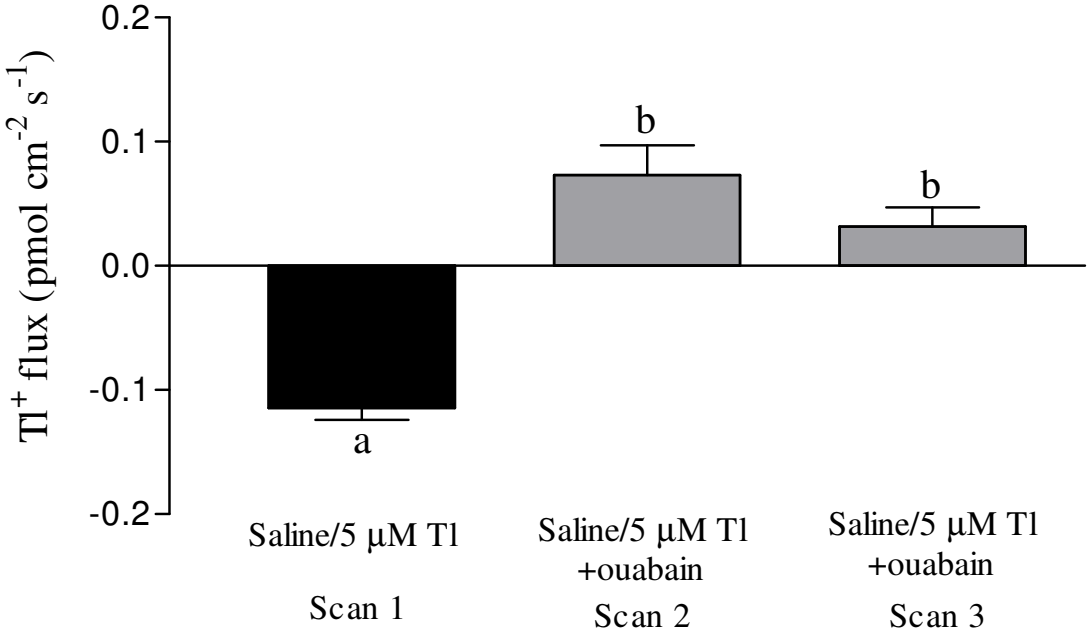
0.2
0.1
0.0
-0.1
-0.2
Tl+ flux (pmol cm-2 s-1)
a
b
b
Saline/5 µM Tl
Saline/5 µM Tl +ouabain
Saline/5 µM Tl +ouabain
Scan 1
Scan 2
Scan 3

Figure 12. The effect of 48 hour exposure to 300 μM Tl^+ on ion flux at the AMG of *C. riparius* larvae. Bars are means ± SEM. N = 6. Statistical analysis was performed by Student's paired t-test. Bars sharing the same letter are not statistically different from each other. (A) K^+ flux. (B) Tl^+ flux.

A

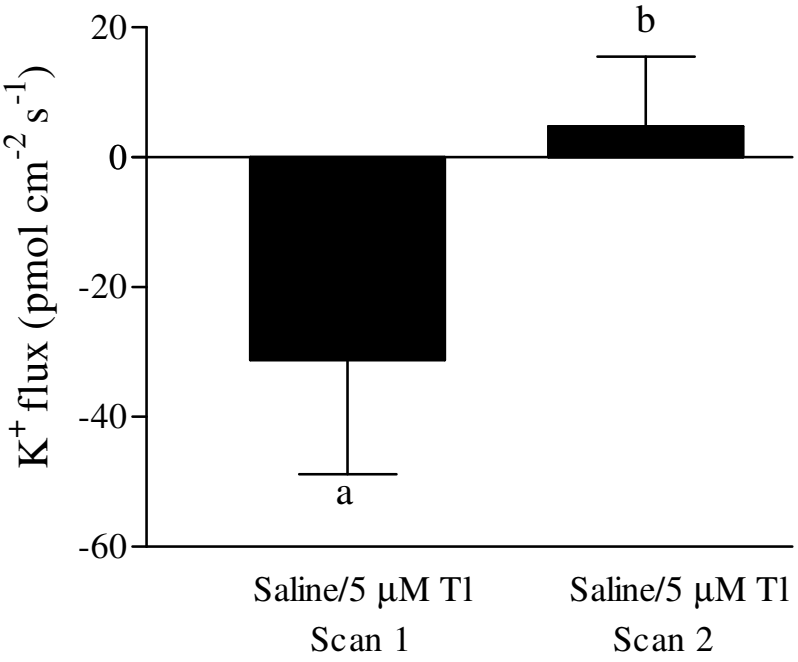
20
0
-20
-40
-60
K+ flux (pmol cm-2 s-1)
b
a
Saline/5 µM Tl
Scan 1
Saline/5 µM Tl
Scan 2

B

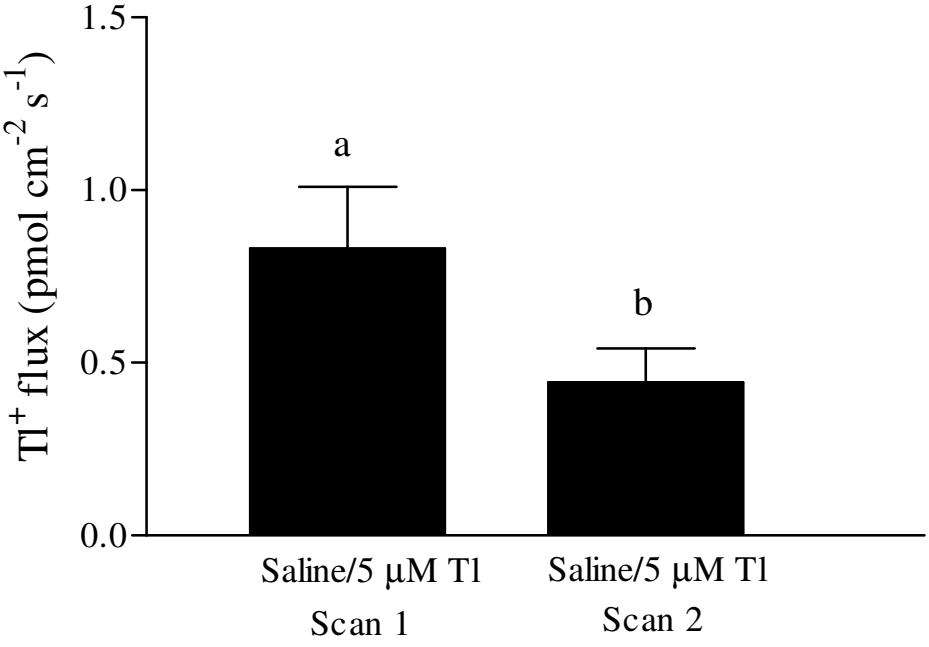
1.5
1.0
0.5
0.0
Tl+ flux (pmol cm-2 s-1)
a
b
Saline/5 µM Tl
Scan 1
Saline/5 µM Tl
Scan 2

Figure 13**.** SIET measurement of ion flux at the AMG of Tl^+-naïve *C. riparius* larvae; controls for the effects of time and changing solutions between scans. Bars are means ± SEM. Statistical analysis was performed by repeated measures ANOVA with Tukey's and Bonferroni's post-hoc test if $p<0.05$. Bars sharing the same letter are not statistically different from each other. (A) K^+ flux. N = 4. (B) Tl^+ flux at the AMG of an intact gut. N = 6. (C) Tl^+ flux at the AMG where the caecae and esophagus have been removed, allowing the bathing medium to enter the lumen. N = 5.

A

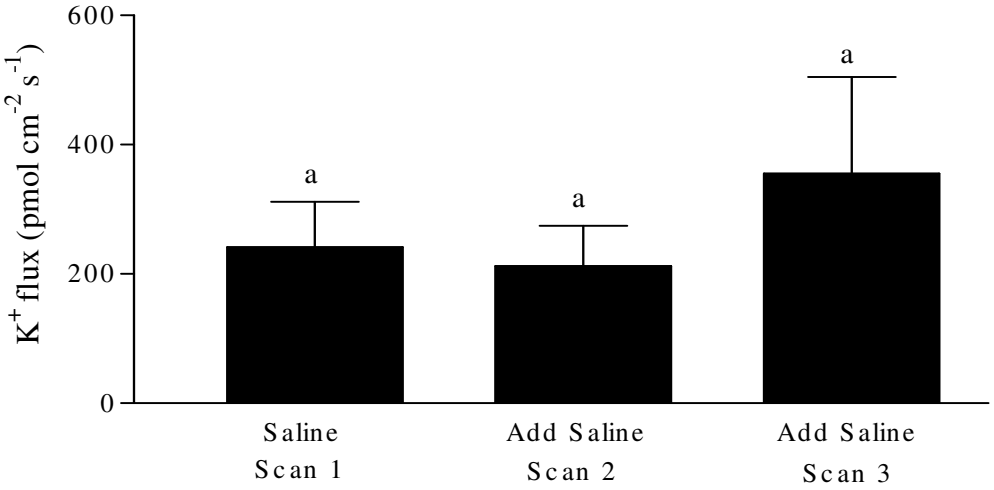
600
400
200
0
K+ flux (pmol cm-2 s-1)
a
a
a
Saline
Scan 1
Add Saline
Scan 2
Add Saline
Scan 3

B

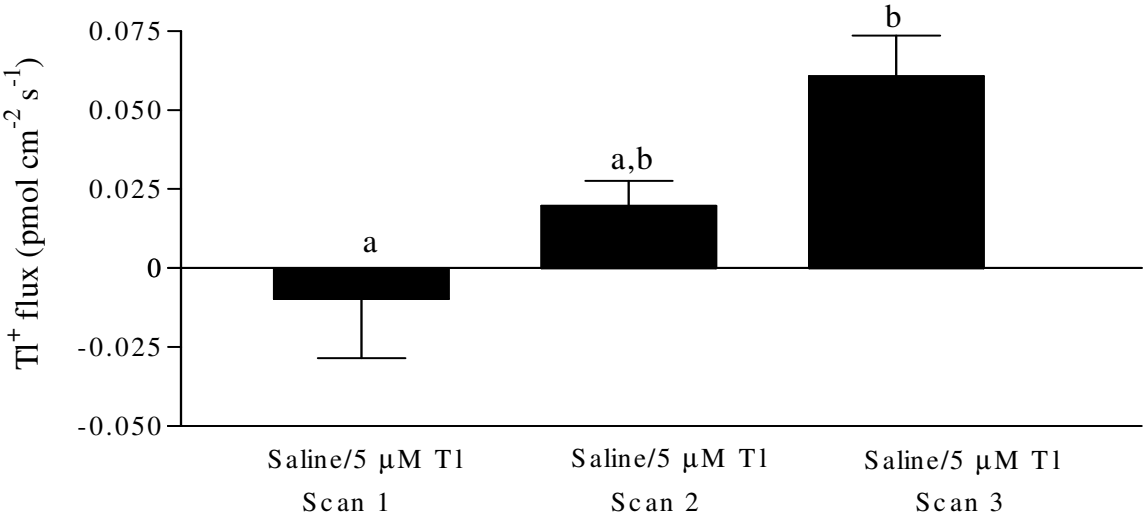
0.075
0.050
0.025
0
-0.025
-0.050
Tl+ flux (pmol cm-2 s-1)
a
a,b
b
Saline/5 µM Tl
Scan 1
Saline/5 µM Tl
Scan 2
Saline/5 µM Tl
Scan 3

C

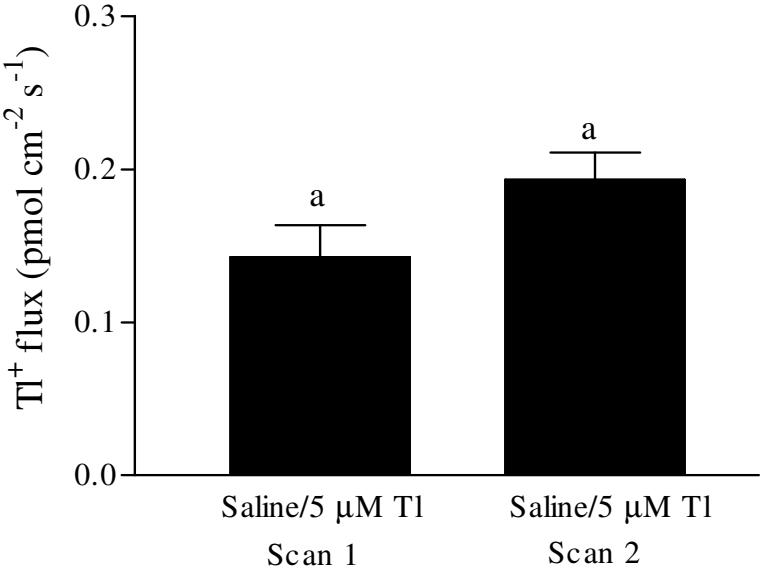
0.3
0.2
0.1
0.0
Tl+ flux (pmol cm-2 s-1)
a
a
Saline/5 µM Tl
Scan 1
Saline/5 µM Tl
Scan 2

Figure 14. The effect of Tl^+ on K^+ flux at the AMG of Tl^+-naïve *C. riparius* larvae. Bars are means ± SEM. Statistical analysis was performed by repeated measures ANOVA with Tukey's and Bonferroni's post-hoc test if $p<0.05$. Bars sharing the same letter are not statistically different from each other. (A) The effect of 5 and 50 μM Tl^+ on K^+ flux. N = 7. (B) The effect of increased duration to 5 μM Tl^+ on K^+ flux. N = 4.

A

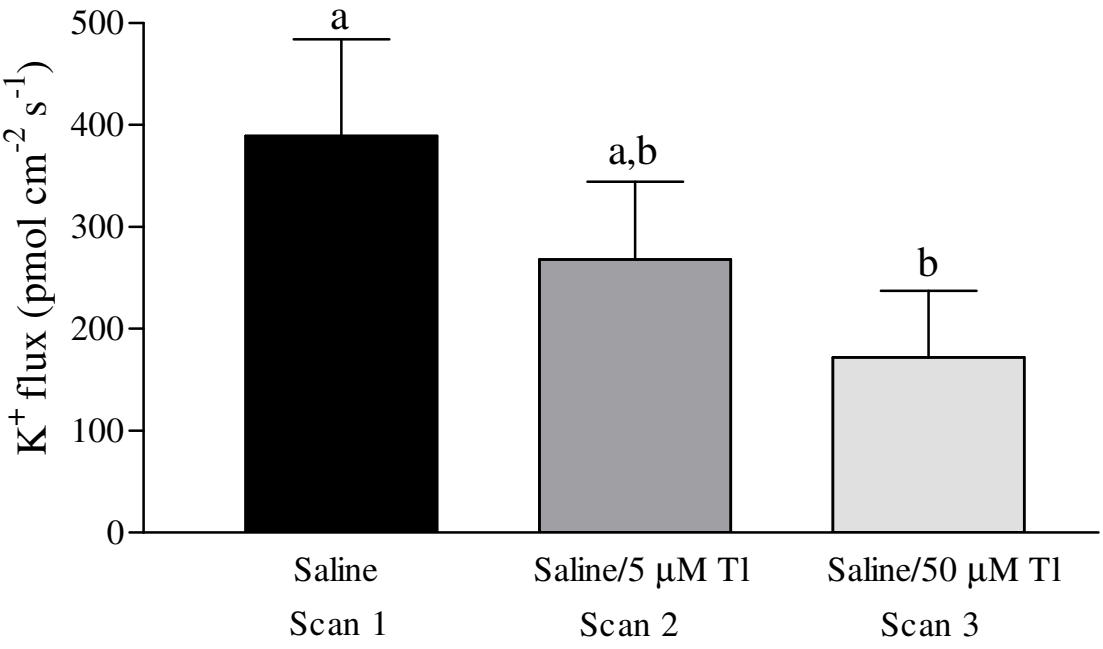
500
400
300
200
100
0
K+ flux (pmol cm-2 s-1)
a
a,b
b
Saline
Scan 1
Saline/5 µM Tl
Scan 2
Saline/50 µM Tl
Scan 3

B

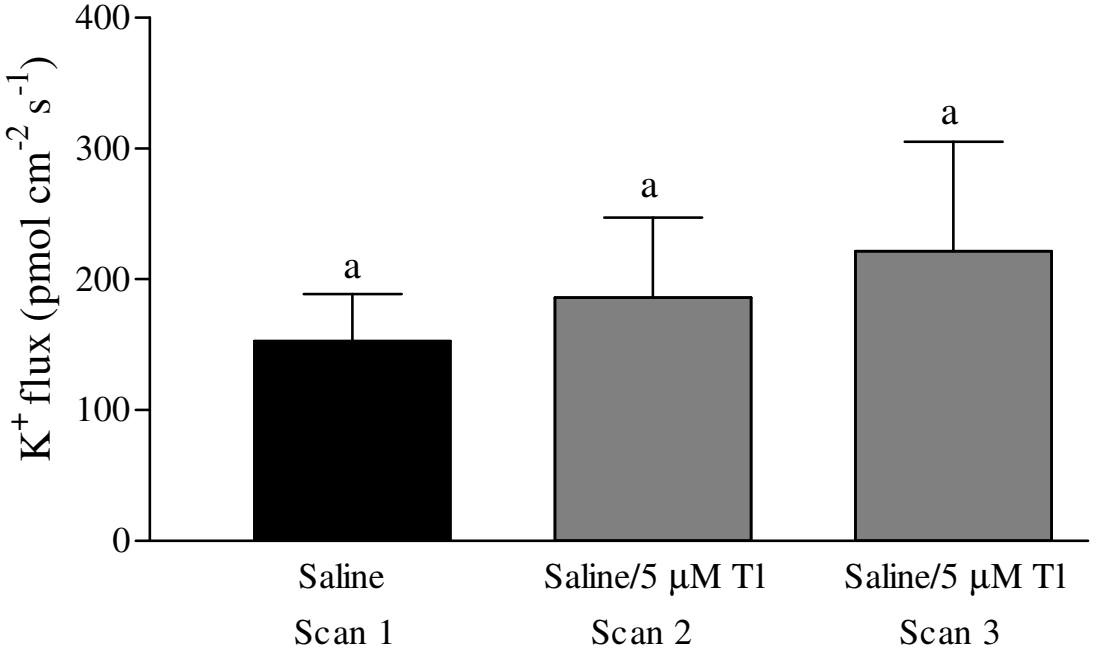
400
300
200
100
0
K+ flux (pmol cm-2 s-1)
a
a
a
Saline
Scan 1
Saline/5 µM Tl
Scan 2
Saline/5 µM Tl
Scan 3

Figure 15. The effect of 48 hour exposure to 300 μM Tl^+ on ion flux at the PMG of *C. riparius* larvae. Bars are means ± SEM. N = 6. Statistical analysis was performed by repeated measures ANOVA with Tukey's and Bonferroni's post-hoc test if $p<0.05$. Bars sharing the same letter are not statistically different from each other. (A) K^+ flux. (B) Tl^+ flux.

A

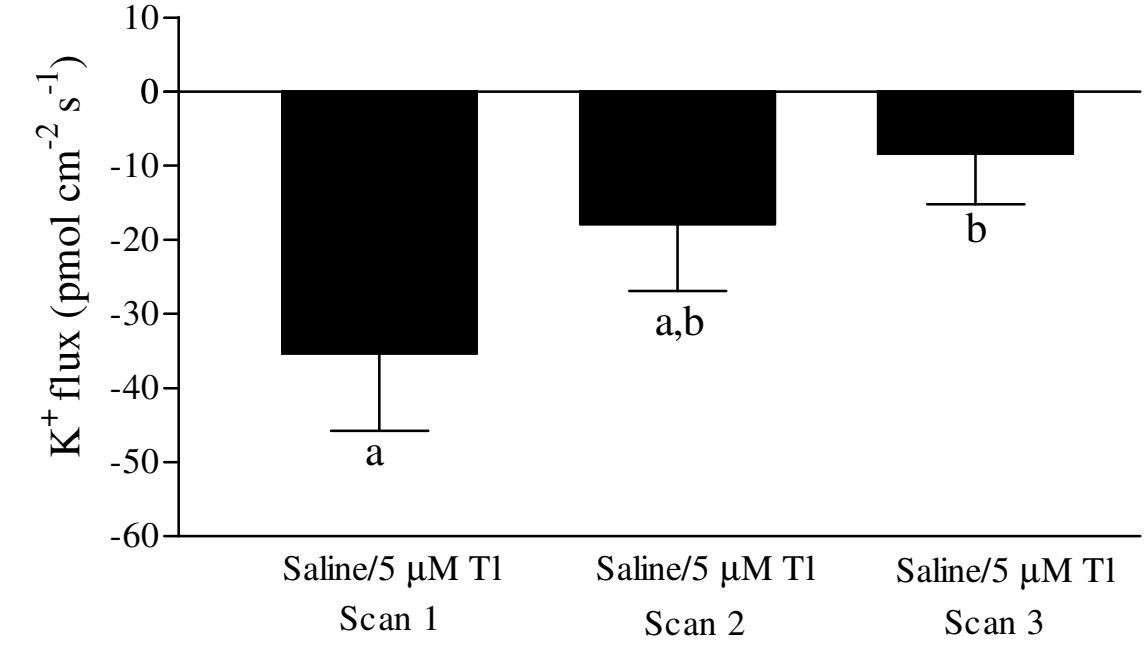
10
0
-10
-20
-30
-40
-50
-60
K+ flux (pmol cm-2 s-1)
a
a,b
b
Saline/5 µM Tl
Scan 1
Saline/5 µM Tl
Scan 2
Saline/5 µM Tl
Scan 3

B

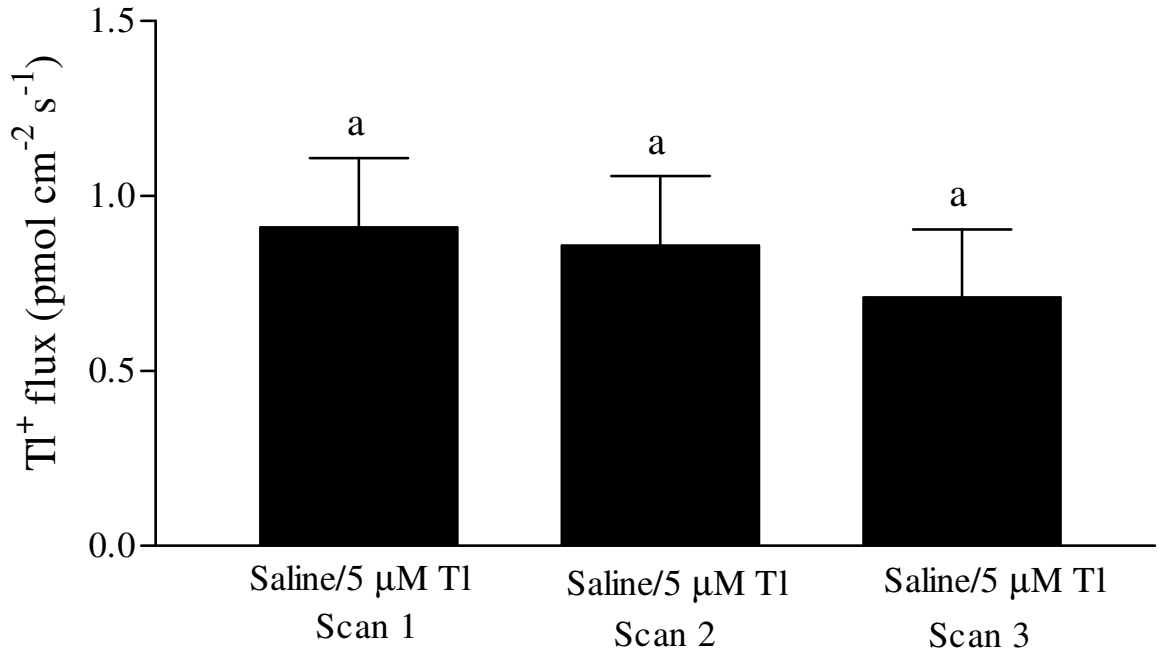
1.5
1.0
0.5
0.0
Tl+ flux (pmol cm-2 s-1)
a
a
a
Saline/5 µM Tl
Scan 1
Saline/5 µM Tl
Scan 2
Saline/5 µM Tl
Scan 3

Figure 16**.** Net ion (K^+ and Tl^+) transport by the caecae, AMG and PMG in *C. riparius* larvae exposed to 300 μM Tl^+ for 48 hours. Bars are means ± SEM.; N = 5-6 per each tissue segment. (A) K^+ fluxes (fmol s^{-1}) corrected for surface area of the corresponding gut segment. Net K^+ transport is the sum of the fluxes from the three gut segments, shown on the right as the gray bar. N = 5-6 per each tissue segment. (B) Tl^+ fluxes (fmol s^{-1}) corrected for surface area of the corresponding gut segment. Net Tl^+ transport is the sum of the fluxes from the three gut segments, shown on the right as the gray bar. N = 5-6 per each tissue segment.

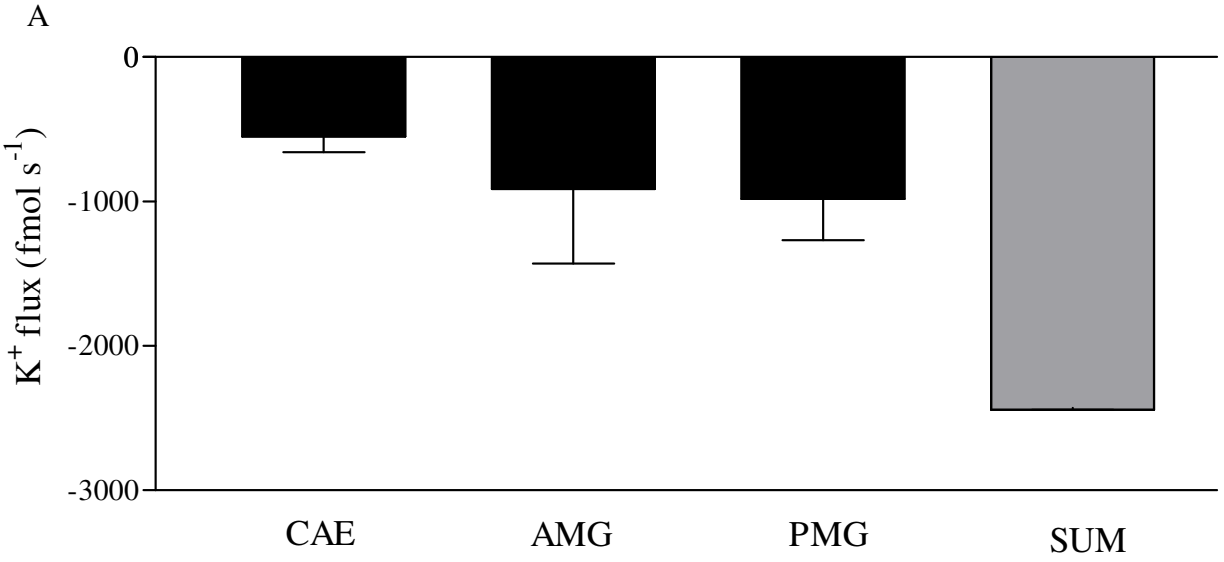
A
0
-1000
-2000
-3000
K+ flux (fmol s-1)
CAE
AMG
PMG
SUM

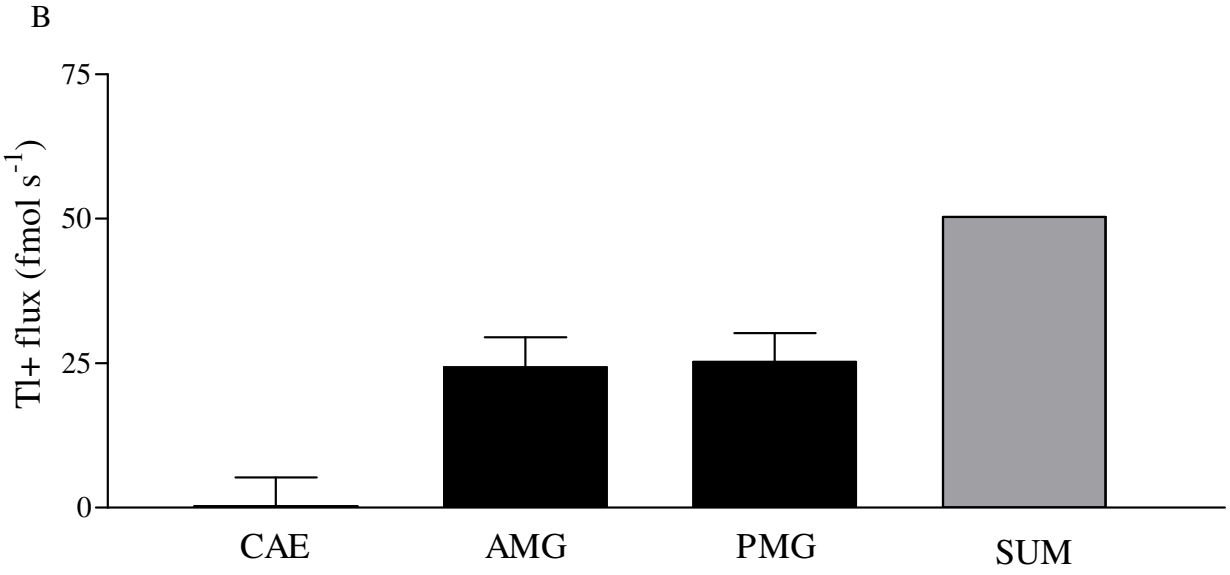
B
75
50
25
0
Tl+ flux (fmol s-1)
CAE
AMG
PMG
SUM

Figure 17**.** SIET measurement of ion flux at the PMG of Tl^+-naïve *C. riparius* larvae; controls for the effects of time and changing solutions between scans. Bars are means ± SEM. Statistical analysis was performed by repeated measures ANOVA with Tukey's and Bonferroni's post-hoc test if $p<0.05$. Bars sharing the same letter are not statistically different from each other. (A) K^+ flux. N = 6. (B) Tl^+ flux. N = 11.

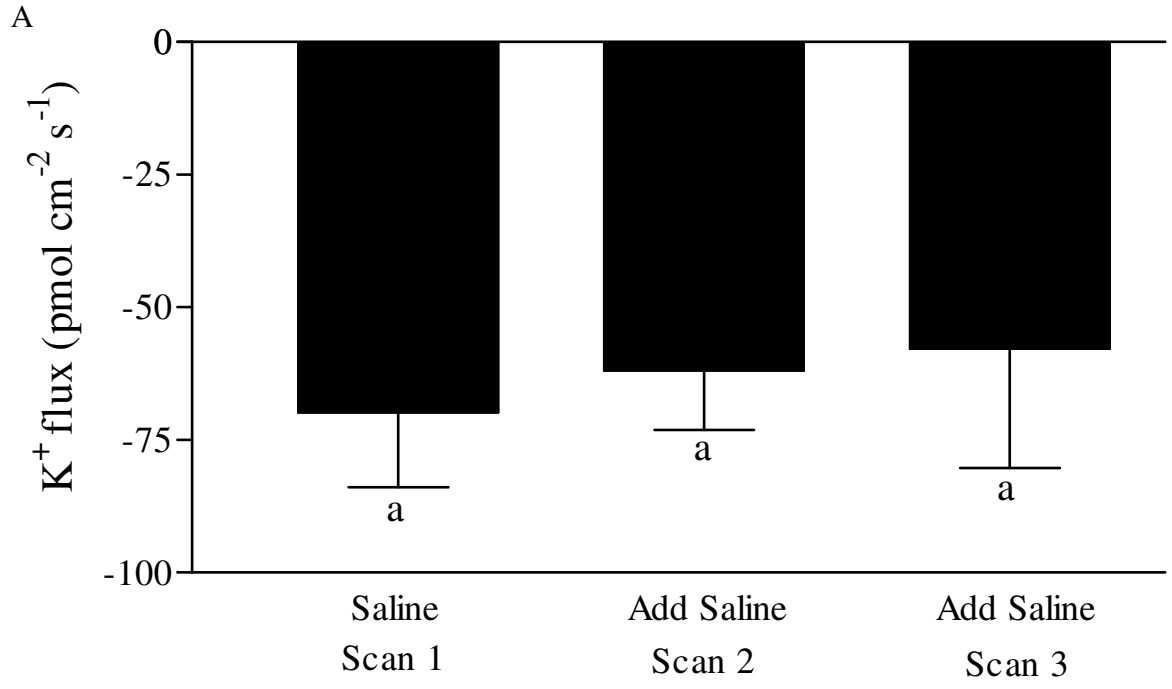
A
0
-25
-50
-75
-100
K+ flux (pmol cm-2 s-1)
a
a
a
Saline
Scan 1
Add Saline
Scan 2
Add Saline
Scan 3

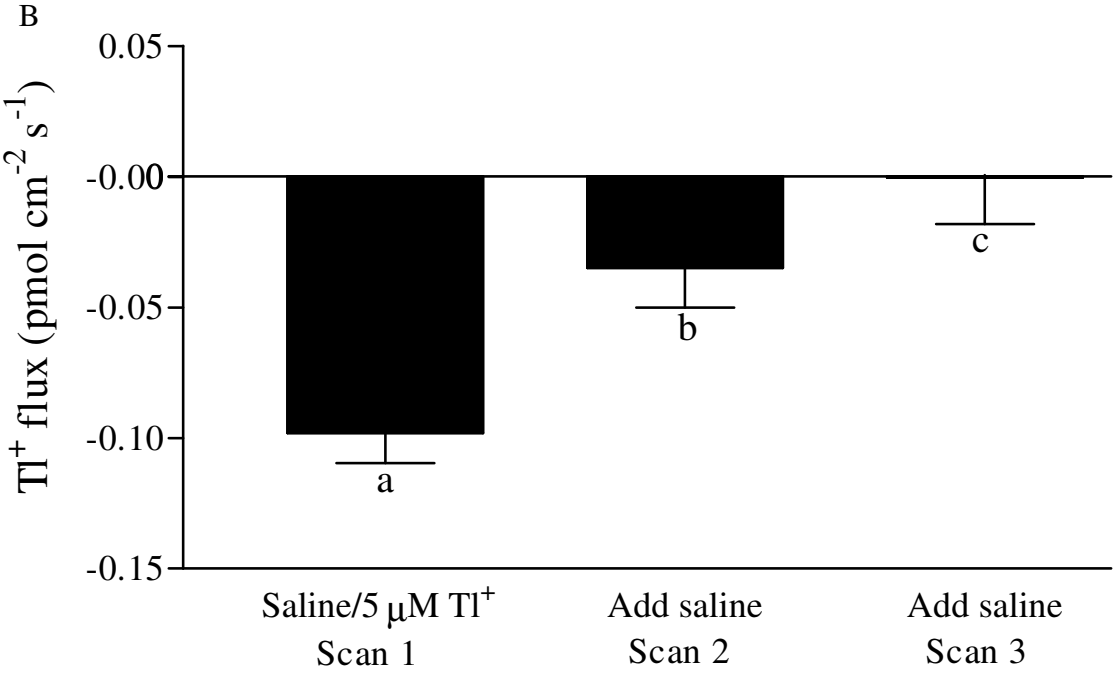
B
0.05
-0.00
-0.05
-0.10
-0.15
Tl+ flux (pmol cm-2 s-1)
a
b
c
Saline/5 μM Tl+
Scan 1
Add saline
Scan 2
Add saline
Scan 3

Figure 18**.** The effect of 5 and 50 μM Tl^+ on K^+ flux at the PMG of Tl^+-naïve *C. riparius* larvae. Bars are means ± SEM. N = 5. Statistical analysis was performed by repeated measures ANOVA with Tukey's and Bonferroni's post-hoc test if $p<0.05$. Bars sharing the same letter are not statistically different from each other.

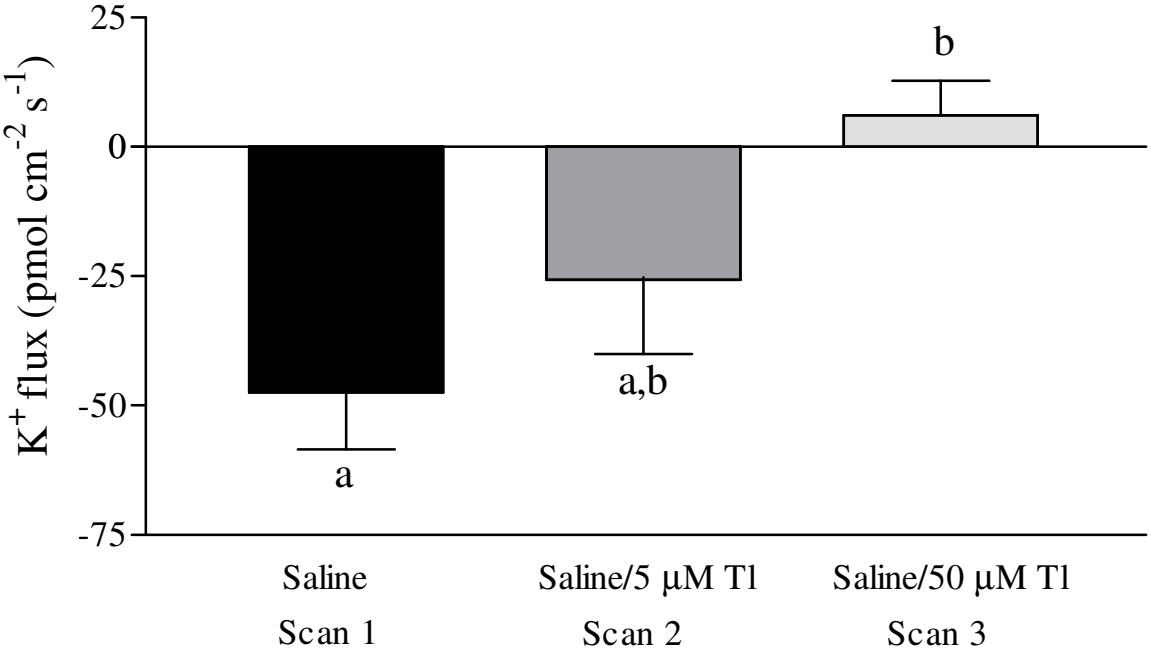
25
0
-25
-50
-75
K+ flux (pmol cm-2 s-1)
a
a,b
b
Saline
Scan 1
Saline/5 µM Tl
Scan 2
Saline/50 µM Tl
Scan 3

Figure 19. The effect of 2 mmol l^{-1} Ba^{2+} on K^+ flux at the PMG of Tl^+-naïve *C. riparius* larvae. Bars are means ± SEM. N = 6. Statistical analysis was performed by repeated measures ANOVA with Tukey's and Bonferroni's post-hoc test if $p<0.05$. Bars sharing the same letter are not statistically different from each other

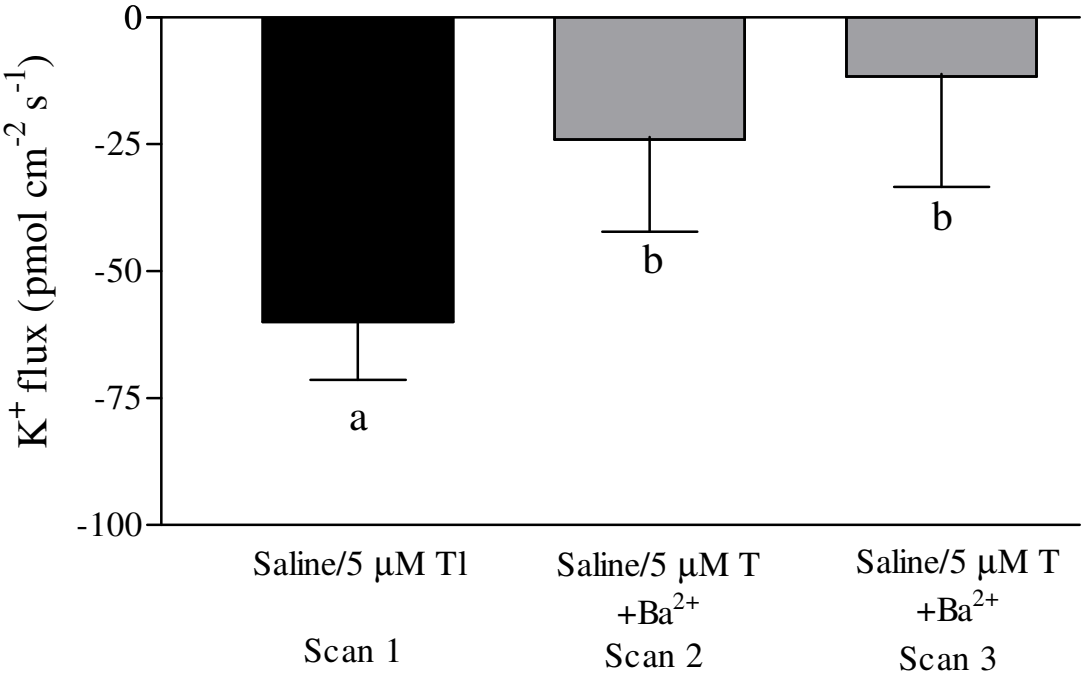
0
-25
-50
-75
-100
K+ flux (pmol cm-2 s-1)
a
b
b
Saline/5 µM Tl
Scan 1
Saline/5 µM T
+Ba2+
Scan 2
Saline/5 µM T
+Ba2+
Scan 3

Figure 20. Schematic diagram of the *C. riparius* gut showing K^+ and Tl^+ fluxes for each gut segment (fmol s^{-1}) in a Tl^+-naïve organism. .Jagged arrows indicate inhibition of the corresponding flux by the experimental treatments. ESO = esophagus, CAE = caecae, AMG = anterior midgut, PMG = posterior midgut, ILE = ileum, LMT = lower Malpighian tubule, MMT = middle Malpighian tubule, DMT = distal Malpighian tubule, AR = anterior rectum, PR = posterior rectum. Note that Ba^{2+} was not tested at the AMG or on Tl^+ flux at the PMG and that ouabain was tested only at the caecae.

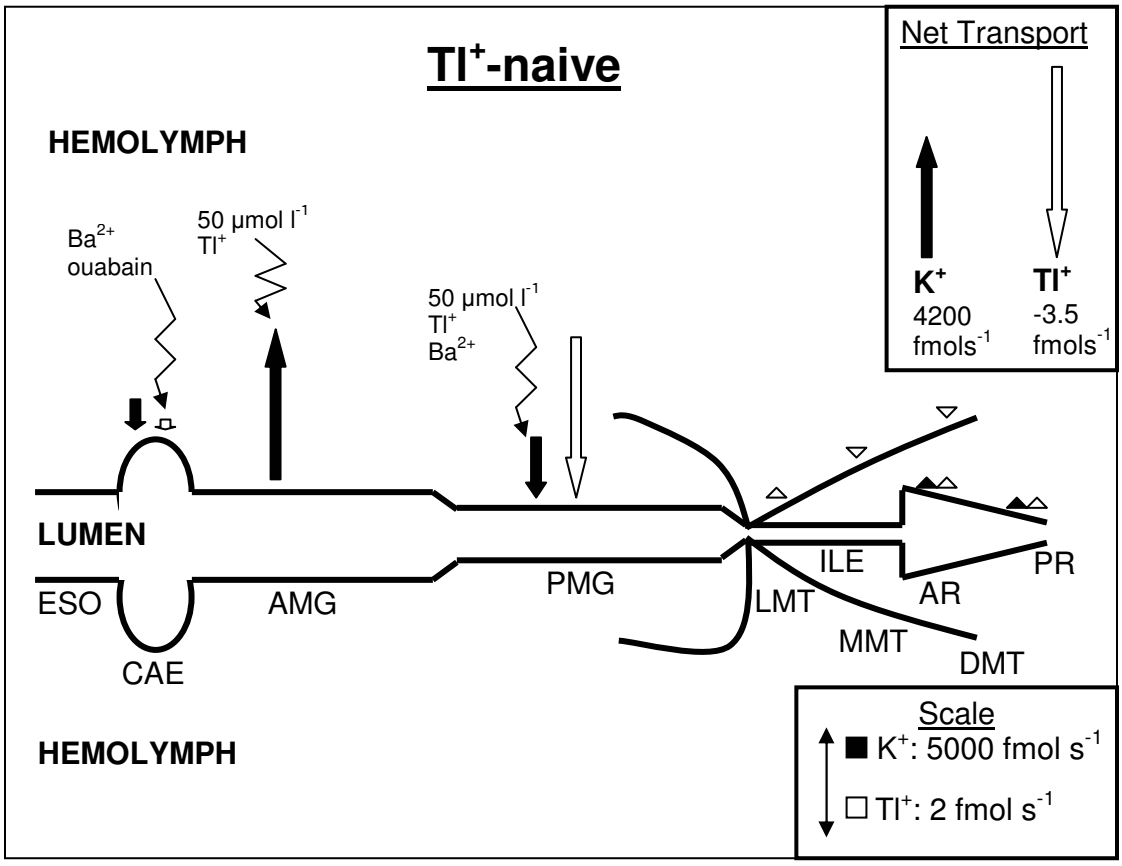
Tl+-naive
HEMOLYMPH
Ba2+
ouabain
50 µmol l-1
Tl+
50 µmol l-1
Tl+
Ba2+
LUMEN
ESO
CAE
AMG
PMG
LMT
ILE
AR
PR
MMT
DMT
HEMOLYMPH
Net Transport
K+
4200
fmols-1
Tl+
-3.5
fmols-1
Scale
K+: 5000 fmol s-1
Tl+: 2 fmol s-1

Figure 21. Schematic diagram of the caecae, AMG and PMG showing K^+ and Tl^+ fluxes (pmol cm^{-2} s^{-1}). The left most arrow denotes the 1st of 2 or 3 consecutive scans. The net flux (fmol s^{-1}) for the entire gut, based on the summation of the first scan for each region, is shown on the right. (A) Tl^+-naïve larvae (B) Tl^+-exposed larvae

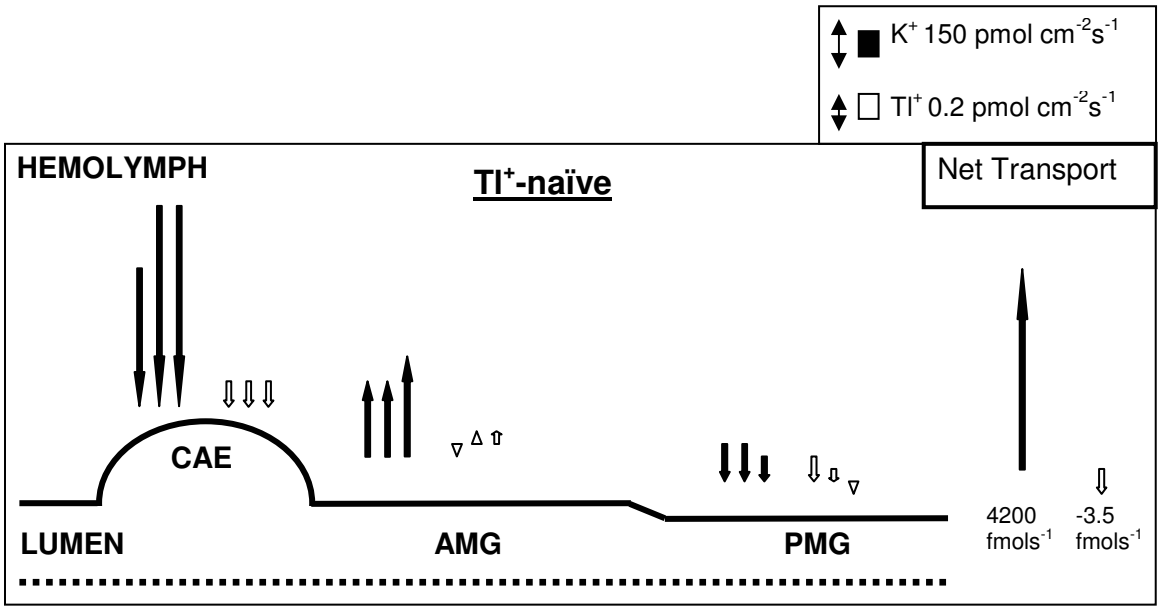
K+ 150 pmol cm-2s-1
Tl+ 0.2 pmol cm-2s-1
HEMOLYMPH
Tl+-naïve
Net Transport
CAE
LUMEN
AMG
PMG
4200 fmols-1
-3.5 fmols-1

A

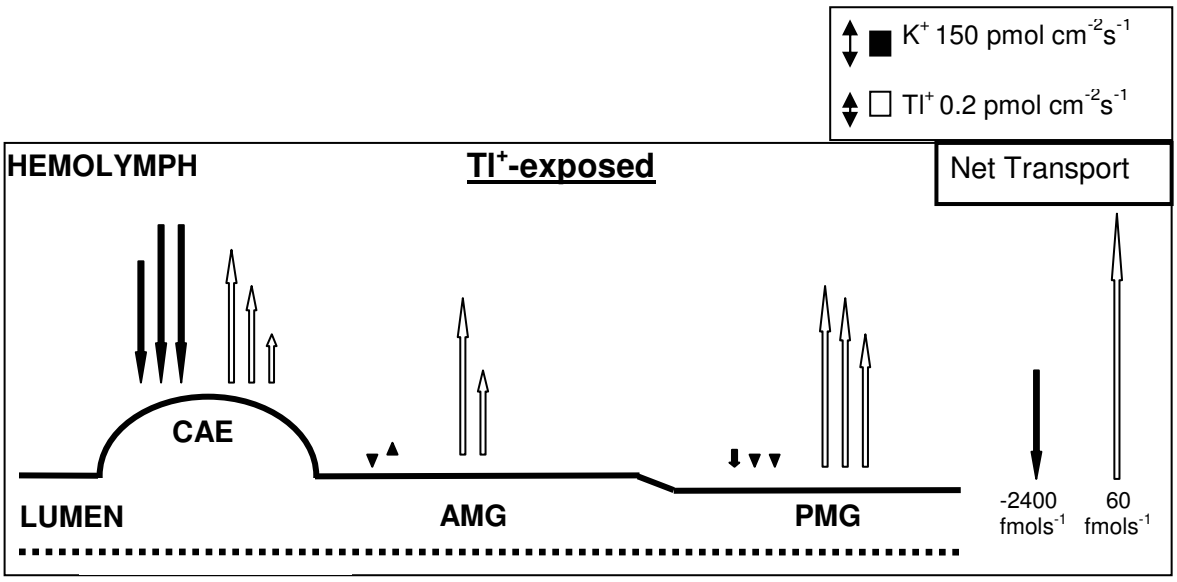
K+ 150 pmol cm-2s-1
Tl+ 0.2 pmol cm-2s-1
HEMOLYMPH
Tl+-exposed
Net Transport
CAE
LUMEN
AMG
PMG
-2400 fmols-1
60 fmols-1

B

Table I. The calibration and scan solutions used for ion (K^+ and Tl^+) flux measurements in this study.

Scan Type	Calibration Solutions	Scan Solution
Single Electrode Holder		
K^+ - isolated gut	50 and 5 mmol l^{-1} K^+ in chironomid saline	Chironomid saline
Tl^+ - isolated gut	50 and 5 µmol l^{-1} Tl^+ in chironomid saline	5 µmol l^{-1} Tl^+ in chironomid saline
K^+ - cuticle and anal papillae	4 and 0.4 mmol l^{-1} K^+ and 1 mmol l^{-1} HEPES in $_dH_20$	Hamilton tapwater with 1 mmol l^{-1} HEPES
Tl^+ - cuticle and anal papillae	50 and 5 µmol l^{-1} Tl^+ and 1 mmol l^{-1} HEPES in $_dH_20$	Hamilton tapwater with 5 µmol l^{-1} Tl^+ and 1 mmol l^{-1} HEPES
Double Electrode Holder		
Control – K^+	5 and 0.5 mmol l^{-1} K^+ in chironomid saline	Scan 1-3: Chironomid saline (5 mmol l^{-1} K)
Control – Tl^+	50 and 5 µmol l^{-1} Tl^+ in chironomid saline	Scan 1-3: 5 µmol l^{-1} Tl^+ in chironomid saline
K^+-Tl^+ Competition Studies (K^+ flux measured only)	5 and 0.5 mmol l^{-1} K^+	Scan 1: Tl-free chironomid saline Scan 2: 5 µmol l^{-1} Tl^+ in chironomid saline Scan 3*: 50 µmol l^{-1} Tl^+ in chironomid saline
Effect of Ba^{2+}	5 and 0.5 mmol l^{-1} K^+ and 50 and 5 µmol l^{-1} Tl^+ in chironomid saline	Scan 1: 5 µmol l^{-1} Tl^+ in chironomid saline Scan 2-3: 5 µmol l^{-1} Tl^+ in chironomid saline + 2 mmol l^{-1} Ba^{2+}
Effect of DMSO	5 and 0.5 mmol l^{-1} K^+ and 50 and 5 µmol l^{-1} Tl^+ in chironomid saline	Scan 1: 5 µmol l^{-1} Tl^+ in chironomid saline Scan 2-3: 5 µmol l^{-1} Tl^+ in chironomid saline + 0.2% DMSO
Effect of ouabain	5 and 0.5 mmol l^{-1} K^+ and 50 and 5 µmol l^{-1} Tl^+ in chironomid saline	Scan 1: 5 µmol l^{-1} Tl^+ in chironomid saline Scan 2-3: 5 µmol l^{-1} Tl^+ in chironomid saline + 100 µmol l^{-1} ouabain
Effect of 48 hour Tl^+-exposure	5 and 0.5 mmol l^{-1} K^+ and 50 and 5 µmol l^{-1} Tl^+ in chironomid saline	Scan 1: 5 µmol l^{-1} Tl^+ in chironomid saline Scan 2-3: 5 µmol l^{-1} Tl^+ in chironomid saline

CHAPTER 3

Abstract

C. riparius are water dwelling benthic larvae and are exceptionally tolerant towards a wide range of toxic metals. They are well protected by both CCME and USEPA water quality guidelines, with acute LC_{50s} several orders of magnitudes above the maximum allowable levels. Previous studies which have looked at Cd^{2+} tolerance in *Chironomus* have found that they can sequester Cd^{2+} in the posterior midgut and Malpighian tubules, and that the Malpighian tubules can also secrete large amounts of Cd^{2+}. In addition, it has been show that Cd^{2+} tolerance in *C. riparius* may involve the avoidance of hypocalcaemia, which is not observed in Cd^{2+} sensitive species. However, few studies have looked at Tl^{+} tolerance by *C. riparius*. Tl is a non-essential metal that can exert toxic effects at low concentrations. It gets released into the environment mainly as the result of anthropogenic activities such as fossil fuel burning and smelting of ores. It is thought to interfere with K dependant processes due to holding the same charge and having a similar ionic radius as K. We determined that the acute (48 hour) LC_{50} of Tl for 4^{th} instar *C. riparius* larvae was 723 μmol l^{-1}, which is ~180000-fold above the CCME water quality guidelines. The uptake of Tl by the whole animal was saturable, with a maximum uptake (J_{max}) of 3666 μmol kg^{-1} wet weight, and K_D of 439 μmol l^{-1} Tl. At the gut, Tl uptake appeared saturable at the lowest four Tl concentrations, with a J_{max} of 2560 μmol kg^{-1} wet weight and K_D at 54.5 μmol l^{-1} Tl. The saturable uptake at the gut may be indicative of a limited capacity of intracellular detoxification, such as storage in lysosomes or binding to metal-binding proteins. Tl uptake by the hemolymph was found

to be non-saturable, and at Tl exposures >600 μmol l^{-1}, the Tl concentrations in the hemolymph were less than exposure concentration. There was a significant decrease in K concentrations in the whole animal at 30 and 545 μmol l^{-1} Tl exposures. In addition, there was a negative correlation between hemolymph K and Tl exposures in the range of concentrations between 0 (control) and 730 μmol l^{-1} Tl. This provides some evidence for an interaction between K and Tl. This paper is the first to look at the tolerance of *C. riparius* towards Tl and its effect on K concentrations in the tissues, and contributes to our knowledge on the mechanisms of non-essential metal tolerance in *C. riparius.*

Introduction

Thallium (Tl) is an inorganic and non-essential metal that can be toxic at low concentrations. In the natural environment, Tl^+ is present at low concentrations. In unpolluted freshwater it is present at concentrations between 5×10^{-5} to 4.9×10^{-5} μmol l^{-1} (Peter and Viraraghavan, 2005). Cheam (2001) reports Tl^+ concentrations in unpolluted freshwater environments across Canada range from 4.1×10^{-5} to 4.0×10^{-4} μmol l^{-1}. In polluted sites that receive waste water, such as mining sites and power plants, Tl^+ concentrations range from 1×10^{-3} to 0.115 μmol l^{-1}.

15 tonnes of Tl is produced world wide annually for industries involved in the production of fiber (optical) glass, semiconductiors and specialized research equipment (Peter and Viraraghavan, 2005). However, the majority of Tl (2000-5000 tonnes) is released into the environment by anthropogenic activities such as the burning of fossil fuels and the refining and smelting of ores (Cheam, 2001). Once Tl^+ enters the environment it can be exposed to aquatic organisms where it can exert toxic effects.

There is less literature available on Tl^+ toxicity towards aquatic species compared to better studied essential and non-essential metals such as copper, nickel, lead, zinc or cadmium, and the exact mechanism of Tl^+ toxicity is not well understood. Mulkey and Oehme (1993) have found that Tl^+ can inhibit cellular respiration and interfere with riboflavin and riboflavin-based cofactors. Since Tl^+ is classified as a soft Lewis acid, it forms more stable bonds with soft ligand donors, such as those rich in sulfur containing compounds (House, 2008). This can cause Tl to bond to a wide range of sulfur rich proteins and interfere with their normal function. Tl^+ is also thought to exert its toxicity

through competition with the physiologically important ion K^+ (Mulkey and Oehme ,1993), due to the same charge and similar ionic radii of the two ions (1.33 and 1.4 Å for K^+ and Tl^+, respectively, Zhou and MacKinnon, 2003). Competition between K^+ and Tl^+ has been shown to occur in plants (Siegel and Siegel, 1976), and Borgmann (1998) reports that only K (and not Ca, Mg, Na or Pb) affect Tl toxicity and uptake by *Hyalella azteca.*

LC_{50} values are an important parameter for comparing the lethality of different toxic metals and for identifying which species are more sensitive. Chronic LC_{50} values provide more useful parameters for measuring sensitive sub lethal end-points, such as reproduction or growth effects (Sibley et al., 1997), and are therefore more useful for setting water quality guidelines. However, acute toxicity tests are also useful for explaining the mechanism of the toxic effect (Watts and Pascoe, 2000).

Chironomus riparius are dipterans found in ecologically diverse habitats, and spend the majority of their life cycle as benthic larvae (Pinder, 1995). They are commonly found in polluted aquatic environments, indicating that they are extremely tolerant towards a wide range of harmful xenobiotics (Pinder, 1995). 1st instar *C. riparius* larvae are the most sensitive to toxic metals (Williams et al., 1986) yet they still have acute (24 hour) LC_{50} values for the waterborne toxic metals Cd, Cu, Pb, Ni and Zn that are well above the Canadian Council of Ministers for the environment (CCME) and US Environmental Protection Agency (USEPA) water quality guidelines (Béchard et al., 2008). 4th instar larvae are even more tolerant, and have an acute LC50 value for Cd^{2+} that is several orders of magnitude above CCME and USEPA guidelines (Gillis and

Wood, 2008). This indicates that *C. riparius* are both well protected and extremely tolerant towards toxic metals.

The mechanism of tolerance employed by *C. riparius* towards toxic metals has been studied by numerous groups in the past. Secretion and sequestration of Cd^{2+} by the gut segments and Malpighian tubules of *C. riparius* has been reported Leonard et al., (2009), and Seidman et al., (1986) has also found a role for the posterior midgut in sequestration of Cd^{2+} in *Chironomus thummi.* Gillis and Wood (2008) propose that *C. riparius* are able tolerate high amounts of Cd^{2+} by preventing hypocalcemia from occurring, possibly due to the lower affinity of Ca transporters for Cd relative to other aquatic organisms. Finally it has been suggested that metal-binding proteins, such as metallothionein, may bind toxic metals (such as Cd^{2+}) and render them inert, and thus contribute to tolerance (Gillis et al., 2002).

In this study we investigated the tolerance of *C. riparius* towards another toxic metal, Tl^{+}, by determining the acute (48 hour) LC50. The accumulation of Tl^{+} by the whole animal, gut and hemolymph, and the subsequent effect on K^{+} concentrations in these tissues was investigated to determine if hypokalemia was occuring.

Methods

1.1. Chironomid larvae

C. riparius larvae were cultured at McMaster University, initiated from ropes obtained from Environment Canada. *C. riparius* egg ropes were hatched in Petri dishes, and first instar larvae were transported to 10 L aquaria containing fine-grained silica sand and aerated dechlorinated Hamilton tap water ('culture water'). The ionic composition of the culture water (in mmol l^{-1}) was Na^+ (0.6), Cl^- (0.8), Ca^{2+} (1.8), K^+ (0.4), Mg^{2+} (0.5) and Tl^+ ($<1.25 \times 10^{-5}$). The water was moderately hard (140 mg l^{-1} $CaCO_3$) and pH was 7.8-8.2. The water was replaced once every ~10 days. The larvae were fed *ad labitum* on ground Nutrafin™ fish flakes (45% protein, 5% crude fat, 2% crude fibre, 8% moisture) and maintained at 21 ± 2 ºC under a 16:8 h light:dark photoperiod. Dissolved organic content (DOC) has been reported as 3.0 mg l^{-1} for our culture water (Gillis and Wood, 2008a). Once the larvae pupated and emerged as adults, the tanks were fitted with an equal sized lid. The lid contained an opening that could be covered with a removable mesh net, allowing egg ropes to be removed and hatched so that the colony was continuously replenishing itself.

1.2. Acute thallium exposures for 48 hour LC_{50} studies

The protocol for acute toxic metal exposures was taken from Gillis and Wood, 2008a). All 250 mL beakers used in the experiment were acid washed in 10% HNO_3 for 48 hours. The Tl exposures were performed in the same room and under the same lighting conditions as the colony to prevent major environmental changes (e.g.

temperature, humidity). The LC50 experiment was performed in culture water (composition described above), and Tl was added from a stock solution of reagent grade $TlNO_3$ (Sigma-Aldrich) dissolved in deionized water. After the Tl exposure solutions were prepared and placed in the beakers, they were covered and aerated for 24 hours. The seven concentrations used for this study were based on preliminary toxicity tests and selected in order to bracket the apparent LC_{50}.

3^{rd} and 4^{th} instar *C. riparius* larvae were removed from the tank and placed in acid washed 250 mL beakers containing aerated culture water for 24 hours prior to adding them to the exposure solution, allowing for gut clearance. After gut clearance, 15 larvae were added to each exposure or control solution of each of the three replicates (i.e. 7 Tl exposures + control x 3 replicates x 15 chironomid/beaker = 360 chironomids total). Water samples were collected for total (unfiltered) and dissolved (filtered) Tl measurements immediately after the addition of the larvae to the beakers, and at the 24 and 48 hour time points. For measurements of dissolved Tl, the water samples were filtered through an Acrodisk™ 0.45 µm in-line-syringe-tip filter. The Tl concentration for each exposure was calculated as the mean of the dissolved Tl at 0 and 48 hours. The mean concentration (± SEM) for the three replicates (in $\mu mol\ l^{-1}$) was 0.01 (±0.003), 3.4 (± 0.17), 26.9 (±0 .82), 277 (±50.23), 544 (±26.49), 730 (±26.45), 966 (±19.13) and 1558 (±109.81). The dissolved Tl concentrations are compared to the nominal Tl concentrations in the results. The mortality was assessed after 24 and 48 hours by gentle prodding of the larvae. Larvae that did not respond were considered dead and removed from the beaker.

After 48 hours, the surviving larvae were removed from the beaker and placed in culture water (i.e. dechlorinated Hamilton tapwater) for five minutes to remove adsorbed Tl. The chironomids were then rinsed with deionized water and blotted dry on a Kimwipe™.

Larvae used for whole animal ion measurements were weighed to the nearest 0.01 mg and placed in1.5 mL microtubes for tissue digestion.

Larvae used for gut and carcass ion measurements were dissected in a saline solution, and the gut and carcass were weighed to the nearest 0.01 mg after excision and transferred to 1.5 mL microtubes. The composition of the saline was based on hemolymph ion measurements performed by Leonard et al., (2009) and contained (in mmol l^{-1}) K^+ (5), Na^+ (74), Ca^{2+} (1), Mg^{2+} (8.5), HCO_3^- (10.2), HEPES (10), glucose (20), and pH was titrated to 7 before use.

Larvae used for hemolymph ion measurements were placed in a slygard lined Petri dish containing mineral oil, and the chironomid was pierced, which caused the hemolymph to leak out. The hemolymph formed a sphere in the hydrophobic environment, and the diameter of the sphere was measured using an eye-piece micrometer. This allowed the volume to be calculated by the following equation:

$$V = (4/3\pi r^3) \times 1000 \qquad \text{(Equation 1)}$$

where V is the volume (in nL), and r is the radius (in mm). The hemolymph samples were then transferred to 1.5 mL microtubes.

1.3. K and Tl Analysis

The concentration of dissolved Tl in the exposure solutions was measured in the 0.45 µm filtered water samples by atomic absorption spectroscopy (AAS) using a Graphite Furnace (GFAAS; Varian SpectrAA -220 with graphite tube atomizer [GTA – 110], Mulgrave, Australia). The concentrations of Tl in the exposure solutions reported throughout this study are the dissolved Tl measurements.

Tl concentrations in the whole-animal, gut and hemolymph were determined for control and Tl-exposed larvae by GFAAS, and K concentrations were determined by flame AAS (FAAS; Varian 220FS SpectaAA, Varian Techtron, Mulgrave, Australia).

Tissues were digested in a similar manner as reported by Gillis and Wood (2008a) and Leonard et al., (2009). Whole animal tissues were digested in 70 µl of concentrated metals grade nitric acid at room temperature for 6 days, after which 30 µl of H_2O_2 was added. 24 hours after the addition of the H_2O_2, 750 µl of 1% nitric acid was added to each sample. Samples that required further dilution for Tl^+ measurements were diluted between 5- to 225- fold with 1% nitric acid. For K^+ measurements, all the samples were diluted 3- fold with 0.2% CsCl (Sigma-Aldrich) in 1% nitric acid.

The gut and hemolymph samples were digested in 30 µl of concentrated metals grade nitric acid at room temperature for 6 days, after which 10 µl of H_2O_2 was added. 24 hours after the addition of the H_2O_2, 100 µl of 1% nitric acid was added to each sample. Samples that required further dilution for Tl measurements were diluted between 3- to 100-fold with 1% nitric acid. For K measurements, the samples were diluted 9- to 15-fold with 0.2% CsCl (Sigma-Aldrich) in 1% nitric acid.

1.4. Statistical Analysis

ToxCalc was used for calculating the acute LC_{50} values by Probit analysis. Comparisons between K and Tl concentrations in the tissues was performed using one-way analysis of variance (ANOVA) followed by Dunnet's and Tukey's post-hoc test if $p < 0.05$. Correlations were tested by Pearson's test for K concentrations in the tissue and Tl exposures. All statistical analyses were performed using GraphPad Instat software (GraphPad InStat, GraphPad software, Inc San Diego, CA, USA). Statistical significance was designated if $p<0.05$. Data are reported as mean ± SEM.

Results

2.1. Total and dissolved Tl concentrations measured by graphite furnace atomic absorption spectroscopy (GFAAS)

There was no significant difference between the total Tl and dissolved Tl concentrations (measured by GFAAS) in the solutions to which the chironomid larvae were added, and the concentrations of Tl remained stable in all solutions over 48 hours (figure 1). However, there was a noticeable difference between the measured Tl (dissolved or total) and nominal Tl concentrations (figure 2). The measured Tl concentrations were on average only ~70% of the nominal value. This may be the result of Tl binding to either the glass beakers during the experiment, or to the plastic vials in which water samples were collected. It is unlikely that Tl binds to the plastic vials, however, as the vials were acidified after the collection of water samples. Because of the differences between nominal and measured Tl concentrations, the physiological parameters (e.g. Tl uptake kinetics) are plotted against the measured dissolved Tl concentrations rather the then nominal Tl concentrations.

2.2. Tl 48-hour LC_{50} in fourth instar C. riparius *larvae*

Fourth instar *C. riparius* larvae showed high tolerance toward waterborne Tl. The 48 hour LC_{50} was 723 μmol l^{-1} (figure 3). There was a large and saturable uptake of Tl by whole animal across all the Tl exposures, with a maximum uptake (B_{max}) of ~3600 μmol kg^{-1} wet weight (figure 4). Fewer larvae survived exposure to higher concentrations of Tl. This meant that at the highest concentrations (i.e. above the LC_{50}) there were fewer

larvae available for measuring the concentrations of Tl and K in the whole animal and the tissues. The calculated values that were based on less than 3 surviving larvae were therefore not included in the statistical analysis.

2.3 Tl concentration-dependent uptake kinetics for the whole animal, gut and hemolymph of C. riparius *larvae*

The uptake of Tl appears to be non-saturable (i.e. linear) at the gut when all the Tl exposure concentrations, shown as the solid line in figure 5, are included. However, there may be some saturation occurring based on analysis of the 4 lowest Tl concentrations, displayed in figure 5 as the dotted curve. At the lower Tl concentrations (3 and 25 μmol l^{-1} Tl), the gut bioconcentrated Tl 50-fold. At concentrations above this, the bioconcentration leveled off and remained ~10-fold.

In contrast to the gut, figure 6 shows there was only a ~3-fold bioconcentration of Tl in the hemolymph at low concentrations (3 and 25 μmol l^{-1}). Interestingly, at concentrations above ~575 μmol l^{-1} there was less Tl in the hemolymph relative to the exposure concentration (e.g. hemolymph Tl of 715 μmol l^{-1} versus 1000 μmol l^{-1} Tl in the exposure medium). This may indicate that the gut provides some defense of the hemolymph at higher Tl concentrations in the water.

The total amount of Tl in the whole animal and gut (μmoles) was determined for each exposure concentration by multiplying the weight of the chironomid or gut (kg) by the concentration of Tl in the respective tissue (μmol kg^{-1} wet weight). Similarly, the

total amount of Tl in the hemolymph was calculated as the product of hemolymph volume (l) and Tl concentration in the hemolymph (μmol l^{-1}). Figure 7 shows the percent of total Tl in the gut or hemolymph (relative to the whole animal) which was calculated from these measured values. The percent of Tl in the carcass is not a measured value, but represents the remaining Tl not accounted for by the gut and hemolymph (i.e. Tl in carcass = [whole animal Tl – (gut Tl + hemolymph Tl)].

Tl in the carcass was ~70% of total Tl, not a surprising finding since the carcass accounts for a significant portion of the chironomid body mass (~60%). The role of the gut in accumulating 20% of total Tl was of interest, given that it represents such a small amount of total body mass (<10%). This may implicate the gut as a site of Tl sequestration which helps contribute to tolerance. In contrast with the gut, the hemolymph accounted for a significantly smaller amount of total Tl given that it represents ~30% of the mass of the larvae.

2.4. The effect Tl exposure on K concentrations in the whole animal, gut and hemolymph of C. riparius *larvae*

The effect of Tl exposure on whole animal K concentrations is shown in figure 8. There was a significant decrease in K concentration at the 30 and 545 μmol l^{-1} Tl concentrations. Thus, there appears to be some effect of Tl on whole body K, although it is not an obvious does-response relationship. The ratio of K loss to Tl gain (by the whole animal) was examined to determine the stoichiometric relationship between the two ions.

If the ratio is > 1, more moles of K are being loss compared to Tl being gained, whereas if the ratio is < 1, more Tl is being gained compared to the K being loss. If the ratio is equal to 1, than the absorption of 1 mole of Tl results in the loss of 1 mole of K. The total K in the whole animal was calculated for each Tl^+-exposure in a similar manner as total Tl in the whole animal (described above), the difference being that whole animal K concentration (μmol g^{-1}) was multiplied by the chironomid weight (g) to determine total K (μmoles) in the whole animal. The K loss was calculated by subtracting total K (μmoles) at the different Tl^+-exposures from the total K in control larvae. The calculated K loss was divided by the Tl gain (calculated above) to determine the ratio. At the 30 and 545 μmol l^{-1} Tl^+-exposures, which showed a significant reduction in whole animal K^+ concentrations, the ratio was 11.43 and 0.61. In general, the ratio was > 1 at the two lowest concentrations, and dropped to < 1 for the Tl^+-exposures > 30 μmol l^{-1}.

There was no significant decrease in K concentration in the gut or hemolymph when *C. riparius* were exposed to Tl (figure 9 and 10). However, there was a negative correlation (r = -0.833) between hemolymph K and Tl exposures in the range of concentrations between 0 (control) and 730 μmol l^{-1} Tl, providing some evidence for an interaction between K and Tl.

Discussion

3.1. Tl 48-hour LC_{50} in fourth instar C. riparius *larvae*

The 48 hour LC_{50} (723 µmol l^{-1}) of *C. riparius* larvae indicates a high tolerance towards Tl compared to other aquatic organisms. For example, the 48-hour LC_{50} of Tl in *Daphnia magna* is ~70 times lower (LeBlanc, 1980), and in the rotifer *Brachionus. calyciflorus* it is approximately 40-fold lower (Calleja et al., 1994), while Pickard et al (2001) reports that the 96 hour LC_{50} for rainbow trout is 20.89 µmol l^{-1}. However, it should be noted that the Tl concentrations tested in this study are above what would normally be found in the environment. The lowest concentration that was tested (3 µmol l^{-1}) is still ~25 times higher than the most Tl- polluted sites in Canada (Cheam, 2001), but is still within the range of contaminated mining sites found in some parts of China (Xiao et al., 2004). The testing at such high concentrations was necessary in order to bracket the LC_{50} of *C. riparius*, which are extremely tolerant to Tl.

The high tolerance towards Tl exposure displayed by *C. riparius* was unsurprising given that *C. riparius* have been found to tolerate toxic concentrations of virtually every metal (essential and non-essential) that has been tested. First instar *C. riparius* larvae are the most sensitive life stage (Williams et al., 1986), but still display remarkable tolerance to toxic metals. Béchard at., (2008) found that the 24 hour LC_{50} concentrations of Pb (2.9 µmol l^{-1}), Cu (32.9 µmol l^{-1}), Cd (83 µmol l^{-1}) and Ni and Zn (>425 and >382 µmol l^{-1}, respectively) for first instar larvae were at least 25 times higher than CCME water quality guidelines.

3.2. Tl concentration-dependent uptake kinetics of the whole animal

The 48-hour LC_{50} of Cd, a divalent toxic metal, is ~10 mmol l^{-1} in fourth instar *C. riparius* larvae (Gillis and Wood, 2008a), which indicates that short term exposures to Tl is more toxic by ~13-fold. In our study, we found that Tl uptake by the whole animal was saturable and dose-dependant (figure 4), whereas Gillis and Wood found that Cd tissue concentrations were highest at the lowest exposure concentrations. This conflicting result may indicate that divalent and monovalent non-essential metals exert their toxicity through independent mechanisms and/or that the detoxification pathways are different. It may also be possible that the high tissue levels of Tl measured in the whole animal were due to adsorbed Tl. However, the adsorption of Tl was minimized by removing the larvae from the Tl exposures at the conclusion of the experiment and placing them in tapwater for ~5 minutes, and then rinsing them in deionized water for a further ~15 seconds. In the future, it may be useful to compare Tl concentrations in the dead and live animals to check for adsorption.

3.3. Tl concentration-dependent uptake kinetics of the hemolymph

The gut was not a perfect barrier to Tl entry into the hemolymph. We found that the hemolymph contained ~3-fold more Tl than the exposure concentrations at low Tl exposures, and that at higher concentrations (above 575 μmol l^{-1}) the hemolymph Tl was ~2/3 of the exposure concentration (figure 5). Given that the hemolymph is on average 1.26 μL (± 0.06), the total Tl content in the hemolymph at the lowest exposure was 0.02

nmoles, and at the highest exposure it was 0.9 nmoles. This is a 45-fold increase in total hemolymph Tl content, even though the exposure concentration increases ~270-fold. Leonard et al., (2009a) reports similar findings for hemolymph Cd concentrations in *C. riparius*. Our findings indicate that Tl gains access to the hemolymph, where it may be able to exert toxic effects on sensitive tissues. Because the bioconcentration of Tl in the hemolymph only occurs at Tl concentrations well below the LC_{50}, it may be that at low exposures there is less need to regulate Tl access into the hemolymph, whereas at higher exposures access into the hemolymph may need to be more limited. This may be indicative of an innate tolerance for toxic metals at low concentrations, perhaps allowing the larvae to expend its energy on more useful activities in the short term, such as leaving the polluted site or maturing more quickly. This strategy has been observed in female killifish from polluted aquatic sites, which were found mature and become reproductive at a younger age (Weis and Weis, 1989)

3.4. Tl concentration-dependent uptake kinetics of the gut

There was some evidence for a saturable uptake of Tl in the gut over the range of the lowest 4 concentrations (figure 6, dotted curve). However, when including all the Tl concentrations it appears that uptake is non-saturable (figure 6, solid curve). Another possibility is that there is both a saturable and a non-saturable component to Tl uptake. For example, in *Oncorhynchus mykiss,* there is saturable uptake of Ni at low exposure concentrations (0 to 30 μmol l^{-1} Ni) and a non-saturable uptake at higher concentrations (> 100 μmol l^{-1} Ni) in the stomach, midintestine and posterior intestine (Leonard et al.,

2009b). The possibility of the saturable uptake of Tl at low concentrations may be indicative of intracellular compartmentalization of Tl within lysosomes, as observed in *Mercenaria* cytosomes for Hg uptake (Fowler, 1975). The saturable uptake may also be caused by the limited availability of metal-binding proteins, such as metallothionein, which can bind toxic metals to decrease their toxicity (Fowler, 1987). Metallothionein has been detected in *C. riparius* and increases in response to increased Cd in the sediment (Gillis et al., 2002). At higher concentrations, the uptake of Tl appears to be by simple diffusion into the gut (i.e. the linear portion of the curve).

3.5. The effect of Tl on K concentrations in the whole animal, gut and hemolymph

There is some evidence for an effect of Tl on K homeostasis. Larvae that were exposed to 30 or 545 μmol l^{-1} Tl had a significantly lower K concentration (18% and 12% of whole animal K, respectively), which would be consistent with an interaction between the two ions (figure 8). One possible explanation for the lack of an effect on K concentration at the other Tl concentrations may be that concentrations of K were measured only in the surviving larvae, which may have been better able to maintain K homeostasis to avert mortality. The ratio of K loss to Tl absorption was > 1 at the lower concentrations (< 30 μmol l^{-1}), and dropped to ~1 or < 1 at higher exposures to Tl. At the exposures < 30 μmol l^{-1} Tl, the large ratio (>1) could be caused by excessive K loss, less Tl absorption, or a combination of both, and vice versa for the smaller ratio (< 1) at the higher

concentrations. Based on the calculated ratios, there appears to be increased K loss at the lower concentrations, which may contribute to toxicity at these exposures.

Although there was not an effect of Tl on K concentrations in the gut or hemolymph, there was a negative correlation between hemolymph K and Tl exposures in the range of concentrations between 0 (control) and 730 μmol l^{-1} Tl (figure 10). This leads us to believe that there may be some interaction with K As mentioned above, the effects on K may be biased by measuring K concentrations in only the surviving organisms. It may also be conceivable that there is no effect on K in the gut and hemolymph. The possibility still exists that the carcass is adversely affected by Tl, or perhaps that the carcass acts as a buffer for K changes in the gut and hemolymph. The carcass contains muscle, which contains high levels of K. It would be of interest to identify whether the tolerance towards Tl displayed by *C. riparius* involves the carcass shifting K from muscle to the hemolymph and gut. This would explain why there were decreases in whole body K at some Tl concentrations, but no corresponding decrease in gut and hemolymph K concentrations.

3.6. Future Studies

There is some evidence for an interaction between K and Tl based on whole animal K measurements. Follow up experiments using Tl concentrations closer to the LC_{50}, in conjunction with simple behavioural studies to determine whether movement is reduced (which would be indicative of impaired muscle and/or nervous system

functioning) would help in deciphering the exact mechanism of Tl toxicity, and whether it does disrupt K homeostasis. It would also be useful to test whether the different parts of the gut and Malpighian tubules can sequester Tl as a method of detoxification, as this would help to explain the tolerance that was observed in *C. riparius* larvae.

References

Béchard, K.M., Gillis, P.L., Wood, C.M. Acute toxicity of waterborne Cd, Cu, Pb, Ni and Zn to first-instar *Chironomus riparius* larvae. *Arch. Environ. Contam. Toxicol.* **54** (2008), pp. 454-459.

Borgmann, U., Cheam, V., Norwood, W.P., and Lechner, J. Toxicity and bioaccumulation of thallium in *Hyallela azteca*, with comparison to other metals and prediction of environmental impact. *Environ. Poll.* **99** (1998), pp.105-114.

Calleja, M.C., Persoone, G., and P. Geladi. Comparative acute toxicity of the first 50 multicenter evaluation of *in vitro* cytotoxicity chemicals to aquatic non-invertebrates. *Arch. Environ. Contam. And Toxic.* **26** (1994), pp. 69-78.

Cheam, V. Thallium contamination of water in Canada. *Water Qual. Res. J. Canada* **36** (2001), pp. 851-877.

Fowler, B. Intracellular compartmentation of metals in aquatic organisms: roles in mechanism of cell injury. *Environ. Health Perspec.* **71** (1987), pp. 121-128.

Fowler, B.A., Wolfe, D.A., and W.F. Hettler. Mercury and iron uptake by cytosomes in mantle epithelial cells of quahog clams (*mercenaria mercenaria*) exposed to mercury. *J. Fish. Res. Bd. Can.* **30** (1975), pp. 1767-1775.

Gillis, P.L., Diener, L.C., Reynoldson, T.B., and D.G. Dixon. Cadmium induced production of a metallothionein-like protein in *Tubifex tubifex* (Oligochaeta) and *Chironomus riparius* (Diptera): correlation with whole body (reproduction and growth) endpoints of toxicity. *Environ. Toxicol. Chem.*, **21** (2002), pp. 1836–1844.

Gillis, P.L, and C.M. Wood, Investigating a potential mechanism of Cd resistance in *Chironomus riparius* larvae using kinetic analysis of calcium and cadmium uptake. *Aqua. Toxi.* **89** (2008), pp.180-187.

House, J.E. 2008. Chemistry of Coordination Compounds. p. 582-583. In J. House, Inorganic Chemistry, Academc Press, Burlington, MA.

LeBlanc, G.A. Acute toxicity of priority pollutants to water flea (*Daphnia magna)*. *Bull. Environ. Contam. Toxicol.* **24** (1980), pp. 684-691.

Leonard, EM., Pierce, L.M., Gillis, P.M., Wood, C.M., O'Donnell, M.J. Cadmium transport by the gut and Malpighian tubules of *Chironomus riparius. Aquat. Toxicol*. **92** (2009a), pp.179-186.

Leonard, E.M. Nadella, S.R., Bucking, C. and C.M. Wood. Characterization of dietary Ni uptake in the rainbow trout *Oncorhynchus mykiss. Aqu. Toxic.* **93** (2009b), pp. 205-216.

Mulkey, J.P. and Oehme, F.W. A review of thallium toxicity. *Veterinary and Human Toxicology* **35** (1993), pp. 445-453.

Pickard, J., Yang, R., Duncan, C., McDevitt, A., and C. Eickhoff. Acute and sublethal toxicity of thallium to aquatic organisms. *Bull. Of. Environ. Contam. And Toxic.* **66** (2001), pp. 94-101.

Peter, J.A.L. and Viraraghavan, T. Thallium: a review of public health and environmental concerns. *Environ. Int.* **31** (2005), pp. 493-501.

Pinder, L.C.V. The habitats of chironomid larvae. In: *The Chironomidae Biology and Ecology of Non-biting Midges*, edited by Armitage P.D., Cranston P.S., and L.C.V. Pinder. London: Chapman and Hall, 1995. pp. 107-135.

Sibley, P.K., Benoit, D.A., and G.T. Ankley. The significance of growth in *Chironomus tentans* sediment toxicity tests: relationship to reproduction and demographic endpoints. *Environ. Toxicol. Chemis.* **16** (1997), pp. 336-345

Seidman, L.A., Bergtrom, G., Gingrich, D.J., and C.C. Ramsen. Accumulation of cadmium by the fourth instar larva of the fly *Chironomus thummi*. *Tiss. Cell* **18** (1986), pp. 395-405.

Siegel, B.Z. and Siegel, S.M. Effect of potassium on thallium toxicity in cucumber seedlings: further evidence for potassium-thallium ion antagonism. *Bioinorganic Chem*. **6** (1976), pp. 341-345.

Watts, M.M., and Pascoe, D. A comparative study of *Chironomus riparius* Meigen and *Chironomus tetnans* fabricius (Diptera: Chironomidae) in aquatic toxicity tests. *Arch Environ. Contam. Toxicol*. **39** (2000), pp. 299-306.

Weis, J.S. and P. Weis. Tolerance and stress in a polluted environment. *Bioscience.* **39** (1989), pp. 89-95.

Williams, K.A., Green, D.W.J., Pascoe, D., and D.E. Gower. The acute toxicity of cadmium to different larval stages of *Chironomus riparius* (Diptera: Chironomidae) and its ecological significance for pollution regulation. *Oecologia.* **70** (1986), pp. 362-366.

Xiao, T., Guha, J., Boyle, D., Liu, C., Chen, J. Environmental concerns related to high thallium levels in soils and thallium uptake by plants in southwest Guizhou, China. *The Science of The Total Environment* **318** (2004), pp. 223-244.

Zhou, Y. and R. MacKinnon. The occupancy of ions in the K^+ selectivity filter: charge balance and coupling of ion binding to a protein conformational change underlie high conductance rates. *J. Mol. Biol.* **333** (2003), pp. 965-975.

Figure 1: Total and dissolved Tl concentrations measured by graphite furnace atomic absorption spectroscopy (GFAAS) at 0 and 48 hours. The horizontal dotted bars indicate the nominal Tl concentrations that were prepared. Error bars are standard error about the mean of three replicates.

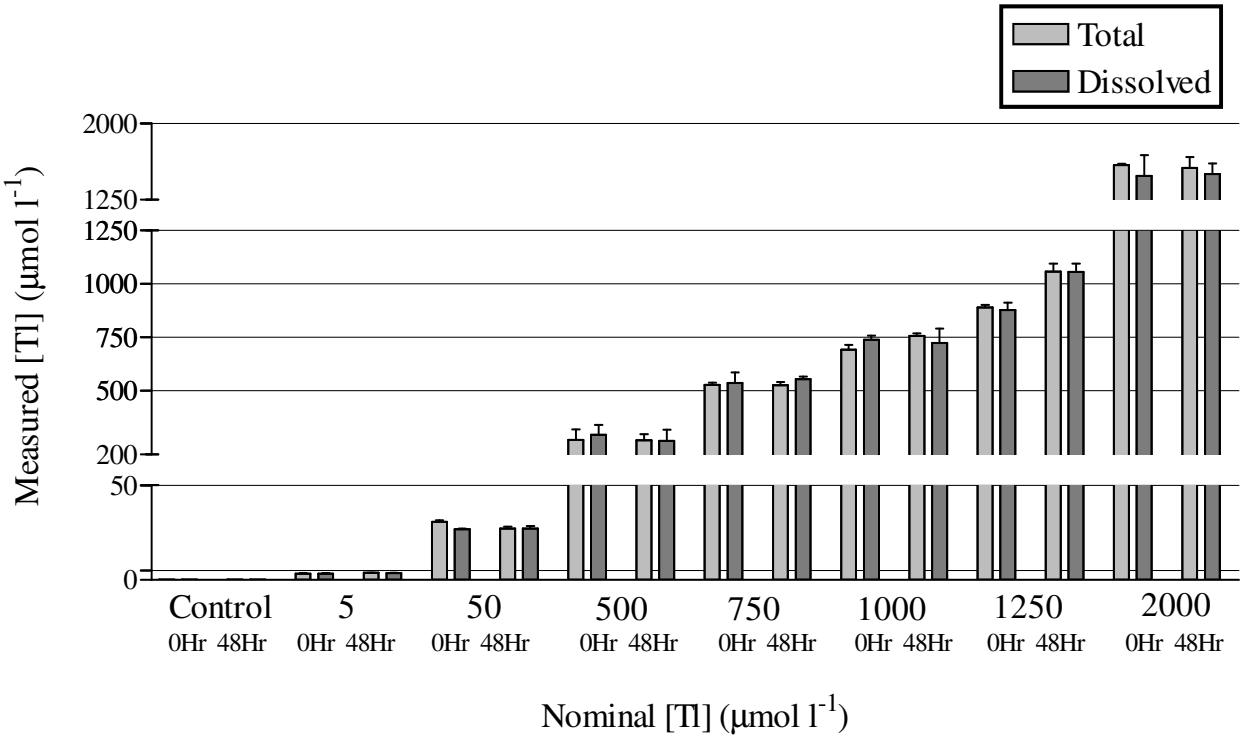
Total
Dissolved
Measured [Tl] (µmol l-1)
2000
1250
1250
1000
750
500
200
50
0
Control
5
50
500
750
1000
1250
2000
0Hr 48Hr
Nominal [Tl] (µmol l-1)

Figure 2: Total and dissolved Tl concentrations measured by graphite furnace atomic absorption spectroscopy (GFAAS) at 0 and 48 hours, as a percent of the nominal value. The measured concentrations were divided by the nominal concentrations and multiplied by 100. The average of all the values is indicated by the horizontal dotted line. Error bars are standard error about the mean of three replicates.

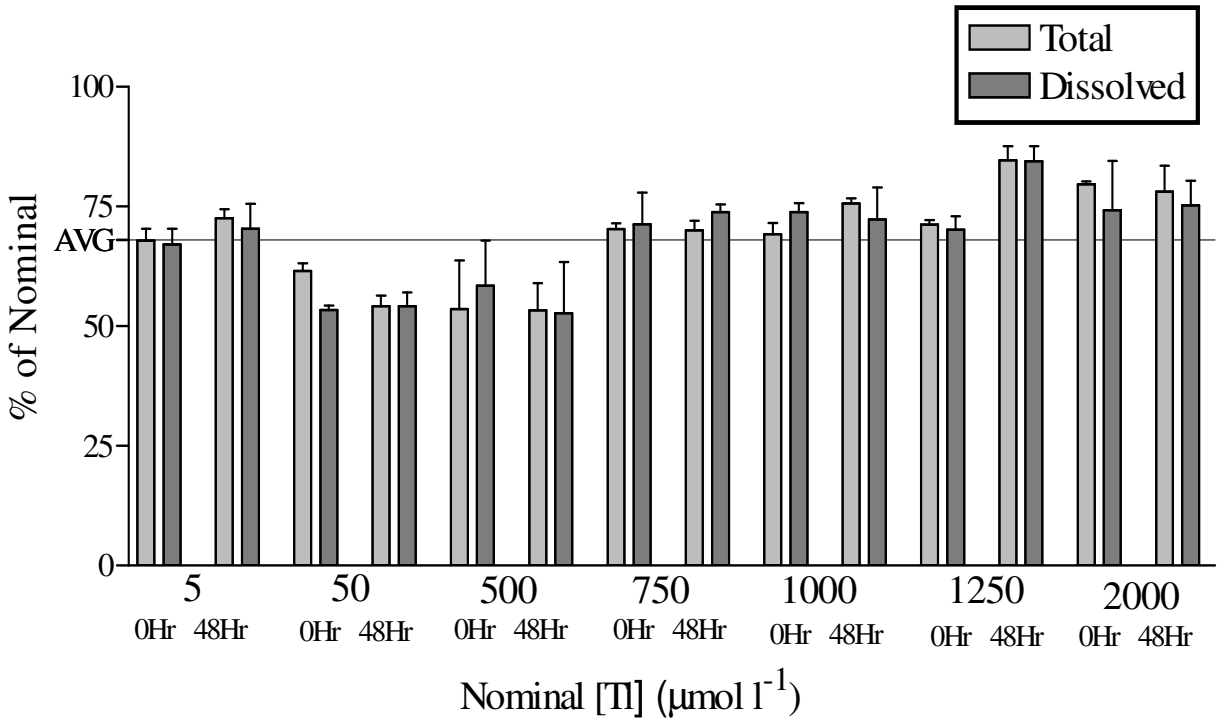
Total
Dissolved
100
75
AVG
50
25
0
% of Nominal
5
50
500
750
1000
1250
2000
0Hr 48Hr
Nominal [Tl] (µmol l-1)

Figure 3: Percentage mortality of 4th instar *C. riparius* larvae, plotted against the dissolved (average of 0 and 48 hours) Tl concentrations. The LC_{50} was performed in triplicate, and chironomids that pupated during the exposure were not counted. Each concentration started with n=13-15 larvae. Error bars are standard error about the mean of the three replicates.

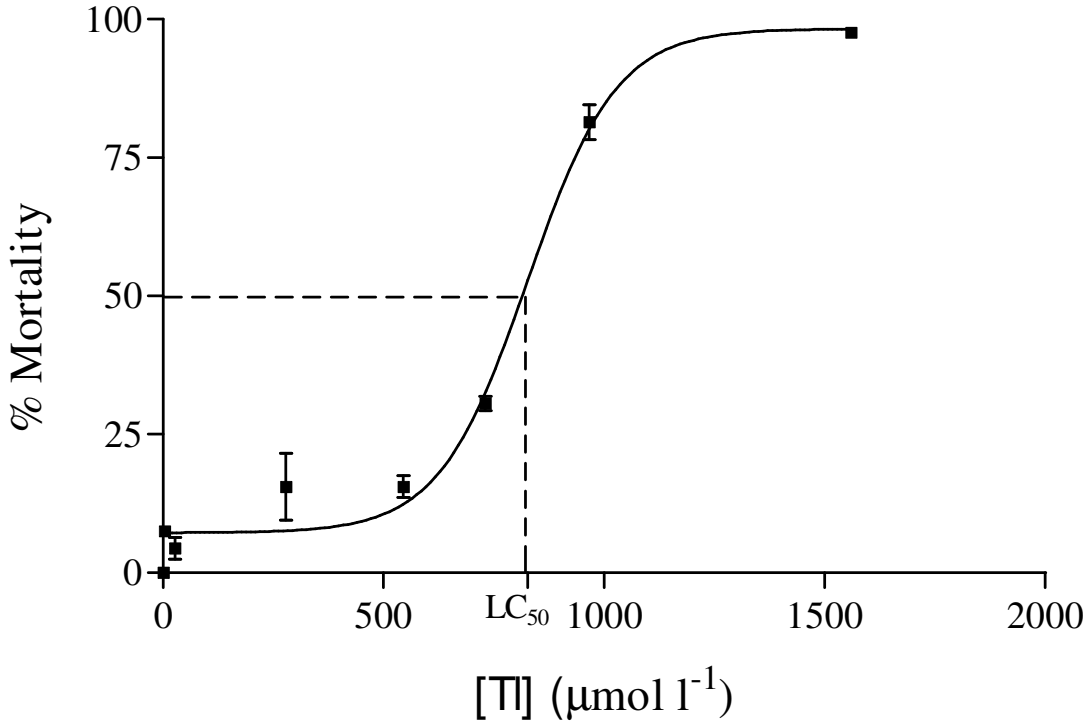
100
75
50
25
0
% Mortality
0
500
LC50
1000
1500
2000
[Tl] (µmol l-1)

Figure 4: Concentration-dependant uptake kinetics of Tl by the whole animal in *C. riparius* larvae. Values are means ± SEM.

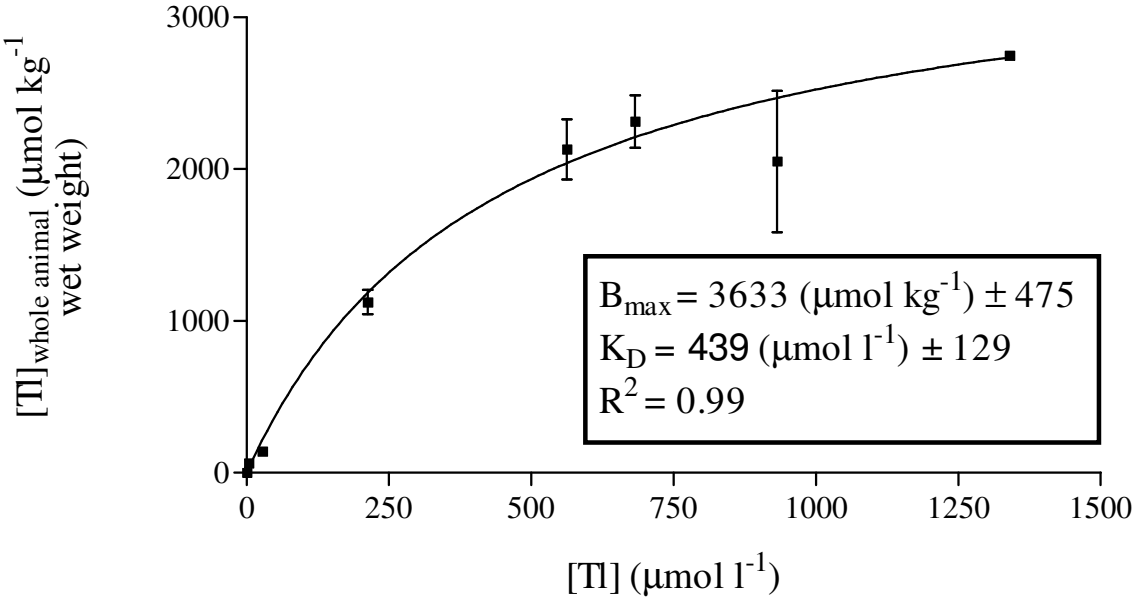
3000
2000
1000
0
0
250
500
750
1000
1250
1500
[Tl]whole animal (µmol kg-1 wet weight)
[Tl] (µmol l-1)
Bmax = 3633 (µmol kg-1) ± 475
KD = 439 (µmol l-1) ± 129
R2 = 0.99

Figure 5: Concentration-dependant uptake kinetics of Tl by the gut in *C. riparius* larvae. Values are means ± SEM.

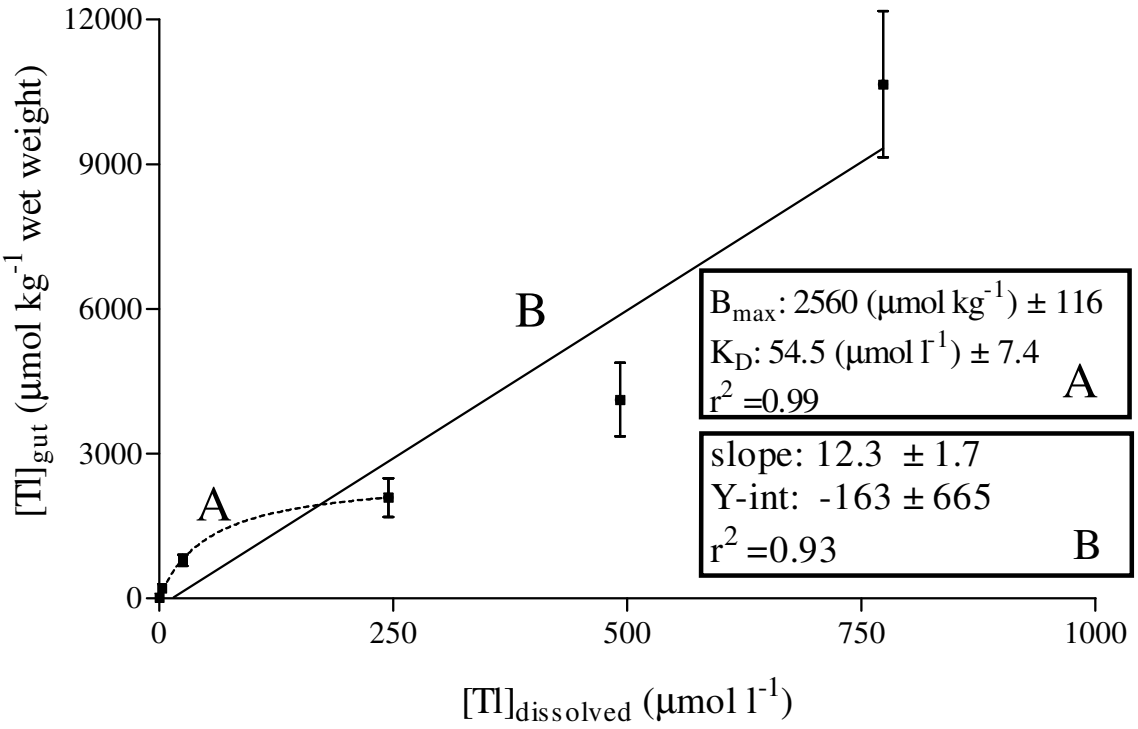
12000
9000
6000
3000
0
0
250
500
750
1000
[Tl]gut (µmol kg-1 wet weight)
[Tl]dissolved (µmol l-1)
A
B
Bmax: 2560 (µmol kg-1) ± 116
KD: 54.5 (µmol l-1) ± 7.4
r2 =0.99
A
slope: 12.3 ± 1.7
Y-int: -163 ± 665
r2 =0.93
B

Figure 6: Concentration-dependant uptake kinetics of Tl by the hemolymph in *C. riparius* larvae. Values are means ± SEM.

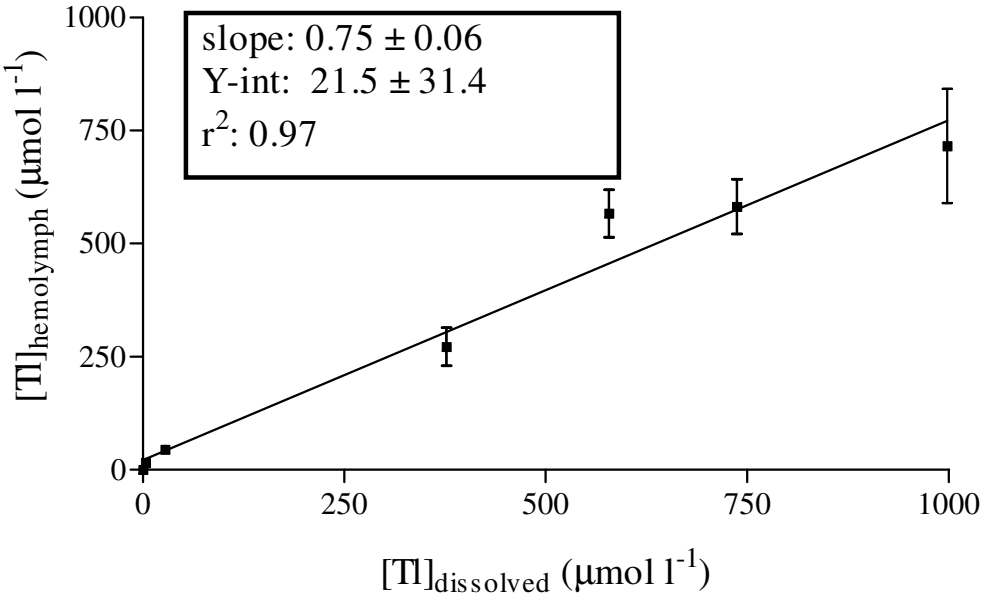
slope: 0.75 ± 0.06
Y-int: 21.5 ± 31.4
r2: 0.97
[Tl]hemolymph (µmol l-1)
[Tl]dissolved (µmol l-1)
0
250
500
750
1000

Figure 7: The total amount of Tl in each body compartment, as a percent of the total Tl in the whole animal. The total thallium in the whole animal, gut and hemolymph were based on measured Tl concentrations and the recorded weight or volume. The % of Tl in the carcass was calculated (i.e. $[Tl]_{carcass} = \{[Tl]_{whole\ animal} - ([Tl]_{Gut} + [Tl]_{Hemolymph})\}$. Values are means ± SEM.

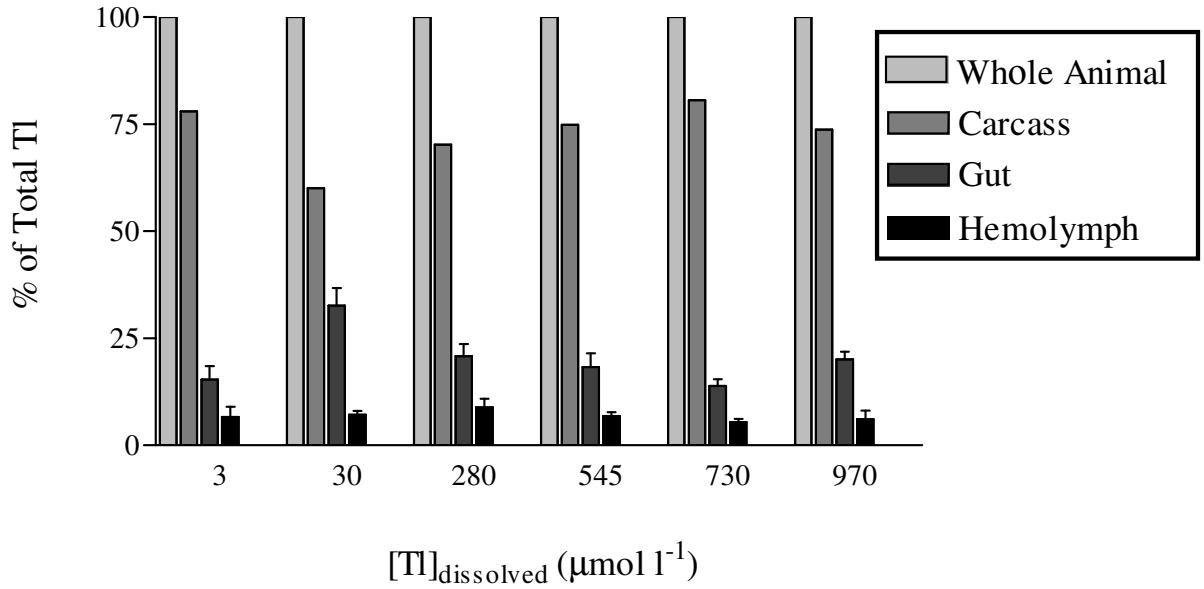
100
75
50
25
0
% of Total Tl
3
30
280
545
730
970
[Tl]dissolved (µmol l-1)
Whole Animal
Carcass
Gut
Hemolymph

Figure 8: Whole animal K concentrations plotted against dissolved Tl concentration. Significance from 0 (control) is indicated by an asterisk (One-way ANOVA with Dunnet's post tests if $p < 0.05$). Correlations between K concentrations and Tl exposure concentration were tested by Pearson's correlation and considered significant if $p < 0.05$. There was no significant correlation.

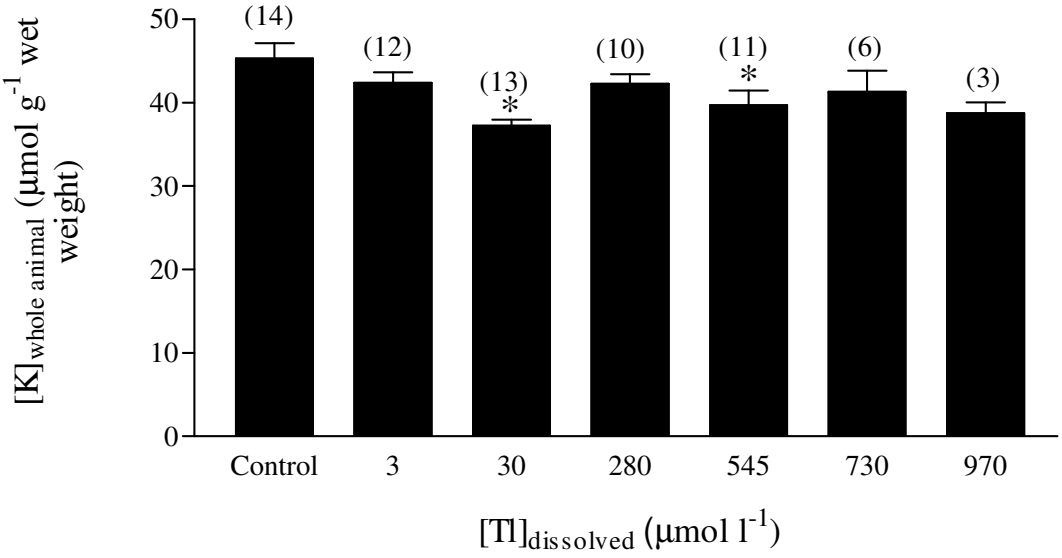
50
40
30
20
10
0
(14)
(12)
(13)
(10)
(11)
(6)
(3)
*
*
Control
3
30
280
545
730
970
[K]whole animal (µmol g-1 wet weight)
[Tl]dissolved (µmol l-1)

Figure 9: Gut K concentrations plotted against dissolved Tl concentration. Correlations between K concentrations and Tl exposure concentration were tested by Pearson's correlation and considered significant if $p < 0.05$. There was no significant correlation.

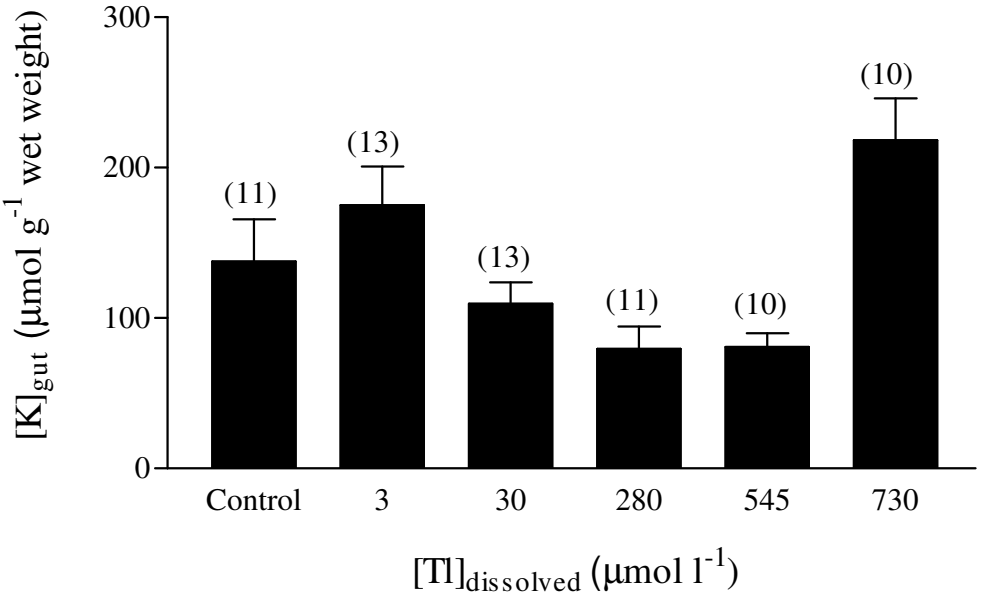
300
200
100
0
(11)
(13)
(13)
(11)
(10)
(10)
Control
3
30
280
545
730
[K]gut (µmol g-1 wet weight)
[Tl]dissolved (µmol l-1)

Figure 10: Hemolymph K concentrations plotted against dissolved Tl concentration. There was a negative correlation ($r = -0.833$, $p = <0.05$) between hemolymph K and Tl exposures in the range of concentrations between 0 (control) and 730 μmol l^{-1} Tl.

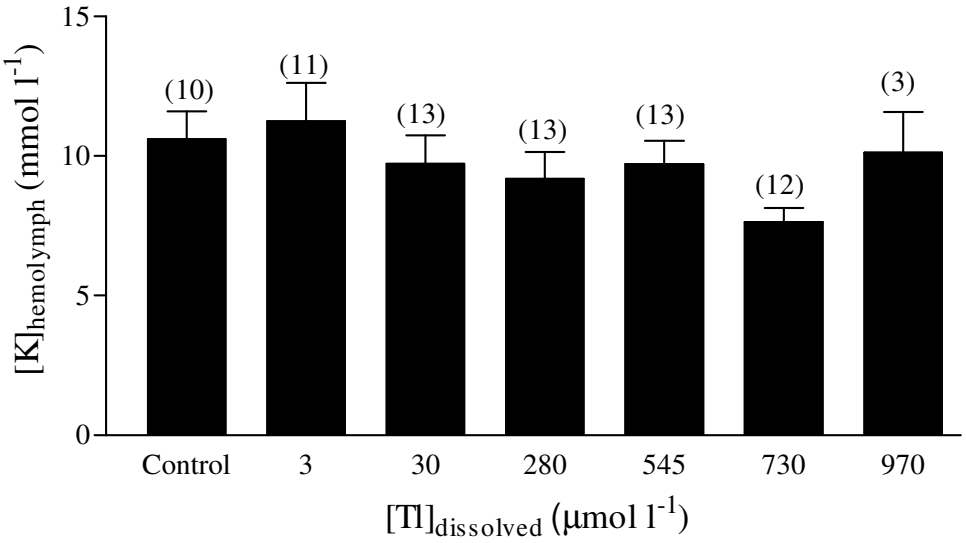
15
10
5
0
$[K]_{hemolymph}$ (mmol l^{-1})
(10)
(11)
(13)
(13)
(13)
(12)
(3)
Control
3
30
280
545
730
970
$[Tl]_{dissolved}$ (µmol l^{-1})

CHAPTER 4

General Discussion

This thesis has examined the tolerance of *C. riparius* towards Tl^+, the transport of Tl^+ and K^+ by isolated tissues, and the accumulation of Tl^+ and K^+ in the whole animal, gut and hemolymph. Taken together, the results suggest complex interactions between K^+ and Tl^+ in *Chironomus*, yet their survival when exposed to high concentrations of Tl^+ indicates efficient mechanisms of detoxification. This general discussion provides a summary of the findings from chapter 2 and 3, followed by a section identifying the conflicting results between the two chapters, with possible explanations. The next section integrates the findings of chapter 2 and 3 to explain the interactions between K and Tl and gives some suggestions for Tl tolerance in *C. riparius*, followed by proposals for future studies.

1.1. Summary of chapter 2

In chapter 2, K^+ and Tl^+ transport directions and magnitudes were compared along the entire isolated gut and Malpighian tubules (MTs) of Tl^+-naïve *C. riparius* larvae using ion-selective microelectrodes and the SIET technique. Flux magnitudes and directions are comparable along most of the gut, consistent with a shared transport mechanism. Even though K^+ and Tl^+ transport appeared to differ at the AMG, this was shown to be caused by an experimental artifact (due to the absence of a luminal source of Tl^+). The major K^+ transporting regions of the gut are the caecae, anterior midgut (AMG) and posterior midgut (PMG). Competition studies performed at these locations provide evidence for an

interaction between the two ions, based on the finding that 50 μmol l^{-1} Tl^+ decreases K^+ flux at the AMG and PMG. At the caecae, the K^+ transport blockers Ba^{2+} and ouabain inhibit Tl^+ flux, but not K^+ flux. This may indicate that there is no interaction between K^+ and Tl^+ at the caecae. However, it is also possible that multiple K^+ transporters are present at the caecae, and that some of these have higher affinities for Tl^+ but are also more sensitive to Ba^{2+} and ouabain. There is also evidence for an interaction between K^+ and Tl^+ based on differences in net transport of these two ions by the gut in Tl^+-naïve and Tl^+-exposed larvae. The sum of the fluxes across all gut segments indicates that the gut secretes Tl^+ (hemolymph towards gut lumen) in Tl^+-naïve larvae, whereas it absorbs Tl^+ (gut lumen to hemolymph) in Tl^+-exposed larvae. Conversely, K^+ is absorbed in Tl^+-naïve larvae, and it is secreted in Tl^+-exposed larvae.

1.2. Summary of chapter 3

In chapter 3, I determined that the acute (48 hour) LC_{50} of 4th instar *C. riparius* larvae to Tl is 723 μmol l^{-1}. This is ~ 180000 above CCME water quality guidelines. The finding that Tl is not very toxic to *C. riparius* fits with previous studies which have looked at tolerance for other toxic metals, such as Cu, Cd, Pb, Zn and Ni (Gillis and Wood 2008a; Gillis and Wood 2008b; Béchard et el., 2008).

The measurement of Tl uptake by the whole animal, gut and hemolymph was determined from GFAAS measurements. K concentrations were also measured in these tissues using FAAS. Tl uptake by the whole animal is saturable, while uptake is non-saturable in the hemolymph. The gut showed some evidence for saturable uptake over the

4 lowest Tl concentrations, possibly due to a limited intracellular compartmentalization of Tl involving lysosomes or metal-binding proteins. However, it is possible that uptake by the gut may be non-saturable over the entire range of tested Tl concentrations. Evidence for an interaction between K and Tl is based on the finding of a significant decrease in K concentrations in the whole animal at some Tl exposures. There is also some evidence for an interaction between the two ions in the hemolymph based on a negative correlation between hemolymph K and Tl exposures in the range of concentrations between 0 (control) and 730 μmol l^{-1} Tl. Calculated values indicate that the majority of total Tl is accumulating within the carcass, which also contains K-rich muscle. The muscle within the carcass may act as a K store and act to maintain K concentrations in the hemolymph, and thus prevent toxicity and contribute to tolerance.

1.3. Conflicting observations between chapters 2 and 3

The interactions between K^+ and Tl^+ in chapter 2 were identified by the measurement of K^+ and Tl^+ fluxes using ion-elective microelectrodes and the SIET technique, whereas in chapter 3 the interactions of the two ions were examined by the measurements of ion concentrations after Tl^+-exposure using AAS. While we did find evidence for interactions between K^+ and Tl^+ from both these approaches, there were also some disagreements between the findings of chapter 2 and 3. These conflicting results are identified and addressed here.

In chapter 2, evidence for an interaction between K^+ and Tl^+ was based on the finding that Tl^+ caused a reduction in K^+ transport at the AMG and PMG. However, in

chapter 3 there were no significant changes in K concentrations in the gut or hemolymph after Tl^+-exposure when K concentrations were measured by FAAS. This difference may be due to compensation of hemolymph and gut K concentrations by K stores in the muscle (described below).

In chapter 2, Tl^+-exposed larvae showed a net secretion of K^+ (i.e. net K loss) by the gut. This would cause total hemolymph K to reach zero after ~40 minutes (Leonard et al., 2009), and total body K^+ to reach zero after ~12 hours. This was obviously not the case, as indicated by the survival of the larvae at these Tl concentrations (chapter 3). In addition to the survival of the larvae, FAAS measurements of K concentrations in the gut and hemolymph showed there was no significant decrease in K at any exposure after 48 hours (although there was some evidence for a negative correlation in hemolymph K concentration and Tl^+-exposure, described in chapter 3). This finding is not completely surprising, since the SIET measurements of K^+ and Tl^+ flux are only performed for ~60 minutes *in vitro,* while the net ion concentrations measured by FAAS are measured *in vivo* after a 48 hour exposure. The disturbance of K^+ homeostasis caused by Tl^+ and indicated by SIET measurements may just be present in the short term (i.e. < ~1 hour).

In chapter 2, SIET measurements indicated that there was a net movement of Tl^+ into the hemolymph after Tl^+-exposure. However, in chapter 3 GFAAS measurements showed the highest concentrations of Tl ($\mu mol\ kg^{-1}$) were present within the gut, not the hemolymph. The apparent disagreement between the findings may be the result of the relatively short SIET measurements of Tl^+ flux (~60 minutes). After 60 minutes, there may be more Tl^+ being transported into the gut (basolateral) as a way of sequestering and

detoxifying Tl^+. Also, there were no luminal measurements of Tl^+ flux performed. If the transport of Tl^+ into the gut was greater across the lumen side than across the basolateral side, it would indicate why there appears to be a net absorption of Tl^+ into the hemolymph as measured by SIET, even though GFAAS measured higher concentrations of Tl in the gut.

1.4. Integration of chapter 2 and 3 findings: K and Tl interactions and Tl-tolerance

Based on SIET measurements of K^+ and Tl^+ fluxes, and measurements of K and Tl concentration by AAS, we have identified that there are interactions between K and Tl. In chapter 2, we were able to identify where Tl^+ gains access to the hemolymph, based on SIET measurements of Tl^+ flux along the gut of Tl^+-exposed larvae. The net absorption of Tl^+ into the hemolymph was confirmed by GFAAS measurements of hemolymph Tl concentrations after exposure to a range of Tl concentrations. GFAAS measurements found higher concentrations of Tl were present in the gut compared to the hemolymph in Tl-exposed larvae. This may indicate a role for the gut in Tl sequestration or secretion, as we found it was possible for Tl to be transported into the gut at the PMG, caecae and MTs in Tl-naïve larvae.

It seems likely that within the carcass, Tl^+ is accumulating mostly within the muscle. This is proposed based on the finding that calculated values (based on GFAAS measurements of Tl in the whole animal, gut and hemolymph) indicate that the majority of total Tl is present within the carcass, and that SIET measurements show Tl^+ is not transported into the abdominal cuticle. Tl^+ entry into the muscle cells may occur because

muscle cells are K^+ rich and excitable, and depolarization requires the movement of large amounts of K^+. Thus, the ionic mimicry of Tl^+ for K^+ may allow Tl^+ to gain access into the muscle cells. Conversely, it may be that the muscle is providing K^+ to the hemolymph to compensate the net K^+ loss measured along the whole gut by SIET in Tl^+-exposed larvae.

The saturable uptake of Tl^+ observed for the whole animal followed the same saturable uptake pattern see for Cd^{2+} (Gillis and Wood, 2008b). An apparent saturable uptake of Tl^+ was also observed at the lower concentrations in the gut. The saturation in the gut may be the result of saturation of K^+ transporters, or limited compartmentalization of Tl^+ within the cell (e.g. within lysosomes or bound to metal-binding proteins). The saturation of Tl^+ in the whole animal may also be the result of limited binding availability to metal binding proteins. However, the limited uptake may also be the result of a maximum capacity of the carcass for Tl^+ being reached. The linear uptake seen in the hemolymph and gut are indicative of passive diffusion, possibly involving both paracellular and transcellular pathways.

1.5. Future studies

The findings of these studies provide evidence for an interaction between K^+ and Tl^+, but also show that *C. riparius* larvae are highly tolerant towards Tl^+. The Tl^+ tolerance likely involves a combination of the strategies that have been reported for Cd^{2+} tolerance – secretion, sequestration and a role for the metal-binding protein, metallothionein. These studies focused mainly on the role of secretion in contributing to

tolerance (in addition to the effects of Tl^+ on K^+). Future studies looking at Tl^+ secretion by the anal papillae in Tl^+-exposed larvae would be beneficial to further understanding the role of secretion by the whole organism and its contribution to Tl^+ tolerance. Whether Tl^+ transport at the anal papillae involves K^+-transporters could be determined through the use of K^+-transporter blockers. It would also be helpful to further investigate the potential of the MTs to secrete Tl^+ through the use of the Ramsay assay. Whether Tl^+ transport along the gut is passive or active could be determined through the addition of cyanide and/or iodoacetate to block oxidative and glycolytic ATP production. Finally, the role of sequestration by the anal papillae, gut and MTs at various Tl^+ concentrations would help in further explaining the tolerance of *C. riparius* for Tl^+.

References

Béchard, K.M., Gillis, P.L., Wood, C.M. Acute toxicity of waterborne Cd, Cu, Pb, Ni and Zn to first-instar *Chironomus riparius* larvae. *Arch. Environ. Contam. Toxicol.* **54** (2008), pp. 454-459

Gillis, P.L, and C.M. Wood. Investigating a potential mechanism of Cd resistance in *Chironomus riparius* larvae using kinetic analysis of calcium and cadmium uptake. *Aquat. Toxcoli.* **89** (2008a), pp.180-187.

Gillis, P.L., and C.M. Wood. The effect of extreme waterborne cadmium exposure on the internal concentrations of cadmium, calcium and sodium in *Chironomus riparius* larvae. *Aquta. Toxcoli.* **1** (2008b), pp. 56-64.

APPENDIX

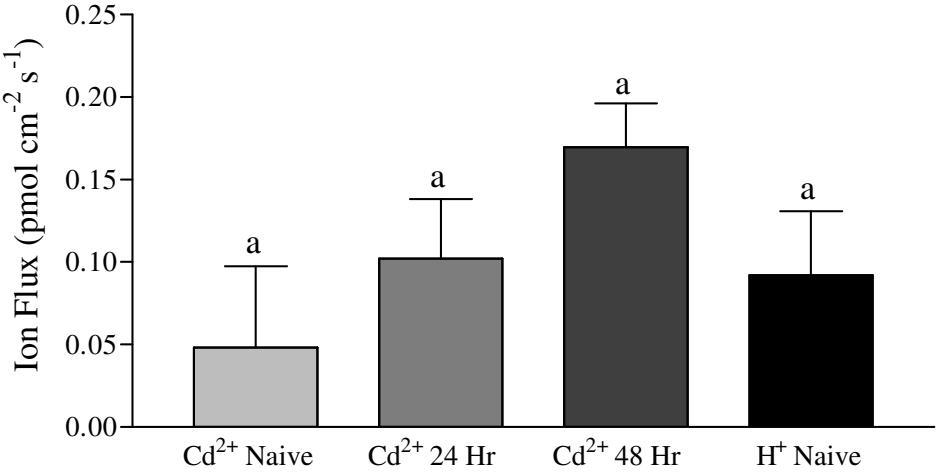

Figure1A: Cd^{2+} and H^{+} flux at the anal papillae of *C. riparius* after 0 (naïve), 24 and 48 hour waterborne exposure to 10 μM Cd. Scanned in dechlorinated Hamilton tap water (pH 7) with 1mM PIPES. Letters sharing the same letter are not significant from each other ($p < 0.05$).

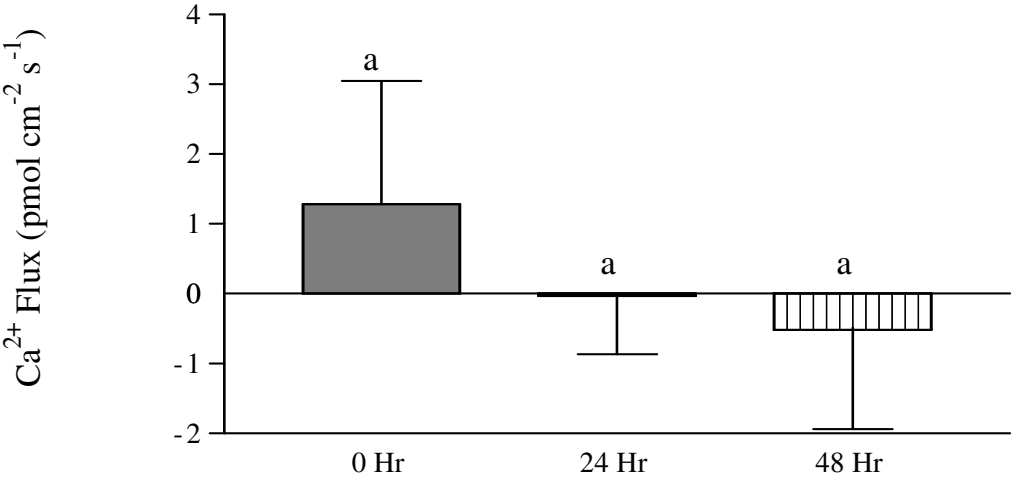

Figure 1B: Ca^{2+} flux at the anal papillae of *C. riparius* after 0 (naïve), 24 and 48 hour waterborne exposure to deionized water . Scanned in dechlorinated Hamilton tap water (pH 7) with 1mM PIPES. Letters sharing the same letter are not significant from each other ($p < 0.05$).

Figure 1A shows Cd^{2+} flux at the anal papillae of chironomids that had no prior exposure to Cd (naïve) and those that had been exposed to 10 μm Cd (in Hamilton tapwater) prior to measurements. Scans were performed in Hamilton tapwater with 1 mM PIPES buffer titrated to pH 7. PIPES was used to keep conditions similar to previous SIET Cd^{2+} measurements performed along the gut by Leonard et al., (2009). The results indicate that the anal papillae do have a role in Cd^{2+} excretion (i.e. from anal papillae to bathing solution). H^+ measurements were also performed to determine the effect of an acidic boundary layer around the AP on the amount of free Cd^{2+} which is available for transport. The H^+ flux causes an acidification of 0.013 pH units 10 μM from the surface compared to 50 μM from the surface, causing a 1.44 nM increase in free Cd^{2+} 10 μM from the surface. This causes an apparent Cd^{2+} efflux artifact of 0.00144 pmol cm^{-2} s^{-1}, which has negligible effects on actual Cd^{2+} efflux measurements.

Figure 1B shows Ca^{2+} flux at the anal papillae of chironomids with no prior exposure to deionized water, and those that had been exposed to deionized water for 24 or 48 hours. Exposure to deionized water was performed to try to increase Ca^{2+} uptake potential when the scans were performed in Ca^{2+} rich dechlorinated Hamilton tapwater with 1 mM PIPES (pH 7). The results indicate the anal papillae are not involved in Ca^{2+} transport under the experimental conditions, which agrees with the results of Ca^{2+} flux measurements using SIET at the anal papillae of *Aedes aegypti* by Donini and O'Donnell (2005). Ca^{2+} transport blockers would confirm whether the Cd^{2+} efflux seen in figure 1B involves Ca^{2+} transporters.